System Performance Analysis of Cooperative Communication in Wireless Ad Hoc Networks

by

Yong Zhou

A thesis
presented to the University of Waterloo
in fulfillment of the
thesis requirement for the degree of
Doctor of Philosophy
in
Electrical and Computer Engineering

Waterloo, Ontario, Canada, 2015

Author's Declaration

I hereby declare that I am the sole author of this thesis. This is a true copy of the thesis, including any required final revisions, as accepted by my examiners.

I understand that my thesis may be made electronically available to the public.

Abstract

Wireless ad hoc networks have been attracting more and more attentions in recent years from both academia and industry, because of their low deployment costs and broad applications. Due to the scarcity of the radio spectrum, supporting concurrent transmissions by exploiting the spatial frequency reuse gain is necessary to enhance spectrum utilization. On the other hand, cooperative communication is a practical technique for realizing the spatial diversity gain to mitigate the detrimental effect of wireless channel and enhance the transmission reliability. Enabling concurrent cooperative transmissions across a network can achieve both types of gains. Due to the broadcast nature of wireless communications, the concurrent cooperative transmissions using the same radio channel generate interference to each other, which is the main performance-limiting factor. Accurate characterization of interference is a fundamental step towards evaluating the performance of cooperative communication in a wireless ad hoc network. However, the distributed network operation, random node locations, interference redistribution due to relay transmissions, and dynamic traffic arrival pose significant challenges in interference characterization.

Under the protocol interference model, this thesis evaluates the effectiveness of cooperative communication in a wireless ad hoc network from a perspective of overall network performance through investigating the network throughput, which captures the tradeoff between single-link cooperation gain and network-wide reduced spatial frequency reuse due to relay transmissions. In particular, based on stochastic geometry, the outage probabilities of direct and cooperative transmissions are derived to characterize single-link cooperation gain. On the other hand, according to a randomized scheduling scheme, the expected numbers of concurrent direct and cooperative transmissions that can be accommodated within the network coverage area are calculated to characterize network-wide reduced spatial frequency reuse. The analytical results show that a locally beneficial cooperation decision is not guaranteed to be network-wide beneficial.

The number of potential relays determines the achievable performance of a cooperative link, and varies for different source-destination pairs due to random relay locations. This thesis proposes an opportunistic cooperation strategy based on the number of potential relays available for each source-destination pair. Under the physical interference model, the correlation of node locations induces the correlation of interference power. Via modeling node locations as a Poisson point process (PPP) and based on the Campbell's theorem, the temporal correlation coefficient of interference power at a destination node is analyzed. In addition, we derive the outage probability of opportunistic cooperation while taking into account the spatial and temporal interference correlation. The overall network performance can be enhanced by adjusting the proportion of concurrent cooperative transmissions.

In addition to random node locations and interference redistribution, dynamic traffic arrival further complicates the interference characterization. This thesis investigates the performance of cooperative communication in a wireless ad hoc network with unsaturated traffic, which introduces a correlation between the interferer density and packet retransmission probability. Based on queueing theory and stochastic geometry, the interference power is characterized from two aspects, namely stationary interferer density and interference correlation in two consecutive time-slots, to evaluate the network performance. The analytical results show that the performance analysis under the assumption of independent interference power overestimates the network performance.

The proposed theoretical performance analysis framework provides a step towards better understanding of the benefits and limitations of cooperative communication in wireless ad hoc networks with spatially random nodes, and in turn provides useful insights on protocol design and parameter setting for large-scale networks.

Acknowledgements

I would like to express my deepest gratitude to my supervisor, Professor Weihua Zhuang, for her invaluable guidance and continuous encouragement. Her excellent supervising skills and commitment to her students are extraordinarily helpful to develop my academic skills.

I gratefully acknowledge my PhD committee members, Professor Xianbin Wang, Professor Liangliang Xie, Professor Oussama Damen, and Professor Peisong Han, for their insightful comments and suggestions, which helped to improve the quality of the thesis. I would also like to thank Professor Oleg Michailovich for participating in my PhD thesis defense.

I would like to thank Professor Sherman (Xuemin) Shen. The weekly group meeting coordinated by Professor Shen gave me a great opportunity to broaden my knowledge. I am indebted to all my colleagues at the Broadband Communication Research (BBCR) group for their research collaborations and beneficial discussions. Their talent and friendship made my experience in Waterloo pleasant.

Thanks also go to Professor Ju Liu, Professor Jiande Sun, and Professor Weihong Zhu at Shandong University for providing recommendation letters when I applied for a PhD program at the University of Waterloo.

Finally, I would like to thank my parents and wife for their endless support, unconditional love, and continuous encouragement.

Dedication

To my family and teachers from whom I have learned so much.

Table of Contents

List of Figures

List of Abbreviations

2D	Two-Dimensional
ACK	Acknowledgement
AF	Amplify-and-Forward
ARQ	Automatic Repeat reQuest
BPP	Binomial Point Process
CF	Compress-and-Forward
CLIR	Cooperative Link Interference Region
CNIR	Cooperative Node Interference Region
CSI	Channel State Information
CT	Cooperative Transmission
DF	Decode-and-Forward
DR	Diamond Region
DT	Direct Transmission
FIFO	First-In First-Out
HOL	Head-of-Line
i.i.d.	Independent and Identically Distributed
IR	Interference Region
LIR	Link Interference Region

MANET	Mobile Ad Hoc Network
MIMO	Multiple-Input Multiple-Output
MRC	Maximal Ratio Combining
NACK	Negative Acknowledgement
NIR	Node Interference Region
PGFL	Probability Generating Functional
PPP	Poisson Point Process
QoS	Quality-of-Service
SC	Selection Combining
SINR	Signal-to-Interference-plus-Noise Ratio
SIR	Signal-to-Interference Ratio
SNR	Signal-to-Noise Ratio

List of Symbols

α	Path loss exponent
β_ν	Reception threshold for packets transmitted at rate ν
ϵ	Parameter to model the singular (i.e., $\epsilon = 0$) and non-singular (i.e., $\epsilon > 0$) path loss models
$\mathrm{erf}(\cdot)$	Error function
$\Gamma(\cdot)$	Gamma function
$\gamma_{XY:n}$	SIR observed by receiver Y when receiving a packet from transmitter X in the nth sub-time-slot
$\gamma_{XY}(t)$	SIR observed by receiver Y when receiving a packet from transmitter X at time-slot t
κ	Distance between a source node and the corresponding center of relay selection region
λ_C	Spatial density of source nodes of cooperative links
λ_D	Spatial density of source nodes of direct links
λ_F	Spatial density of selected relays that forward packets in the second sub-time-slot
$\lambda_I(t)$	Spatial density of unintended (active) transmitters at time-slot t
λ_R	Spatial density of relay nodes
λ_S	Spatial density of source nodes

Λ_T	Packet arrival rate in packets per time-slot
$\lambda_{em}(t)$	Spatial density of emerging nodes at time-slot t
$\lambda_{reR}(t)$	Spatial density of retransmitting relays at time-slot t
$\lambda_{reS}(t)$	Spatial density of retransmitting source nodes at time-slot t
$\lambda_{re}(t)$	Spatial density of retransmitting nodes at time-slot t
$\mathbb{E}[X]$	Expectation of random variable X
$\mathbb{N}^+$	Set of positive natural numbers
$\mathbb{P}[\mathcal{E}]$	Probability of event $\mathcal{E}$
$\mathbb{R}^2$	Two-dimensional space
$\mathbf{1}(\cdot)$	Indicator function
$\mathcal{A}_{CT}$	Area of the link interference region of a cooperative link
$\mathcal{A}_{DR_0(\omega)}$	Area of the diamond-shaped relay selection region with angle ω for the typical source-destination pair
$\mathcal{A}_{DT}$	Area of the link interference region of a direct link
$\mathcal{A}_N$	Network coverage area
$\mathcal{A}_R$	Area of a circular relay selection region
$\mathcal{A}_{TR(v)}$	Area of the triangular region with height v
$\mathcal{E}_{11}$	Event that there are no qualified relays when there exists at least one potential relay
$\mathcal{E}_{12}$	Event that the received SNR at destination node D_0 in the second sub-time-slot is smaller than $\beta_{2\nu}$ when relay set Ω_0 is not empty
$\mathcal{E}_{21}$	Event that relay set Ω_0 is empty
$\mathcal{E}_{22}$	Event that the received SIR at destination node D_0 in the second sub-time-slot is smaller than $\beta_{2\nu}$ when relay set Ω_0 is not empty

$\mathcal{E}_{31}$	Event that destination node D_0 fails to decode the packet at time-slot t, and relay set $\Omega_0(t)$ is empty
$\mathcal{E}_{32}$	Event that destination node D_0 fails to decode the packet at time-slot t, and source node S_0 has the best channel to destination node D_0 while relay set $\Omega_0(t)$ is not empty
$\mathcal{E}_{33}$	Event that source node S_0 has the best channel to destination node D_0
$\mathcal{E}_{41}$	Event that the direct link is not reliable at both time-slots t and $t+1$
$\mathcal{E}_{42}$	Event that no relays have reliable links to the source and destination nodes at time-slots t and $t+1$, respectively
$\mathcal{R}_{CT}^{I}$	Interference range of the cooperative transmission
$\mathcal{R}_{DT}^{I}$	Interference range of the direct transmission
$\mathrm{Var}(X)$	Variance of random variable X
$\mu(\cdot)$	Intensity measure
ν	Packet transmission rate in bit/s
ω	Angle of a diamond-shaped relay selection region
$\Omega_0(t)$	Set of qualified relays for the typical source-destination pair at time-slot t
Φ_C	PPP formed by the spatial locations of source nodes of cooperative links
Φ_D	PPP formed by the spatial locations of source nodes of direct links
Φ_F	PPP formed by the spatial locations of the selected relays that forward packets in the second sub-time-slot
$\Phi_I(t)$	PPP formed by the spatial locations of unintended transmitters at time-slot t
$\Phi_R(t)$	PPP formed by the spatial locations of relays at time-slot t
$\Phi_S(t)$	PPP formed by the spatial locations of source nodes at time-slot t
$\Phi_{em}(t)$	PPP formed by the spatial locations of emerging nodes at time-slot t

$\Phi_{reR}(t)$	PPP formed by the spatial locations of retransmitting relays at time-slot t
$\Phi_{reS}(t)$	PPP formed by the spatial locations of retransmitting source nodes at time-slot t
$\Phi_{re}(t)$	PPP formed by the spatial locations of retransmitting nodes at time-slot t
ψ_{XY}	SNR observed by node Y when receiving a packet from node X
ρ	Temporal correlation coefficient of interference power at a destination node in the first and second sub-time-slots
ρ_C	Temporal correlation coefficient of interference power at a destination node due to the adjacent locations of the source and relay nodes of cooperative links in the first and second sub-time-slots
ρ_D	Temporal correlation coefficient of interference power at a destination node due to the common locations of the source nodes of direct links in the first and second sub-time-slots
σ	Packet service rate in packets per time-slot
τ	Coordinate difference between a source node and its selected relay
θ_C	Cooperation threshold in terms of the number of potential relays
ϱ_u	Utilization factor
B	Channel bandwidth in Hz
CR_0	Constrained relay selection region for the typical source-destination pair
D_i	Destination node D_i
$d_i(t)$	Location coordinate of destination node D_i at time-slot t
D_{CT}^L	Semi-major axis of the link interference region of a cooperative link
D_{CT}^S	Semi-minor axis of the link interference region of a cooperative link
D_{DT}^L	Semi-major axis of the link interference region of a direct link

D_{DT}^{S}	Semi-minor axis of the link interference region of a direct link
$d_{XY}(t)$	Euclidean distance between nodes X and Y at time-slot t
$DR_0(\omega)$	Diamond-shaped relay selection region with angle ω for the typical source-destination pair
$f_X(x)$	Probability generating function of random variable X
$g\left(x\left(t\right)-y\left(t\right)\right)$	Path loss over a link with length $d_{XY}(t)$
G	Network throughput gain in using cooperative transmissions
G_S	Single-link cooperation gain
$H_{XY:n}$	Random distance-independent fading coefficient between nodes X and Y in the nth sub-time-slot
$H_{XY}(t)$	Random distance-independent fading coefficient between nodes X and Y at time-slot t
$I_{CD_0:1}\left(\Phi_C\right)$	Aggregate interference power from the source nodes of cooperative links in the first sub-time-slot at destination node D_0
$I_{D_0:1}\left(\Phi_D,\Phi_C\right)$	Aggregate interference power in the first sub-time-slot at destination node D_0
$I_{D_0:2}\left(\Phi_D,\Phi_F\right)$	Aggregate interference power in the second sub-time-slot at destination node D_0
$I_{D_0}(t)$	Aggregate interference power observed by destination node D_0 at time-slot t
$I_{DD_0:n}\left(\Phi_D\right)$	Aggregate interference power from the source nodes of direct links in the nth sub-time-slot at destination node D_0
$I_{FD_0:2}\left(\Phi_F\right)$	Aggregate interference power from the relays of cooperative links in the second sub-time-slot at destination node D_0
$I_{R_i}(t)$	Aggregate interference power observed by relay R_i at time-slot t
K_i	Number of potential relays for source-destination pair i

L_D	Link length (i.e., distance between a source node and its intended destination node)
L_i	Link L_i
L_N	Network-wide reduced spatial frequency reuse
N	Total number of links within the network coverage area
N_{CT}	Expected number of concurrent cooperative transmissions
N_{DT}	Expected number of concurrent direct transmissions
N_E	Expected number of concurrent transmissions
$P(k,n)$	Probability that k links can be scheduled after checking the first n links
p_m	Medium access probability
P_t	Transmission power in mW
Q	Interference-free probability between any two links
q_e	Probability of having an empty relay set
q_f	Failure probability of the packets transmitted by emerging nodes
q_s	Probability of source node retransmitting
Q_{CT}	Interference-free probability between any two cooperative links
q_{CT}	Outage probability of the cooperative transmission
q_{CT}^{MRC}	Outage probability of the cooperative transmission with MRC
q_{CT}^{SC}	Outage probability of the cooperative transmission with SC
Q_{DT}	Interference-free probability between any two direct links
q_{DT}	Outage probability of the direct transmission
q_{out}^{Conv}	Outage probability of the conventional ARQ scheme
q_{out}^{Coop}	Outage probability of the cooperative ARQ scheme

$q_{out}^{CT}(k)$	Outage probability of the cooperative transmission given k potential relays
q_{out}^{OC}	Outage probability of opportunistic cooperation
$R_{b'}^{i}$	Best relay of source-destination pair i for the cooperative transmission with MRC
R_{b}^{i}	Best relay of source-destination pair i for the cooperative transmission with SC
r_C	Radius of a circular constrained relay selection region
R_i	Relay node R_i
$r_i(t)$	Location coordinate of relay R_i at time-slot t
R_{F1}	Furthermost potential relay in the upper half of the relay selection region
R_{F2}	Furthermost potential relay in the lower half of the relay selection region
S_i	Source node S_i
$s_i(t)$	Location coordinate of source node S_i at time-slot t
T_{CT}	Network throughput of cooperative transmissions
T_{DT}	Network throughput of direct transmissions
V_1	Y-coordinate of the furthermost potential relay
W	Noise power
Z	Average delay (sum of the service delay and queueing delay)
Z_q	Queueing delay
Z_s	Service delay
$\overline{F}_X(x)$	Complementary cumulative density function of random variable X

Chapter 1

Introduction

1.1 Wireless Ad Hoc Networks

Wireless ad hoc networks have recently received extensive interests, due to their low deployment costs and promising applications (e.g., device-to-device communications in next generation cellular networks [1]). A wireless ad hoc network is formed by a group of nodes that can dynamically self-organize and self-configure the network into an arbitrary topology, and can also establish and maintain the connectivity among themselves. As all nodes are free to move independently and randomly, the network topology changes unpredictably. Each node can serve as a data source or destination, or a relay to help forwarding data on behalf of its neighboring nodes. Due to the scarcity of the radio spectrum, it is almost impossible to allocate an exclusive channel for each source-destination pair, especially in a wireless ad hoc network. By separating concurrent transmissions in space using the same radio channel, as shown in Figure 1.1, spatial frequency reuse is an efficient method to enhance spectrum utilization [2].

The infrastructure-less nature of a wireless ad hoc network renders it very suitable for applications that are constrained by economic conditions and/or geographical locations. For instance, a typical application scenario includes fast establishment of a communication network in battlefield, a natural disaster area where network infrastructures are out-of-work, and an emergency rescue area without adequate network coverage.

The wireless channel suffers from large-scale path loss, time-varying shadowing, and multi-path fading due to node mobility, which result in unpredictable channel conditions. On the other hand, due to the broadcast nature of wireless communications, as shown in

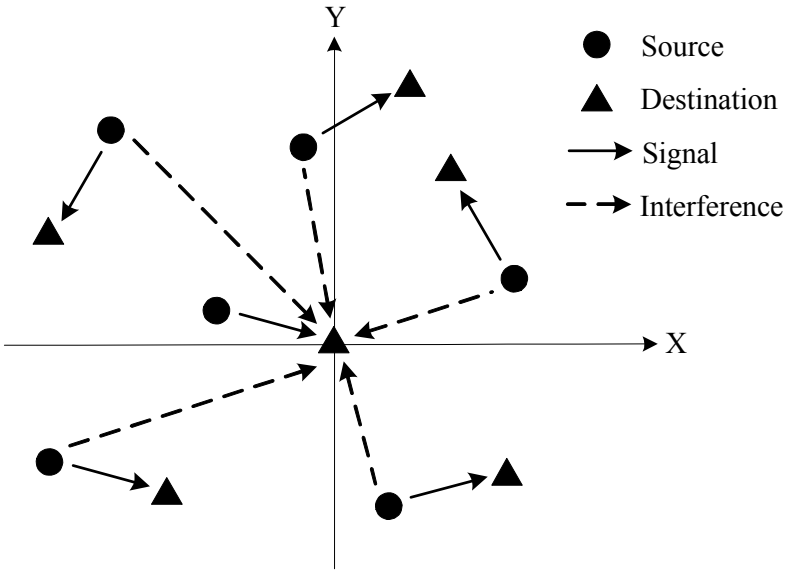

Figure 1.1: An illustration of a wireless ad hoc network with multiple concurrent direct transmissions separated in space using the same radio channel. For clarity, only the interference to the destination node located at the origin is depicted.

Figure 1.1, the concurrent transmissions using the same radio channel generate interference to each other, which undesirably affects the packet reception at a destination node. All these detrimental aspects should be addressed to use limited radio resources for an increasing service demand and to satisfy quality-of-service (QoS) requirements. Additionally, due to the ad hoc networking nature, the network management and operation should be distributed. In particular, each node makes its transmission decision based on only local information, which should be obtained at low costs as well as in a distributed manner. As a result, the randomness of channel fading coefficients, spatial node locations, transmission decisions, and packet traffic patterns complicates the design, modeling, evaluation, and optimization of a wireless ad hoc network.

1.2 Cooperative Communications

Via exploiting spatial diversity and multiplexing gains, multiple-input multiple-output (MIMO) [3] combined with space-time signal processing [4] can effectively mitigate the detrimental effects of wireless channel impairments to improve channel capacity and en-

hance transmission reliability. The deployment of multiple antennas on a single node, however, may not be feasible due to the limited physical size and cost constraints. As a result, cooperative communication [5, 6, 7] as an alternative approach has been proposed, in which cooperative diversity can be achieved by coordinating multiple nearby nodes to work together and form a virtual antenna array.

The process of cooperative communication can be divided into two phases, namely information sharing and cooperative transmission phases, which are carried out by fully utilizing the wireless broadcast and cooperative advantages, respectively. The neighboring nodes, which overhear a packet that is transmitted from a source node, can help forwarding the packet to the intended destination node when necessary. By combining two or more copies of the same packet that are transmitted through independent links, a spatial diversity gain can be achieved at the destination node to enhance reception quality. Different from a traditional point-to-point link, a cooperative link is characterized by the extra relay(s) and two-phase transmission. The abstraction of wireless links is broadened by the introduction of cooperative links. According to the forwarding operations adopted by the relays, the cooperative relaying schemes can be classified into three categories, namely amplify-and-forward (AF), decode-and-forward (DF), and compress-and-forward (CF) [8]. In an AF scheme, the relays simply amplify and forward a received noisy signal to the destination node, in which the level of noise in a signal is also enlarged. In a DF scheme, the relays decode the received signal and then forward the re-encoded signal to the destination node, while the relays in a CF scheme forward a quantized or compressed version of signal to the destination node.

Cooperative communication has been widely studied for the physical layer, and the cooperative advantages have been demonstrated by analyzing different relaying strategies from the viewpoint of information theory. It is shown that the fundamental advantage of cooperative communication is the spatial diversity gain. For different application scenarios, the spatial diversity gain achieved at the physical layer can be mapped to specific advantages at the link layer as needed, such as increasing transmission rate and throughput, reducing transmission power and improving spatial frequency reuse, enhancing transmission reliability, and enlarging transmission range and network coverage [9, 10].

The main objective of a cooperative transmission scheme is to fully map the cooperative diversity gain at the physical layer to the cooperative advantages at the link layer. However, due to the distributed network operation, time-varying channel fading, and co-channel interference, the link-layer performance of a cooperative link may not always be better than that of a direct link. In particular, the effectiveness of cooperative communication depends on many factors, including the protocol overhead, relay selection strategy, instantaneous channel fading, number of available relays, and link length. Additionally, due to interfer-

ence among concurrent transmissions, the cooperative transmissions should be activated when necessary and beneficial from a perspective of overall network performance. As a result, an efficient cooperative transmission scheme should identify an appropriate cooperation opportunity, select the best relay(s), and coordinate the cooperative transmission at low cost and complexity. It is necessary to develop an accurate theoretical performance analysis framework, so as to attain a better understanding of the performance of cooperative communication and provide useful insights on the design of efficient cooperative transmission schemes in a wireless ad hoc network.

The outage probability is a widely-used performance metric to evaluate the transmission reliability. It is defined as the probability that the received signal-to-interference-plus-noise ratio (SINR) falls below a required reception threshold. The transmission capacity, which is introduced in [11], is a performance metric that measures the maximum number of concurrent successful transmissions per unit area, subject to a constraint on the outage probability. A stricter requirement on the outage probability results in lower frequency of spatial reuse as well as lower transmission capacity, and vice versa. Two categories of performance analysis for cooperative communications can be distinguished in the literature. In the first category, the node locations are known and fixed; while the second category includes the scenario with random node locations.

1.2.1 Cooperative Communication in Fixed Topology Networks

The scenario with fixed relay locations without co-channel interference is studied in [12, 13, 14, 15, 16, 17, 18]. A fixed topology scenario with a single source-destination pair and multiple relays, as shown in Figure 1.2(a), is the simplest case for analyzing the performance of different relay selection strategies. Opportunistic relaying [12] and selection cooperation [13] are two representative single relay selection approaches. In opportunistic relaying, the relay that maximizes the minimum signal-to-noise ratio (SNR) of the source-relay and relay-destination links is selected. The outage probabilities of opportunistic AF and DF relaying under different fading channels are derived in [14] and [15], respectively. On the other hand, in selection cooperation, the relay with the best channel quality to the destination node is selected. An exact closed-form expression of outage probability of selection cooperation is derived for independent non-identical Rayleigh fading channels in [16]. The idea of single relay selection is generalized to multiple relay selection in [17, 18] to achieve a higher cooperation gain. As the complexity of selecting multiple relays increases exponentially with respect to the number of relays, relay ordering can be utilized to sort the relays before relay selection according to specific metrics [17]. With such an ordering, linear complexity is required to select multiple relays. Without power control, employing

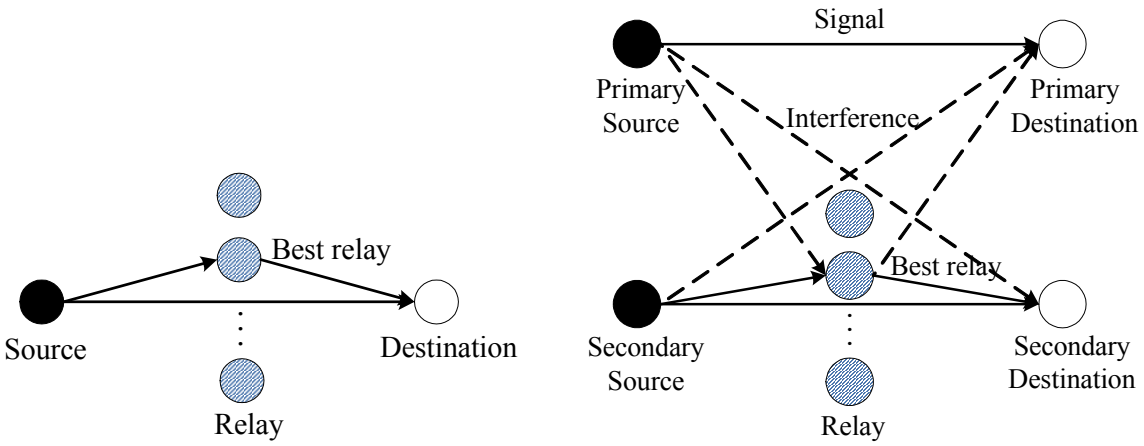

(a) Single relay selection for a single source-destination pair

(b) Single relay selection for a cognitive networks

Figure 1.2: An illustration of single relay selection for a single source-destination pair and a cognitive network.

more relays leads to a higher spatial diversity gain, but incurs higher interference power. In contrast, a single-relay cooperative scheme is easier to implement and achieves full-order spatial diversity without sacrificing spectrum efficiency by selecting the best relay [12]. Because of its simplicity and efficiency, the single-relay cooperative scheme is used in many existing studies.

For the scenario with a single source-destination pair, only time-varying channel fading is considered when selecting the best relay. However, both time-varying channel fading and co-channel interference should be considered when developing a relay selection scheme for a network that allows concurrent transmissions over a single radio channel. As a relay may not achieve the highest cooperation gain and generating the least interference power at the same time, the tradeoff between these two effects should be balanced, in order to maximize overall network performance while satisfying the QoS constraint of each link. Existing works that address this issue mainly focus on a cognitive scenario with a fixed topology, as shown in Figure 1.2(b), where one primary link shares the spectrum with one secondary link. The primary source is unaware of the secondary link and transmits directly to the primary destination. The secondary source enables a cooperative transmission so as to enhance its own transmission reliability and avoid generating intolerable interference to the primary destination. Generally, the QoS constraint of the primary link is specified by the maximum tolerable interference level or outage probability requirement. Under the

QoS constraint, the secondary source and its selected relay should adaptively adjust their transmission power according to the interference level generated to the primary destination [19]. The outage probability of the secondary link is derived and the analytical result shows that the performance of the secondary link is severely degraded due to limiting the transmission power and suffering interference from the primary link. However, such performance degradation can be compensated by increasing the number of potential relays, which increases the probability of selecting a better relay. With a constant transmission power, the best relay that can achieve the highest cooperation gain for the secondary link without incurring intolerable interference to the primary link should be selected [20]. Moreover, the interference due to relay transmissions can be mitigated by enabling cooperative beamforming at multiple relays to forward the packet [21].

All these studies focus on the performance analysis for a fixed topology network with either one or two source-destination pairs which, although providing useful insights on the potential benefits of cooperative communication, cannot characterize the performance of cooperative communication in a random topology network with multiple source-destination pairs.

1.2.2 Cooperative Communication in Random Topology Networks

The stochastic geometry [22, 23] as a powerful mathematical tool can be used to deal with random network topologies by treating node locations in a probabilistic manner. For a wireless ad hoc network with indiscriminate node placement or substantial node mobility, as shown in Figure 1.3, the Poisson point process (PPP) is widely used to model random node locations [24, 25]. The PPP model is necessary for preserving the highest level of analytical tractability, which can provide useful insights into the impact of both network and design parameters on the network performance.

The scenario with a single isolated source-destination pair and randomly positioned relays is studied in [26, 27, 28, 29]. Via modeling the relay locations as a homogeneous PPP, the outage probabilities of both opportunistic relaying and selection cooperation are analyzed for Rayleigh fading channels in [26]. Through the use of a bi-angular coordinate system, the performance analysis is extended for general fading channels in [27]. An uncoordinated cooperation scheme is proposed in [28], where each relay contends to cooperate with a specific probability calculated based on both local channel state information (CSI) and spatial distribution of relays. The authors in [29] derive the outage probabilities of opportunistic relaying that selecting the best relay with instantaneous and statistical CSI,

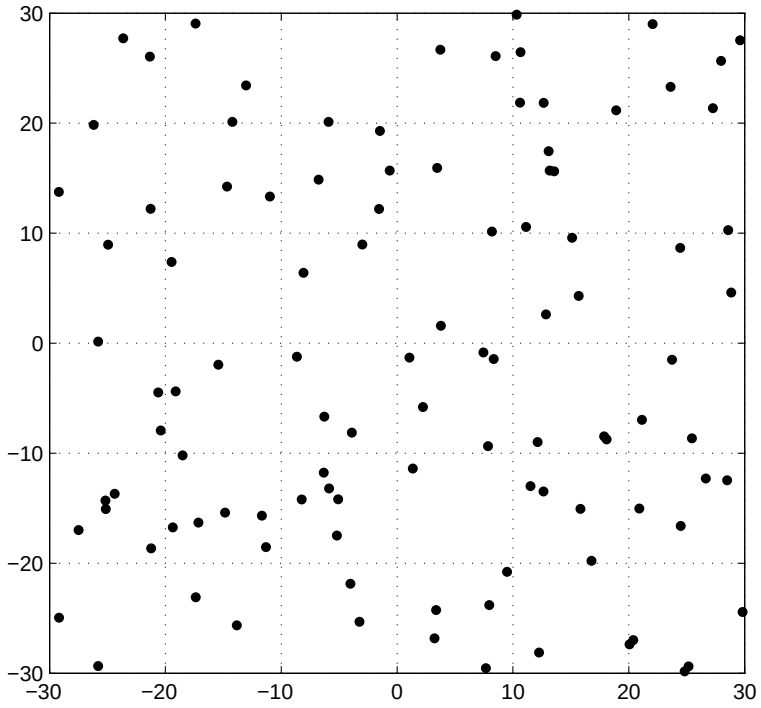

Figure 1.3: An illustration of random node locations modeled by a PPP.

and investigate the impact of different levels of CSI on the outage performance. These studies focus on the performance analysis for the scenario with a single isolated source-destination pair and randomly positioned relays, which cannot be directly extended to the scenario with multiple source-destination pairs.

In a wireless ad hoc network composed of many spatially scattered source-destination pairs, communication suffers from various impairments, such as path loss, channel fading, co-channel interference, and noise. Note that the co-channel interference is treated as noise when evaluating the outage probability based on SINR. As the co-channel interference is the main performance-limiting factor, performance analysis with an accurate interference characterization model can provide a better understanding of the overall network performance. The co-channel interference can be approximated by a Gaussian random process for tractability in performance analysis [30]. However, the Gaussian approximation does not completely characterize the co-channel interference, as it depends on many factors, includ-

ing the interferer distribution, medium access probability, traffic pattern, and propagation channel. Via modeling the spatial locations of concurrent transmitters as a homogeneous PPP, the co-channel interference at any time instant can be characterized, which allows for accurate performance evaluation for both direct transmissions [31, 32] and cooperative transmissions [33, 34, 35, 36, 37]. Taking into account channel fading, the authors in [31] derive the transmission capacity of direct transmissions by utilizing a tight bound of the signal-to-interference ratio (SIR) distribution. By exploiting instantaneous CSI, the channel inversion power control and threshold-based scheduling schemes are proposed to enhance the transmission capacity. Based on the Poisson shot noise field theory, the authors in [32] analyze the outage probability of an opportunistic ALOHA scheme in a mobile ad hoc network (MANET).

Such a performance analysis framework is applied to a cooperative spectrum sharing network in [33], which shows that the spectrum efficiency can be enhanced by exploiting the spatial diversity gain. Based on point process theory, the authors in [34] analyze the asymptotic outage probability and diversity gain for downlink relaying in a cellular network. The performance analysis is extended to an interference-limited hierarchical spectrum sharing network in [35], where the dominant interference is eliminated by forming a primary exclusive region around each receiver. A QoS region, within which any relay can be selected to satisfy a specified QoS constraint, is introduced in [36]. Altieri *et al.* propose a random relay activation strategy for a decentralized wireless network in [37], where each relay operates in full-duplex mode. The outage probability is analyzed for Rayleigh fading channels to investigate the tradeoff between the cooperation gain and additional interference due to relay transmissions. These studies focus on the scenario where the source nodes always have packets to transmit (i.e., a saturated traffic condition) under the assumption that the interference power observed at adjacent locations and in consecutive time-slots is independent.

The packet delivery probability and spatial network throughput of direct transmissions in wireless ad hoc networks with unsaturated traffic are derived in [38] and [39], respectively. On the other hand, the impact of interference correlation on the performance of direct transmissions is investigated recently in [40, 41, 42, 43, 44, 45, 46, 47]. The authors in [40] investigate three main factors that affect interference correlation, i.e., node locations, traffic pattern, and propagation channel. For different combinations of these influential factors, the correlation coefficients of interference power in two consecutive time-slots are derived. Considering the interference correlation due to node locations in [41, 42] and traffic pattern in [43], the authors derive the outage probabilities of direct transmissions and show that the interference correlation reduces the packet delivery probability. The authors in [44] investigate the diversity loss due to interference correlation in a Poisson

network with multi-antenna receivers. Such a performance analysis framework is extended to derive the packet delivery probability and diversity order of cooperative transmissions in a Poisson field of interferers in [45] and [46] respectively, while taking into account the correlation of interference power observed by the relay and destination nodes. The performance analysis is extended by selecting the best relay from multiple potential relays in [47]. By assuming the same set of interferers during the transmission periods of the source and relay nodes, these studies focus on a saturated traffic scenario where only the considered source-destination pair is activating the cooperative transmission.

1.3 Motivation and Research Contributions

Due to the interaction among concurrent transmissions, each source-destination pair should make a cooperation decision from a perspective of overall network performance, so as to prevent cooperation that benefits only its own link but reduces overall network performance. To facilitate the cooperation decision making, it is necessary to develop a theoretical performance analysis framework to evaluate the performance dependency upon system parameters. As interference is the main performance-limiting factor, accurate characterization of interference is a key step towards evaluating the network performance. Specifically, the interference incurred by a cooperative link is different from the interference incurred by a direct link, as an additional relay or relays take part in the transmission of one packet. In other words, the cooperative links redistribute the interference over the network coverage area due to relay transmissions. Without taking into account the interference redistribution incurred by concurrent cooperative transmissions, the network-wide performance of cooperative communication cannot be characterized.

Relay selection plays a pivotal role in determining the performance of a cooperative transmission scheme. Selecting the best relay among randomly positioned relays while taking into account the spatial frequency reuse is challenging, as both random relay locations and time-varying channel fading should be considered. Furthermore, due to the distributed network operation and random relay locations, the cooperative transmission should be activated by each source-destination pair when necessary and beneficial. A comprehensive study of the impact of cooperative communication on the overall network performance is important for the design of efficient cooperative transmission schemes.

The main objective of this research is to evaluate the effectiveness of cooperative communication in a wireless ad hoc network from a perspective of overall network performance, rather than the performance of a single source-destination pair. This research provides a

step towards better understanding of the benefits and limitations of cooperative communication. The main contributions of this thesis are summarized as follows.

• Under the protocol interference model, we develop a theoretical performance analysis framework for cooperative communication in a wireless ad hoc network with randomly positioned single-hop source-destination pairs and relays. The effectiveness of cooperative communication is evaluated from a perspective of overall network performance, through constructing a diamond-shaped constrained relay selection region to investigate the performance tradeoff achieved by spatial diversity gain and by spatial frequency reuse gain;

• We propose a single-relay opportunistic cooperation strategy to activate the cooperative transmission by each source-destination pair when necessary and beneficial from a perspective of overall network performance, leading to a mixture of direct and cooperative transmissions. Under the physical interference model, we characterize the spatial and temporal correlation of interference power, and derive the outage probability of the proposed opportunistic cooperation strategy in terms of important network and protocol parameters;

• We investigate the impact of traffic unsaturation on the performance of an asynchronous cooperative transmission scheme. To evaluate the network performance, we characterize the interference power by deriving the stationary interferer density and identifying the interference correlation in two consecutive time-slots, based on queueing theory and stochastic geometry. The uniqueness of the stationary interferer density is proved.

1.4 Outline of the Thesis

The rest of the thesis is organized as follows. The system model under consideration is described in Chapter 2. Chapter 3 constructs a diamond-shaped relay selection region to study the tradeoff between the single-link cooperation gain and network-wide reduced spatial frequency reuse due to relay transmissions in a wireless ad hoc network [48, 49]. From a perspective of overall network performance, cooperation is beneficial only when the achieved single-link cooperation gain can compensate for the reduction in network-wide spatial frequency reuse. Chapter 4 proposes an opportunistic cooperation strategy in a wireless ad hoc network, where each source-destination pair activates the cooperative transmission only when the number of potential relays is not smaller than a cooperation threshold, leading to mixture of direct and cooperative transmissions as well as the spatial and temporal correlation of interference power [50]. Chapter 5 studies the performance of cooperative communication in a wireless ad hoc network with unsaturated traffic [51]. We

derive the outage probability and average packet delay of a typical source-destination pair as a function of important network and protocol parameters. Finally, Chapter 6 concludes this thesis and identifies some further research topics.

Chapter 2

System Model

2.1 Network Topology

Consider a wireless ad hoc network with nodes independently and randomly distributed in a two-dimensional (2D) coverage area. Data packets are transmitted from source nodes over a single frequency channel with bandwidth B in Hz. Time is partitioned to slots of a constant duration. We model two different cases regarding the spatial distribution of source nodes. In Chapter 3, the spatial locations of source nodes at any time-slot are specified by a binomial point process (BPP). Specifically, N source nodes are independently and uniformly distributed within the network coverage area. On the other hand, in Chapters 4 and 5, the spatial locations of source nodes at time-slot $t \in \mathbb{N}^+$ form a homogeneous PPP $\Phi_S(t) = \{s_1(t), s_2(t), \cdots\} \subset \mathbb{R}^2$ with density λ_S (average number of nodes per unit area). To explicitly illustrate the impact of the distance between the source and destination nodes on the effectiveness of cooperative communication, each source node, S_i, has an associated destination node, D_i, located at a fixed distance L_D away with a random direction, i.e., $d_i(t) \in \mathbb{R}^2$, $i = 1, 2, \cdots$. The destination nodes are not part of PPP $\Phi_S(t)$. Extension to the scenario with random link length is straightforward [52].

All other nodes, without their own packets to transmit and receive, are denoted as relays (e.g., R_i), and they are always willing to forward packets from the source nodes. The spatial locations of relays at time-slot t are modeled by another homogeneous PPP, $\Phi_R(t) = \{r_1(t), r_2(t), \cdots\} \subset \mathbb{R}^2$ with density λ_R. The capital letters (e.g., S_i, R_i, and D_i) and lowercase letters (e.g., $s_i(t)$, $r_i(t)$, and $d_i(t)$) represent the nodes and their locations at time-slot t, respectively. We add a typical source-destination pair (i.e., $S_0 - D_0$) in the network, which does not affect the statistics of the PPP because of the stationary property.

We focus on analyzing the performance of the typical source-destination pair, which holds for any source-destination pair in the network according to the Slivnyak's theorem [53].

2.2 Propagation Channel

All source and relay nodes transmit with the same power, denoted as P_t. The channel between any pair of nodes is characterized by both small-scale Rayleigh fading and large-scale path loss. All the distance-independent fading coefficients are independent and identically distributed (i.i.d.) random variables with unit mean. As in [41], a general path loss model is given by

$$g\left(x(t)-y(t)\right)=\frac{1}{\epsilon+d_{XY}^{\alpha}(t)},\quad \epsilon\geq 0 \tag{2.1}$$

where ϵ is a parameter to model the singular (i.e., $\epsilon=0$) and non-singular (i.e., $\epsilon>0$) path loss models, $d_{XY}(t)=\|x(t)-y(t)\|$ denotes the Euclidean distance between two points in the 2D plane with coordinates $x(t)$ and $y(t)$, and α denotes the path loss exponent.

As Chapters 3 and 4 focus on the average network performance achieved in one time-slot, the time-index is omitted in these two chapters for simplicity of notation. For instance, $\Phi_S(t)$, $\Phi_R(t)$, $s_i(t)$, $r_i(t)$, and $d_{XY}(t)$ are denoted as Φ_S, Φ_R, s_i, r_i, and d_{XY}, respectively.

2.3 Interference Model

The protocol interference model and physical interference model are two widely-used models. In Chapter 3, we study the impact of interference on spatial frequency reuse under the protocol interference model. The interference range defines a region within which the transmission from an interferer interrupts a packet reception [54]. The impact of interference is binary with respect to the interference range. The interference from an interferer within the interference range of a receiver is intolerable, while the interference from an interferer outside the interference range is negligible. Thus, a packet transmission from source node S_0 to destination node D_0 is successful only if the following conditions are satisfied: $\psi_{S_0D_0}\geq\beta_\nu$ and $d_{S_kD_0}>\mathcal{R}_{DT}^{I}$, for every S_k, $k>0$, transmitting concurrently, where $\psi_{S_0D_0}$ denotes the SNR observed by destination node D_0 when receiving a packet from source node S_0, β_ν denotes the required reception threshold for the packets transmitted at rate ν (in bit/s), and $\mathcal{R}_{DT}^{I}$ denotes the interference range for the direct transmission.

Define the required reception threshold $\beta_\nu \equiv 2^{\nu/B} - 1$ so that $\nu = B \cdot \log_2(1 + \beta_\nu)$, based on Shannon's formula. In a two-hop cooperative transmission, rate 2ν is utilized in both hops to achieve the target rate ν between the source and destination nodes. The required reception threshold and interference range for the cooperative transmission are denoted as $\beta_{2\nu}$ and $\mathcal{R}_{CT}^{I}$, respectively.

Under the physical interference model (in Chapters 4 and 5), power levels of the signals from all unintended active transmitters are added and the sum is considered as interference power, leading to a possible transmission failure at a destination node. The noise power is negligible compared to the interference power; hence, we consider an interference-limited wireless network. Thus, a packet transmitted from source node S_0 is successfully received by destination node D_0 if the instantaneous SIR is not smaller than the required reception threshold.

2.4 Packet Transmission

We consider both saturated (in Chapters 3 and 4) and unsaturated (in Chapter 5) traffic scenarios. Each source node has a buffer of infinite length. With saturated traffic, each source node always has a data packet for transmission. In the unsaturated traffic scenario, the initial queue length is independently and randomly chosen, and new data packets arrive at each source node according to a Poisson process with rate Λ_T (average number of packets per time-slot). All data packets are served in a first-in first-out (FIFO) manner.

All source nodes are synchronized in time and the concurrent transmissions are enabled across different spatial locations. Before a packet transmission, the coordination signaling among a source node, its intended destination node, and neighboring relays is required [55]. The protocol overhead incurred by coordination signaling and relay selection is not considered. Each source node transmits to its intended destination node via either one-hop direct transmission or two-hop cooperative transmission. For both direct and cooperative transmissions, all data packets have equal length and each data packet is transmitted in exactly one time-slot. Each node has a single omni-directional antenna and operates in half-duplex mode.

Chapter 3

Throughput Analysis of Cooperative Communication with Frequency Reuse

This chapter investigates the network throughput achieved by both spatial diversity and spatial frequency reuse in a wireless ad hoc network with randomly positioned single-hop source-destination pairs and relays under the protocol interference model. Compared to conventional direct transmissions, cooperative transmissions can enhance single-link transmission reliability, but reduce network-wide spatial frequency reuse due to relay transmissions. To study the tradeoff between these two competing effects, we construct a geographically constrained region for relay selection. The network throughput, defined as the product of the success probability of each link and the expected number of concurrent transmissions, is derived as a function of the total number of links, relay density, size of relay selection region, and link length. The performance analysis is carried out for both selection combining (SC) and maximal ratio combining (MRC) at the destination receiver. Extensive simulations are conducted to validate the performance analysis.

3.1 Motivation

In a wireless ad hoc network, two types of gains can be achieved by utilizing spatial resources, namely spatial diversity gain and spatial frequency reuse gain. Existing works mainly focus on how to exploit either maximal spatial diversity gain or maximal spatial

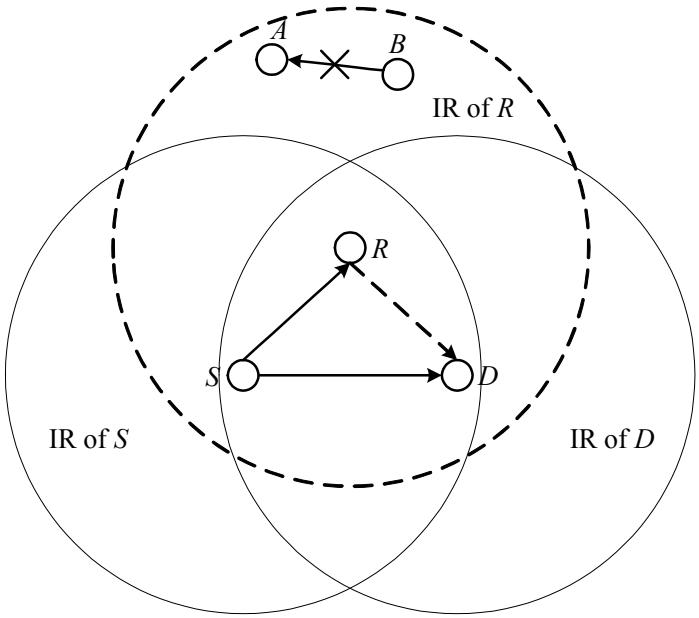

Figure 3.1: An illustration of the IR enlargement due to relay transmission under the protocol interference model.

frequency reuse gain [56, 57]. Maximizing one of the gains, however, does not necessarily maximize the other. Take a network scenario with two source-destination pairs, as shown in Figure 3.1, as an example. Under the protocol interference model, while relay R can enhance the transmission reliability of the concerned link $S - D$ by achieving a spatial diversity gain, it can also enlarge the interference region (IR) of the concerned link to block the transmission of its neighboring link $B - A$. Generally, cooperation occupies more spatial resources to achieve the spatial diversity gain, at a potential cost of reducing the spatial frequency reuse gain due to relay transmissions. There exists a tradeoff between the single-link cooperation gain and network-wide reduced spatial frequency reuse, which implies that a locally beneficial cooperation decision is not guaranteed to be network-wide beneficial. As a result, the effectiveness of cooperation should be evaluated from a perspective of overall network performance, rather than the performance of a single source-destination pair.

A study on cooperative communication in a wireless ad hoc network is presented in [58], which employs a unit disk graph model to analyze the penalty of the enlarged IR. This method suffers from three limitations: First, the link density is not considered, which is an influential factor for the reduction in network-wide spatial frequency reuse; Second,

the unit disk graph model cannot accurately characterize the IRs for both direct and cooperative links; Third, relay selection is not considered, which determines the single-link cooperation gain. It is desirable to fully understand the benefits and limitations of cooperative communication. In this chapter, we characterize both single-link cooperation gain and network-wide reduced spatial frequency reuse in a wireless ad hoc network, while taking into account the spatial distributions of sources and relays, constrained relay selection region, and time-varying channel fading. We evaluate the effectiveness of cooperative communication from a perspective of overall network performance, in terms of the total number of links, relay density, size of relay selection region, and link length.

3.2 Cooperative Transmission and Relay Selection

A single relay is considered for the cooperative transmission; hence, each source node and its best relay share one time-slot in transmitting the same packet. The DF scheme is adopted by the best relay. A time-slot is partitioned equally to two sub-time-slots [59]. Each source node transmits a packet at rate 2ν in the first sub-time-slot. Due to the broadcast nature of wireless communications, whether or not the intended destination node and neighboring relays can successfully receive the packet depends on both instantaneous channel fading and path loss. A CSI-based relay selection strategy is employed to select the best relay, which forwards the packet to the intended destination node at rate 2ν in the second sub-time-slot. Finally, the destination node decodes the packet using either SC or MRC. In SC, the destination node selects only one link from the direct and forward links for packet decoding. On the other hand, in MRC, the destination node combines the signals from both the direct and forward links for packet decoding. Hence, two cooperative transmission schemes are considered, that is CSI-based relay selection with SC and MRC, respectively. Studying both SC and MRC can provide insights for the tradeoff between performance and complexity.

At the link layer, as each transmission requires handshaking, each node of one link becomes both a transmitter and receiver during the transmission of one packet. The IR of a direct (or cooperative) link is the combination of the IRs of the source and destination (and relay) nodes. As more nodes take part in the transmission of one packet, a cooperative link occupies more spatial resources, which reduces the spatial frequency reuse. As shown in Figure 3.1, the size of the IR occupied by a cooperative link is determined by the relay location. Because all relays are randomly distributed across the network, the size of the IR of each cooperative link is random and it may be large enough to significantly reduce the spatial frequency reuse. To restrict the size of the IR occupied by each cooperative link, a

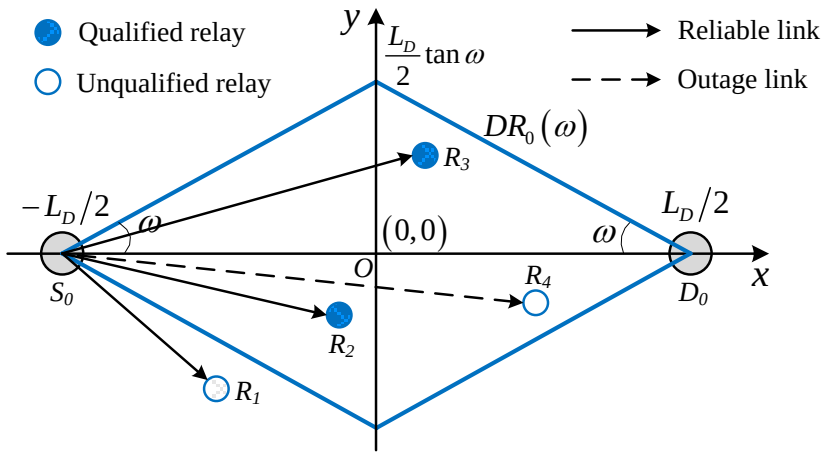

Figure 3.2: A diamond-shaped constrained relay selection region under the rectangular coordinate system. Only the relays within the constrained relay selection region (e.g., R_2, R_3, and R_4) and successfully receive the packet from the source node (e.g., R_2 and R_3) are qualified relays (e.g., R_2 and R_3).

simple way is to construct a constrained geographical region for relay selection. The relays within the relay selection region are called potential relays and only the potential relays can contend to be the best relay. In order to select the best relay and in turn achieve full-order spatial diversity, the packet collision at each potential relay should be avoided and the signaling among the potential relays for relay selection should be collision-free. As a result, all potential relays should be protected from interference. The size of the IR of a cooperative link is determined by the relative location of the furthermost potential relay, which can be controlled by adjusting the size of the relay selection region. Such a relay selection region establishes a connection between single-link cooperation gain and network-wide reduced spatial frequency reuse. A larger relay selection region leads to a higher cooperation gain by incorporating more potential relays, at the cost of reducing the network-wide spatial frequency reuse.

We consider a diamond-shaped relay selection region for each cooperative link, as it covers the best relay locations by introducing a small enlarged IR and only has one parameter. As shown in Figure 3.2, a source node and its intended destination node locate at two endpoints of one diagonal, i.e., $(-L_D/2, 0)$ and $(L_D/2, 0)$, respectively. Such a diamond region (DR) is characterized by an angle ω, which determines the size of the constrained relay selection region. The potential relays that successfully receive the packet from source node S_0 in the first sub-time-slot are referred to as qualified relays, which form a relay set,

denoted as Ω_0. Mathematically, relay set Ω_0 can be expressed as

$$\Omega_0 = \{R_i : r_i \in \Phi_R \cap DR_0(\omega), \psi_{S_0R_i} \geq \beta_{2\nu}\} \tag{3.1}$$

where $DR_0(\omega)$ denotes the constrained relay selection region with angle ω for the typical source-destination pair, $\psi_{S_0R_i} = \frac{P_t \cdot H_{S_0R_i} \cdot d^{-\alpha}_{S_0R_i}}{W}$ denotes the SNR at relay R_i when receiving a packet from source node S_0, $H_{S_0R_i}$ denotes the random distance-independent fading coefficient between source node S_0 and relay R_i, W denotes the noise power, and $\epsilon = 0$ models the singular path loss model.

The fading coefficients and node locations remain invariant during one time-slot. We assume that each qualified relay knows its qualification status and has instantaneous CSI between itself and its intended destination node. A back-off scheme can be utilized to select the best relay in a distributed manner, which requires only local CSI [60]. When relay set Ω_0 is not empty, a qualified relay with the best channel to the destination node obtains the shortest back-off duration and contends to be the best relay first. Other qualified relays quit contention as soon as they receive the signaling from the best relay, denoted as R_b^0, which is given by

$$R_b^0 = \arg \max_{R_i \in \Omega_0} \{H_{R_iD_0} \cdot d^{-\alpha}_{R_iD_0}\}. \tag{3.2}$$

In addition to spatial diversity, spatial frequency reuse is another way to enhance spectrum efficiency. As all links are randomly distributed across the network coverage area and interact with each other, the optimal scheduling problem is shown to be NP-hard in [61]. For simplicity, a randomized scheduling scheme proposed in [62] is employed to activate non-interfering links for concurrent transmissions. The main idea of the randomized scheduling scheme is to check all links in a random order and remove a new link if it interferes with existing ones. The remaining links can be activated concurrently without interrupting each other. Two links interfere with each other when any node of one link locates within the interference range of any node of the other link.

The network throughput, defined as the product of the success probability of each link and the expected number of concurrent transmissions, measures the expected number of concurrent successful transmissions within the network coverage area, given the total number of links and relay density. The network throughput for the direct and cooperative transmissions can be, respectively, expressed as

$$\begin{aligned} T_{DT} &= (1 - q_{DT}) \cdot N_{DT} \\ T_{CT} &= (1 - q_{CT}) \cdot N_{CT} \end{aligned} \tag{3.3}$$

where q_{DT} and q_{CT} represent the outage probabilities of direct and cooperative transmissions respectively, N_{DT} and N_{CT} represent the expected numbers of concurrent direct and cooperative transmissions respectively. Due to the enlarged IR, N_{CT} is not larger than N_{DT}.

The expected number of concurrent direct transmissions is affected by the total number of links (i.e., N), while the expected number of concurrent cooperative transmissions is further affected by the size of relay selection region (i.e., ω) and relay density (i.e., λ_R). The values of parameters ω and λ_R can be set to balance the tradeoff between spatial diversity and spatial frequency reuse. Specifically, with an increase of ω or λ_R, the single-link cooperation gain is enhanced as more potential relays are available and the probability of selecting a reliable relay increases. On the other hand, with an increase of ω or λ_R, the IR of a cooperative link is enlarged and the network-wide spatial frequency reuse is reduced, which will be discussed in Section 3.4.

From a perspective of overall network performance, the network throughput gain in using the cooperative transmission over the direct transmission can be expressed as

$$G = \frac{(1 - q_{CT}) \cdot N_{CT}}{(1 - q_{DT}) \cdot N_{DT}} = G_S \cdot L_N \tag{3.4}$$

where $G_S = \frac{1-q_{CT}}{1-q_{DT}}$ represents the single-link cooperation gain and $L_N = \frac{N_{CT}}{N_{DT}}$ represents the network-wide reduced spatial frequency reuse.

According to (3.4), cooperation in a wireless ad hoc network is beneficial only when the achieved single-link cooperation gain can compensate for the reduction in network-wide spatial frequency reuse, that is, $G_S \cdot L_N > 1$. To evaluate the effectiveness of cooperative communication, we derive the single-link cooperation gain and network-wide reduced spatial frequency reuse in Sections 3.3 and 3.4, respectively.

3.3 Single-link Cooperation Gain

In this section, we characterize the single-link cooperation gain by comparing the success probabilities of cooperative and direct transmissions. Based on stochastic geometry, we derive the outage probability of the CSI-based relay selection strategy for both SC and MRC, while taking into account the spatial distribution of relays, constrained relay selection region, and time-varying channel fading.

3.3.1 CSI-based Relay Selection with SC

With SC at the destination receiver, an outage event occurs when both the direct and forward links cannot support the required transmission rate. Specifically, as a source node transmits a packet at rate 2ν in the first sub-time-slot, the direct link fails when the SNR at the destination node is smaller than $\beta_{2\nu}$. On the other hand, the forward link fails when one of the following events occurs: 1) There are no potential relays within $DR_0(\omega)$; 2) Event $\mathcal{E}_{11}$ - there are no qualified relays when there exists at least one potential relay; 3) Event $\mathcal{E}_{12}$ - destination node D_0 fails to decode the packet from the best relay in the second sub-time-slot when relay set Ω_0 is not empty. Hence, the outage probability, denoted as q_{CT}^{SC}, is given by

$$q_{CT}^{SC} = \mathbb{P}\left(\psi_{S_0D_0} < \beta_{2\nu}\right) \cdot \left[\mathbb{P}\left(K_0 = 0\right) + \sum_{k=1}^{\infty} \mathbb{P}\left(K_0 = k\right) \cdot \mathbb{P}\left(\mathcal{E}_{11} \cup \mathcal{E}_{12} \,|K_0 = k\right)\right] \tag{3.5}$$

where K_0 represents the number of potential relays for the typical source-destination pair, and Events $\mathcal{E}_{11}$ and $\mathcal{E}_{12}$ can be expressed as

$$\begin{aligned} \mathcal{E}_{11} &= \{\Omega_0 = \emptyset, K_0 > 0\} \\ \mathcal{E}_{12} &= \left\{\Omega_0 \neq \emptyset, \psi_{R_b^0 D_0} < \beta_{2\nu}\right\}. \end{aligned} \tag{3.6}$$

The outage probability can be evaluated in terms of the relay density, size of relay selection region, and link length, as stated in the following proposition.

Proposition 1. *Given a diamond-shaped relay selection region $DR_0(\omega)$, as shown in Figure 3.2, the outage probability of the CSI-based relay selection strategy with SC at the destination receiver, given by (3.5), can be written as*

$$\begin{aligned} q_{CT}^{SC} &= \left[1 - \exp\left(-ML_D^{\alpha}\right)\right] \\ &\quad \times \exp\left[-2\lambda_R \int_0^{\frac{L_D}{2}\tan\omega} \int_{\frac{y}{\tan\omega}-\frac{L_D}{2}}^{\frac{L_D}{2}-\frac{y}{\tan\omega}} \exp\left(-M\left(d_{S_0R}^{\alpha} + d_{RD_0}^{\alpha}\right)\right) \mathrm{d}x\mathrm{d}y\right] \end{aligned} \tag{3.7}$$

where $M = \frac{\beta_{2\nu}W}{P_t}$, $d_{S_0R} = \sqrt{(x + \frac{L_D}{2})^2 + y^2}$, and $d_{RD_0} = \sqrt{(x - \frac{L_D}{2})^2 + y^2}$.

The outage probability in (3.7) decreases as the relay density increases, and it can be calculated numerically in MAPLE. For the special case of $\alpha = 2$, the integration can be

replaced by the series summation in the following corollary, which can be calculated more efficiently [63].

Corollary 1. *For the special case of $\alpha = 2$, the outage probability given in (3.7) can be simplified as*

$$\begin{aligned} q_{CT}^{SC} &= \left[1 - \exp\left(-ML_D^{\alpha}\right)\right] \\ &\quad \times \exp\left[-\frac{\sqrt{2\pi}}{\sqrt{M}}\lambda_R \int_0^{\frac{L_D}{2}\tan\omega} \exp\left(-2My^2 - \frac{ML_D^2}{2}\right) \operatorname{erf}\left(\sqrt{2M}\left(\frac{L_D}{2} - y\right)\right) \mathrm{d}y\right] \\ &= \left[1 - \exp\left(-ML_D^{\alpha}\right)\right] \\ &\quad \times \exp\left[-\sum_{k=0}^{\infty} \frac{\lambda_R 2^{2k+2} M^k}{(2k+1)!! \exp\left(ML_D^2\right)} \mathcal{B}\left(4t^2 - 2L_D t, \frac{L_D}{2}(1 - \tan\omega), \frac{L_D}{2}\right)\right] \end{aligned} \tag{3.8}$$

where $\operatorname{erf}(x) = \frac{2}{\sqrt{\pi}} \int_0^x e^{-t^2} \mathrm{d}t$ *is the error function and*

$$\mathcal{B}(h(t), m, n) = \int_m^n \exp\left[-Mh\left(t\right)\right] t^{2k+1} \mathrm{d}t. \tag{3.9}$$

3.3.2 CSI-based Relay Selection with MRC

With MRC at the destination receiver, in the following analysis, the source node is treated equivalently as a qualified relay and it transmits the packet in the second sub-time-slot only when it is selected as the best relay, i.e., all qualified relays keep silent. Let $R_{b'}^0$ denote the best relay in this cooperation scheme. The instantaneous SNR of the channel between $R_{b'}^0$ and D_0 is given by

$$\psi_{R_{b'}^0 D_0} = \max\left\{\psi_{R_b^0 D_0}, \psi_{S_0 D_0}\right\}. \tag{3.10}$$

An outage event occurs when the destination node fails to decode the packet after combining the signals transmitted by the source node and the best relay in the first and second sub-time-slots, respectively. Hence, the outage probability, denoted as q_{CT}^{MRC}, is given by

$$q_{CT}^{MRC} = \mathbb{P}\left(\psi_{S_0 D_0} + \psi_{R_{b'}^0 D_0} < \beta_{2\nu}\right). \tag{3.11}$$

Proposition 2. *Given a diamond-shaped relay selection region $DR_0(\omega)$, as shown in Figure 3.2, the outage probability of the CSI-based relay selection strategy with MRC at the destination receiver, given by (3.11), can be written as*

$$q_{CT}^{MRC} = \left[1 - \exp\left(-\frac{M}{2}L_D^{\alpha}\right)\right] \exp\left(-2\lambda_R \int_0^{\frac{L_D}{2}\tan\omega} \int_{\frac{y}{\tan\omega}-\frac{L_D}{2}}^{\frac{L_D}{2}-\frac{y}{\tan\omega}} \mathcal{I}(x,y)\mathrm{d}x\mathrm{d}y\right) \quad (3.12)$$

where

$$\mathcal{I}(x,y) = \frac{-\exp\left[-M\left(d_{S_0R}^{\alpha} + d_{RD_0}^{\alpha}\right)\right] + \exp\left[-\frac{M}{2}\left(L_D^{\alpha} + d_{RD_0}^{\alpha}\right) - Md_{S_0R}^{\alpha}\right]}{\left[1 - \exp\left(-\frac{M}{2}L_D^{\alpha}\right)\right]\left[(d_{RD_0}/L_D)^{\alpha} - 1\right]}. \quad (3.13)$$

Similarly, the outage probability in (3.12) decreases as the relay density increases, and it can be numerically evaluated in MAPLE.

In the direct transmission, a source node utilizes the whole time-slot to transmit a packet at rate ν. An outage event occurs when the SNR at the destination node is smaller than β_ν. Hence, the outage probability for the direct transmission is given by $q_{DT} = 1 - \exp\left(-\frac{\beta_\nu W}{P_t}L_D^{\alpha}\right)$. Finally, by comparing the success probabilities of cooperative and direct transmissions, single-link cooperation gain G_S can be obtained.

3.4 Network-wide Reduced Spatial Frequency Reuse

In this section, we characterize the reduction in network-wide spatial frequency reuse by comparing the expected numbers of concurrent cooperative and direct transmissions that can be accommodated within the network coverage area. Taking into account the spatial distributions of both source-destination pairs and relays, we calculate the expected numbers of concurrent direct and cooperative transmissions based on a randomized scheduling scheme [62].

Let $P(k,n)$ denote the probability that k links can be scheduled for concurrent transmissions after checking the first n links. Denote Q as the interference-free probability between any two links. After checking the first n links, there are k links that can be scheduled concurrently if 1) $(k-1)$ links are scheduled after checking the first $(n-1)$ links, and link n does not interfere with the scheduled $(k-1)$ links; 2) k links are scheduled after checking the first $(n-1)$ links, and link n interferes with at least one of the scheduled k

links. Hence, we have

$$P(k,n) = P(k-1,n-1)\cdot Q^{k-1} + P(k,n-1)\cdot(1-Q^k). \tag{3.14}$$

With the initial values $P(1,1)=1$, $P(1,2)=1-Q$, and $P(2,2)=Q$, we can iteratively calculate $P(k,N)$ for all $k \leq N$. Hence, the expected number of concurrent transmissions can be calculated by $N_E = \sum_{k=1}^{N} k \cdot P(k,N)$. To calculate the expected number of concurrent transmissions, the interference-free probability between any two direct (cooperative) links should be derived. The interference-free probability between two direct links depends on the distance between the source and destination nodes, while the interference-free probability between two cooperative links is further affected by the size of relay selection region and relay density.

As the IR of a direct (cooperative) link is the combination of the IRs of the source and destination (and relays), it can be approximated as an elliptical region [48]. We calculate the interference-free probability between any two direct (cooperative) links in the following two subsections.

3.4.1 Direct Link

As shown in Figure 3.3, we approximate the IR of a direct link by an elliptical region, and refer to it as node interference region (NIR). Any node of other active links (e.g., $L_j, j \neq i$) should locate outside NIR_i to avoid interrupting link L_i. However, to guarantee both S_j and D_j locate outside NIR_i is not trivial, as the locations of S_j and D_j are not independent and they are placed L_D apart. For simplicity, we introduce a link interference region (LIR), which is also an elliptical region but larger than the NIR, to capture the interference relationship among different links. Specifically, LIR_i is an elliptical region centered at the center of link L_i, and the lengths of the semi-major axis and semi-minor axis are given by

$$\begin{aligned} D_{DT}^{L} &= \mathcal{R}_{DT}^{I} + L_D \\ D_{DT}^{S} &= \mathcal{R}_{DT}^{I} + \frac{L_D}{2}. \end{aligned} \tag{3.15}$$

As illustrated in Figure 3.3, the LIR radii are increased by $L_D/2$ from those of the NIR. Thus, for any two direct links (e.g., L_i and L_j), if the center of link L_j is outside LIR_i, both S_j and D_j are guaranteed to locate outside NIR_i, which implies that two links are

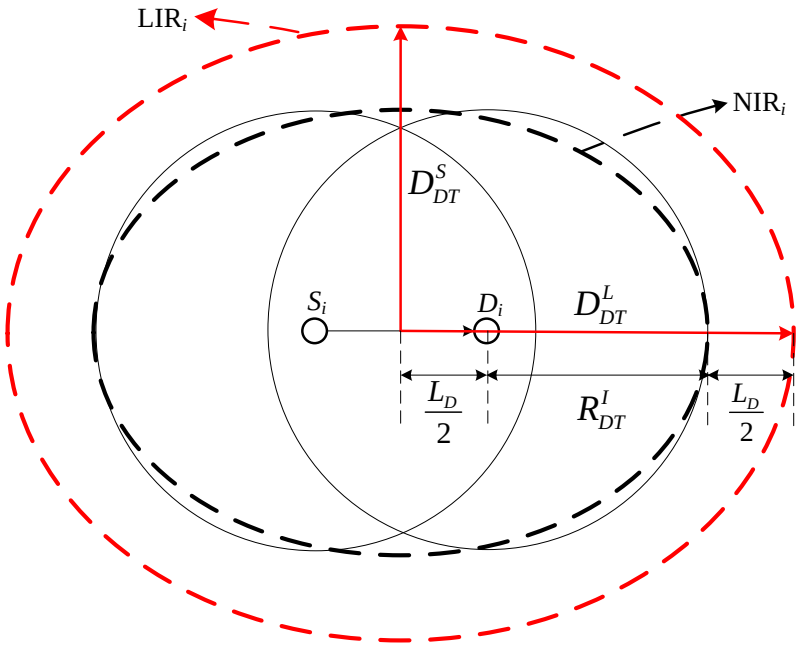

Figure 3.3: Approximated IR of a direct link.

interference-free. Note that the reverse condition, the center of link L_i locating outside LIR$_j$, is not required, as the interference relationship between the nodes is reciprocal.

The elliptical LIR area of a direct link is given by $\mathcal{A}_{DT} = \pi D^L_{DT} D^S_{DT}$. Because of the uniform distribution of nodes, the interference-free probability between any two direct links can be calculated by $Q_{DT} = 1 - \frac{\mathcal{A}_{DT}}{\mathcal{A}_N}$, where $\mathcal{A}_N$ is the network coverage area.

3.4.2 Cooperative Link

As discussed in Section 3.2, all potential relays should be protected from interference and the IR of a cooperative link is determined by the relative location of the furthermost potential relay in each side of the link. Due to the symmetry, we take the upper half of the relay selection region, as shown in Figure 3.4, as an example. The furthermost potential relay refers to the potential relay that has the largest Y-coordinate. Denote V_1 as the Y-coordinate of the furthermost potential relay. As the potential relays are randomly distributed within $DR_0(\omega)$, V_1 is a random variable, which takes value in $\left[0, \frac{L_D}{2}\tan\omega\right]$. To calculate the average size of the IR occupied by a cooperative link, we calculate the expected value of V_1 as follows.

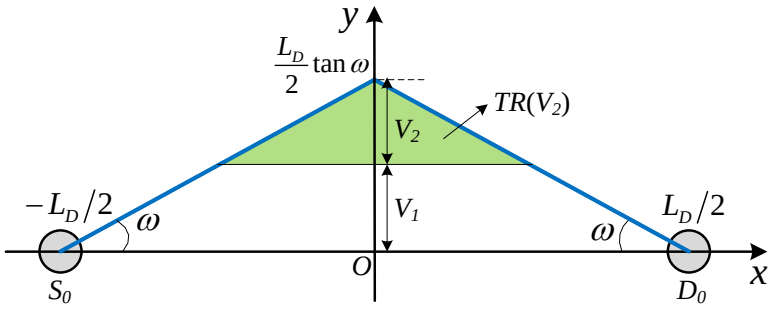

Figure 3.4: The upper half of the relay selection region.

Proposition 3. *The expected value of the Y-coordinate of the furthermost potential relay in the upper half of the relay selection region,* $\mathbb{E}[V_1]$*, is given by*

$$\mathbb{E}\left[V_1\right] = \frac{L_D}{2}\tan\omega - \sqrt{\frac{\pi\tan\omega}{4\lambda_R}}\,\mathrm{erf}\left(\frac{L_D}{2}\sqrt{\lambda_R\tan\omega}\right). \tag{3.16}$$

From (3.16), $\mathbb{E}[V_1]$ increases with λ_R and ω. This is because, with an increase of λ_R and ω, the probability of having a faraway potential relay increases. Let R_{F1} and R_{F2} denote the furthermost potential relays at both sides, at $(0, \mathbb{E}(V_1))$ and $(0, -\mathbb{E}(V_1))$ on average, respectively. The IR of a cooperative link is calculated according to the average locations of the furthermost potential relays.

The IR of a cooperative link is also approximated as an elliptical region, referred to as cooperative node interference region (CNIR). Similarly, as shown in Figure 3.5, we define a cooperative link interference region (CLIR), which is centered at the center of link L_i and the lengths of the semi-major axis and semi-minor axis are given by

$$\begin{aligned} D_{CT}^{L} &= \mathcal{R}_{CT}^{I} + L_D \\ D_{CT}^{S} &= \mathcal{R}_{CT}^{I} + \frac{L_D}{2} + \mathbb{E}(V_1). \end{aligned} \tag{3.17}$$

For any two cooperative links (e.g., L_i and L_j), if the center of CLIR_j locates outside CLIR_i, both L_i and L_j can transmit concurrently without interrupting each other. The elliptical CLIR area can be calculated by $\mathcal{A}_{CT} = \pi D_{CT}^{L} D_{CT}^{S}$. Accordingly, the interference-free probability between any two cooperative links is given by $Q_{CT} = 1 - \frac{\mathcal{A}_{CT}}{\mathcal{A}_N}$.

The calculation of the interference-free probability between any two links is slightly

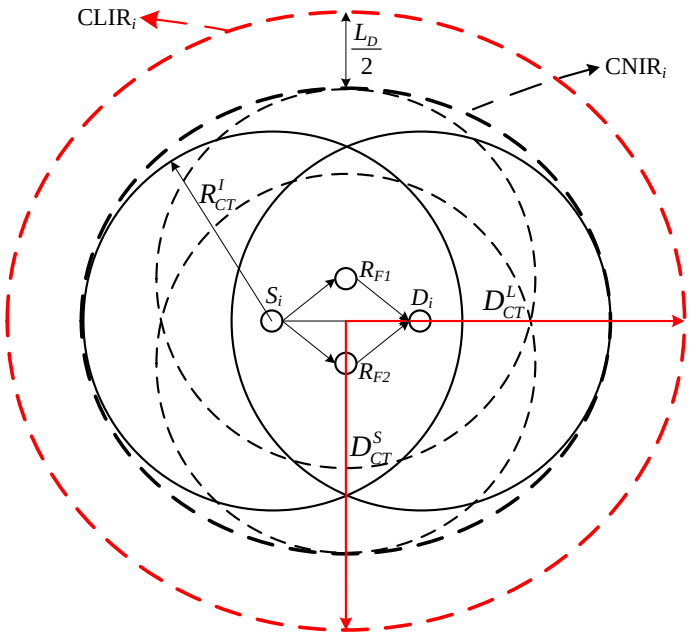

Figure 3.5: Approximated IR of a cooperative link.

conservative, as some links may be blocked although they do not actually cause collisions. According to the simulation results in Section 3.5, the results calculated by this method is rather accurate and the computation complexity is quite low. The expected numbers of concurrent direct and cooperative transmissions, N_{DT} and N_{CT}, can be calculated by substituting Q_{DT} and Q_{CT} into (3.14). By comparing these two numbers, the network-wide reduced spatial frequency reuse L_N can be obtained. Finally, we can derive the network throughput and network throughput gain by substituting the corresponding values into (3.3) and (3.4), respectively.

3.5 Numerical Results

This section presents analytical (A) and simulation (S) results for both direct and cooperative transmissions in a wireless ad hoc network. In the simulation, a circular network coverage area with radius 2000 m is considered. Based on [64] and [65], the interference ranges of direct and cooperative transmissions, $\mathcal{R}^I_{DT}$ and $\mathcal{R}^I_{CT}$, are set to be 60 m and 70 m, respectively. The transmission rate (ν) and channel bandwidth (B) are normalized to

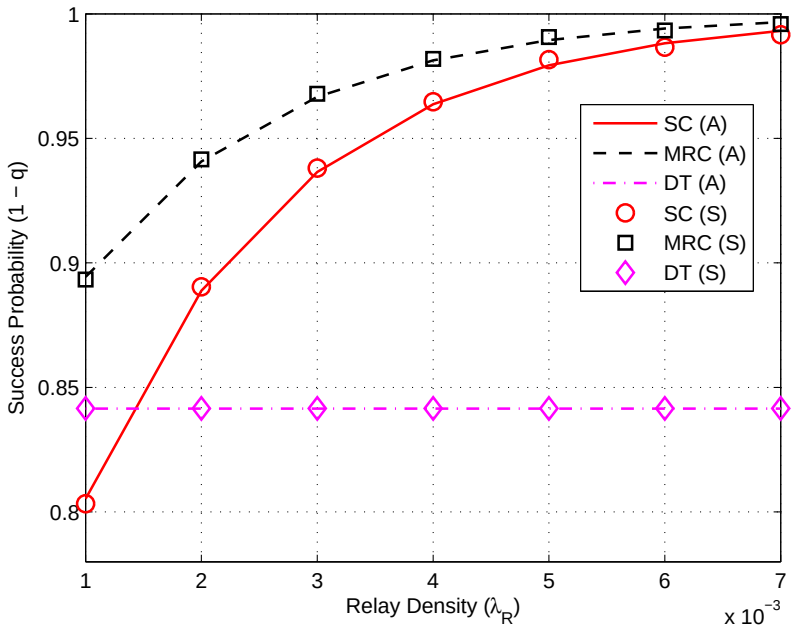

Figure 3.6: Success probability versus relay density (in nodes/m^2) when $\omega = \pi/6$ and $L_D = 50$ m.

be 1 Mbit/s and 1 MHz, respectively. The reception threshold of direct transmissions (β_ν) is set to be $\sqrt{2}-1$, which is calculated based on Shannon's formula and the normalized reception threshold of cooperative transmissions (i.e., $\beta_{2\nu} = 1$). In addition, we set $P_t = 0.06$ mW, $W = -50$ dBm, and $\alpha = 2$. The simulation results are obtained by averaging 10^5 realizations of the random network topology.

3.5.1 Transmission Success Probability and Single-Link Cooperation Gain

In this subsection, we study the impact of relay density λ_R, angle of relay selection region ω, and link length L_D on the transmission success probability and single-link cooperation gain.

Figure 3.6 shows the success probabilities of direct transmission (DT) and cooperative transmission (SC and MRC) versus the relay density with parameters $\omega = \pi/6$ and $L_D = 50$ m, where the analytical results are obtained based on (3.7) and (3.12). When the relay

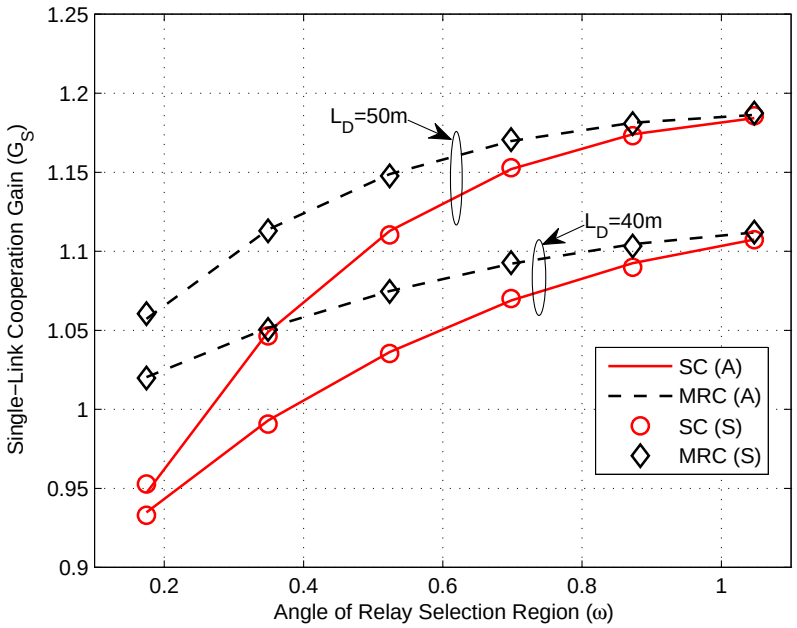

Figure 3.7: Single-link cooperation gain versus angle of relay selection region for $L_D = 50$ m and 40 m when $\lambda_R = 0.003$ nodes/m^2.

density is low, the cooperative transmission with an SC receiver performs worse than the direct transmission, because the probability of having a reliable relay is low and the cooperative transmission requires a higher reception threshold for the SNR. It is observed that the success probabilities of both cooperative transmission schemes increase with the relay density, while that of the direct transmission does not change. This is due to the fact that, with an increase of λ_R, more potential relays are available for relay selection, which results in a higher probability of selecting a reliable relay. By combining the signal from the direct link, the cooperative transmission with an MRC receiver outperforms that with an SC receiver. However, the performance gap between the cooperative transmission schemes reduces with an increase of λ_R, because the channel quality of the forward link becomes better, which reduces the importance of the direct link for packet decoding.

Figure 3.7 illustrates the single-link cooperation gain achieved by cooperative transmission versus the angle of relay selection region for $L_D = 50$ m and 40 m when $\lambda_R = 0.003$ nodes/m^2. The cooperation gain increases with the size of relay selection region, as more spatial resources are allocated to each cooperative link and more potential relays are avail-

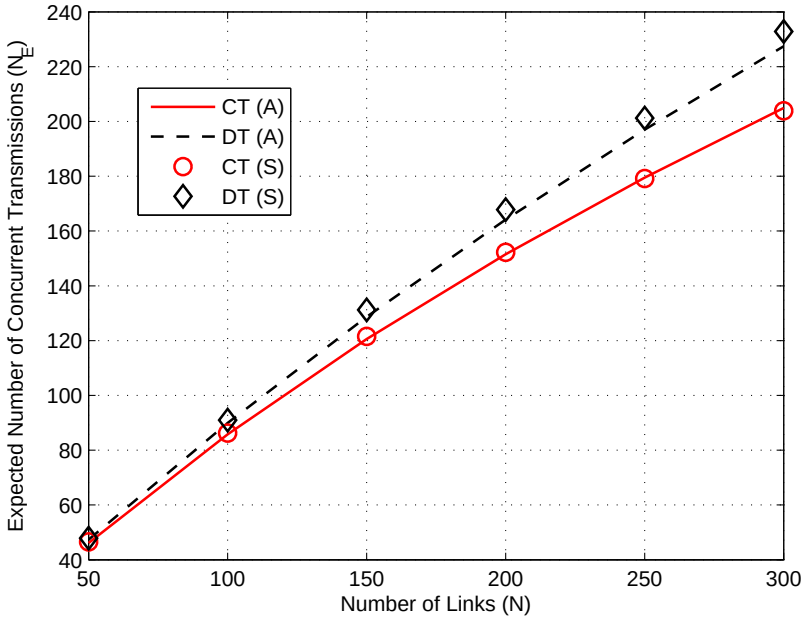

Figure 3.8: Expected numbers of concurrent direct and cooperative transmissions versus total number of links when $\omega = \pi/3$, $\lambda_R = 0.003$ nodes/m^2, and $L_D = 50$ m.

able for spatial diversity. Similarly, the performance gap between the cooperative transmission schemes shrinks with an increase of ω. The cooperation gain at $L_D = 40$ m is smaller than that at $L_D = 50$ m. This observation shows that the cooperative transmission is preferable when the link length is large (i.e., the channel quality of the direct link is poor).

3.5.2 Expected Number of Concurrent Transmissions and Network-Wide Reduced Spatial Reuse

Figure 3.8 plots the expected numbers of concurrent DT and cooperative transmission (CT) versus the total number of links with parameters $\omega = \pi/3$, $\lambda_R = 0.003$ nodes/m^2, and $L_D = 50$ m. The expected numbers of concurrent transmissions increase with the total number of links. As expected, the expected number of concurrent cooperative transmissions is always smaller than that of concurrent direct transmissions, as the enlarged IR due to relay transmissions reduces the network-wide spatial frequency reuse. The gap between the expected numbers of concurrent direct and cooperative transmissions expands with

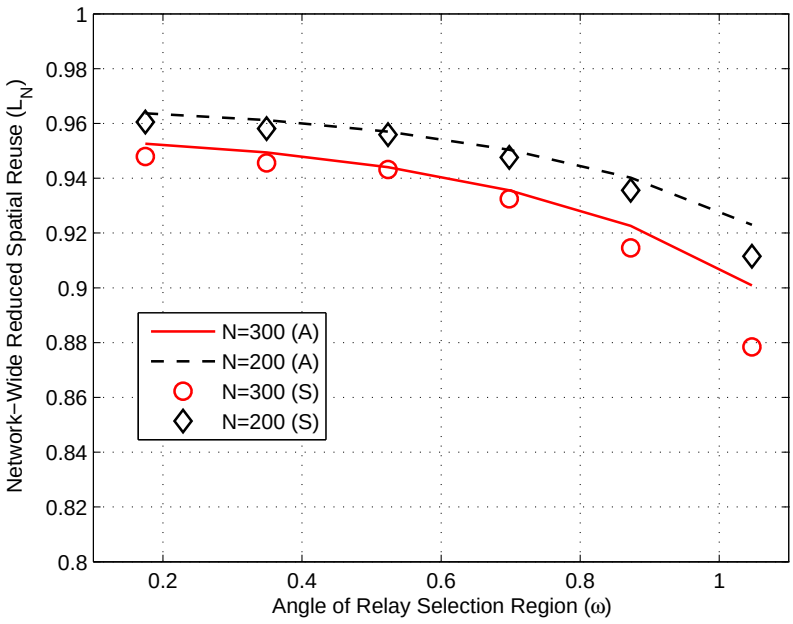

Figure 3.9: Network-wide reduced spatial frequency reuse versus angle of relay selection region for $N = 200$ and 300 when $\lambda_R = 0.003$ nodes/m^2 and $L_D = 50$ m.

an increase of N. This is because the adverse effect of the enlarged IR becomes more significant as N increases.

Figure 3.9 shows the network-wide reduced spatial frequency reuse versus the angle of relay selection region for $N = 200$ and 300 with parameters $\lambda_R = 0.003$ nodes/m^2 and $L_D = 50$ m. The spatial frequency reuse reduces as the angle of relay selection region increases. As ω increases, each cooperative link occupies more spatial resources on average for spatial diversity, which reduces the spatial resources available for spatial reuse. The reduction in network-wide spatial frequency reuse at $N = 300$ is larger than that at $N = 200$. This observation shows that, when the link density is high, the cooperative transmission is more likely to cause link blockage (i.e., the limitation of the cooperative transmission becomes more significant). Due to the conservative calculation of the interference-free probability between any two links, there exists a small deviation between the analytical and simulation results.

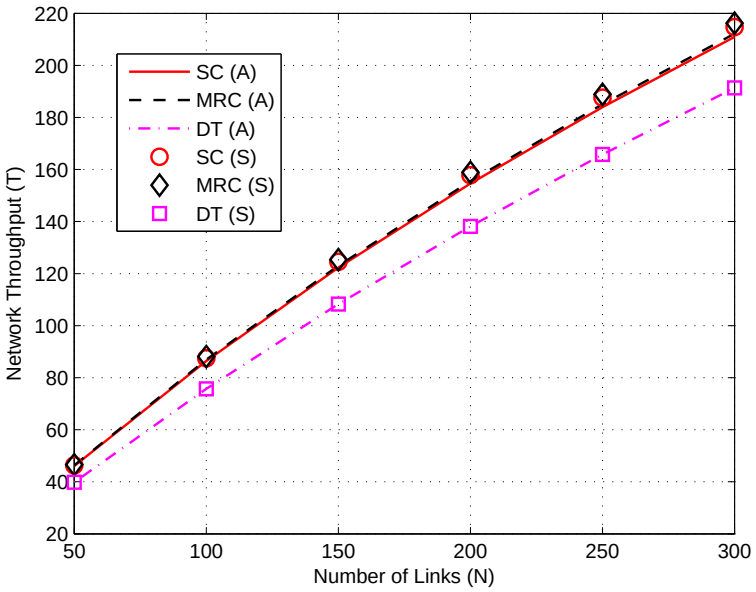

(a) $\omega = \pi/6$ and $\lambda_R = 0.006$ nodes/m^2

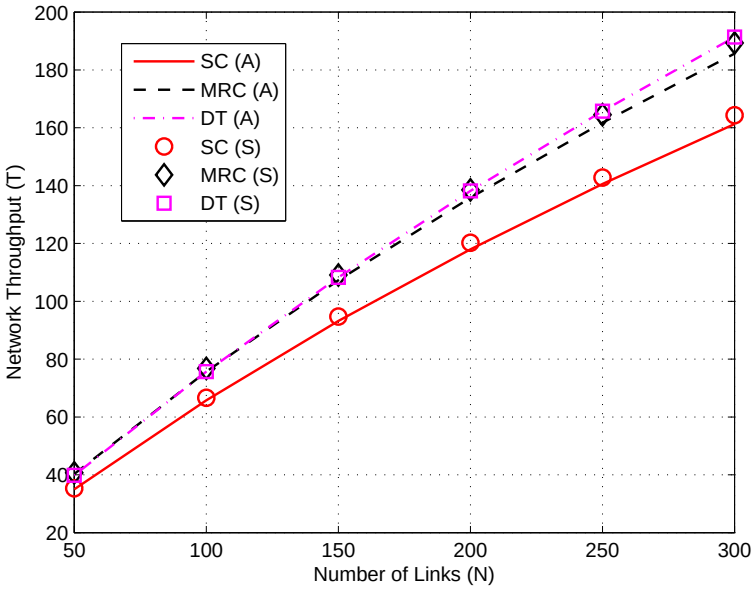

(b) $\omega = \pi/3$ and $\lambda_R = 0.0002$ nodes/m^2

Figure 3.10: Network throughput versus total number of links when $L_D = 50$ m.

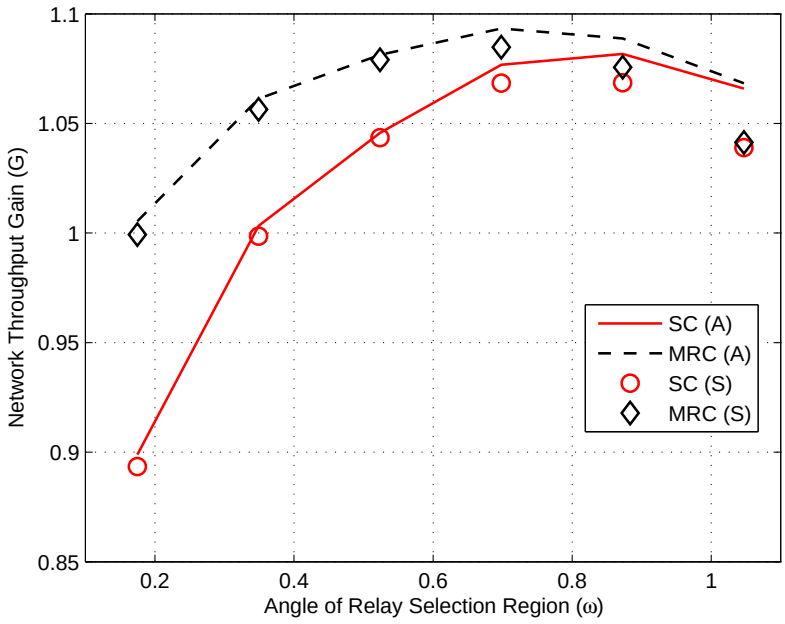

Figure 3.11: Network throughput gain versus angle of relay selection region when $\lambda_R = 0.003$ nodes/m^2, $L_D = 50$ m, and $N = 300$.

3.5.3 Network Throughput

In this subsection, we account for both the transmission success probability and expected number of concurrent transmissions, and study the impact of the total number of links, size of relay selection region, relay density, and link length on the network throughput.

Figure 3.10 illustrates the network throughput of the direct and cooperative transmissions versus the total number of links when $L_D = 50$ m. The network throughput of all schemes increase with N. With a small relay selection region and a high relay density, as shown in Figure 3.10(a), both cooperative transmission schemes outperform the direct transmission, as the single-link cooperation gain outweighs the reduction in network-wide spatial frequency reuse. On the other hand, with a large relay selection region and a low relay density, as shown in Figure 3.10(b), the direct transmission achieves higher network throughput than both cooperative transmission schemes. This implies that the cooperative transmission is not always beneficial and its effectiveness depends on the size of relay selection region and relay density.

Figure 3.11 plots the network throughput gain versus the angle of relay selection region

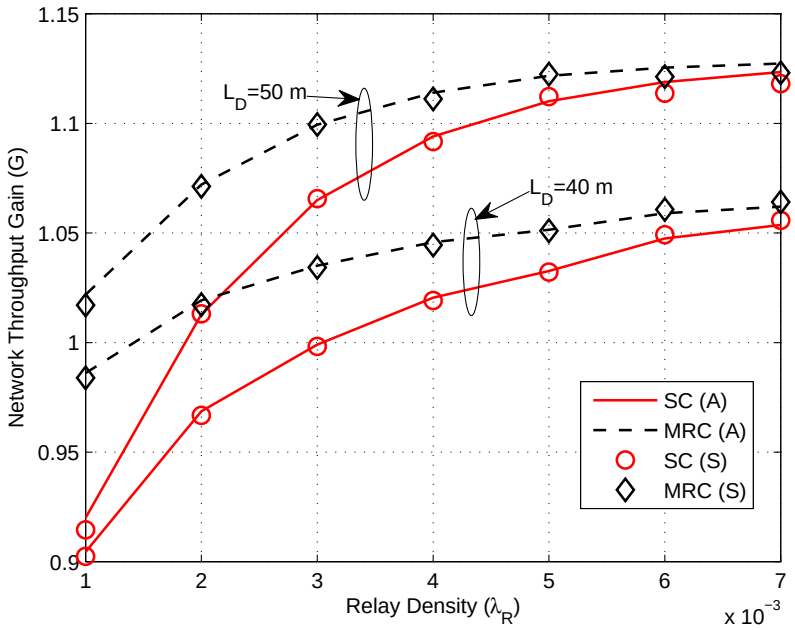

Figure 3.12: Network throughput gain versus relay density (in nodes/m^2) for $L_D = 40$ m and 50 m when $\omega = \pi/6$ and $N = 200$.

with parameters $\lambda_R = 0.003$ nodes/m^2, $L_D = 50$ m, and $N = 300$. With the variation of the angle of relay selection region, there exists a peak point of the network throughput gain. Take the cooperative transmission with MRC as an example. The network throughput gain increases with ω when $\omega < 2\pi/9$, and decreases with ω when $\omega > 2\pi/9$. Note that when $\omega > 2\pi/9$ the increasing rate of the single-link cooperation gain is smaller than the decreasing rate of the network-wide reduced spatial frequency reuse. This implies that the size of relay selection region can be set to balance the tradeoff between spatial diversity and spatial frequency reuse. In addition, we observe that the direct transmission outperforms the cooperative transmission with SC when $\omega < \pi/9$, as the number of potential relays is not large enough to enhance the overall network performance. Comparing the results in Figures 3.7 and 3.11, due to the reduced spatial frequency reuse, the network throughput gain is always smaller than the single-link cooperation gain, and the cooperative transmission that is beneficial for a single source-destination pair may not be beneficial for the whole network. Hence, the effectiveness of cooperation should be evaluated from a perspective of overall network performance.

Figure 3.12 shows the network throughput gain of both cooperative transmission schemes

versus the relay density for $L_D = 40$ m and 50 m with parameters $\omega = \pi/6$ and $N = 200$. The network throughput gain increases with the relay density, as more potential relays are available for each cooperative link. When $L_D = 40$ m, the cooperative transmission with SC is beneficial only if $\lambda_R > 3 \times 10^{-3}$ nodes/m^2, while the cooperative transmission with MRC is beneficial only if $\lambda_R > 1.4 \times 10^{-3}$ nodes/m^2. This implies that a smaller number of potential relays is required for the cooperative transmission with MRC, at the cost of requiring higher implementation complexity. On the other hand, the network throughput gain at $L_D = 40$ m is smaller than that at $L_D = 50$ m. This confirms that the effectiveness of cooperation depends on the link length and the cooperative transmission is effective when the link length is large.

3.6 Summary

This chapter presents the network throughput of cooperative communication in a wireless ad hoc network with randomly positioned single-hop source-destination pairs and relays. The objective is to evaluate the effectiveness of cooperative communication from a perspective of overall network performance. We construct a diamond-shaped relay selection region to study the tradeoff between spatial diversity gain of a single link and reduced spatial frequency reuse of the whole network. We derive the network throughput of the proposed cooperation scheme in terms of the total number of links, relay density, size of relay selection region, and link length. The cooperative transmission is not always beneficial and its effectiveness depends on all these influential factors. Due to the reduced spatial frequency reuse, the network throughput gain is always smaller than the single-link cooperation gain. Extensive simulations are conducted to validate the performance analysis.

Chapter 4

Opportunistic Cooperation with Interference Correlation

Compared with conventional direct transmissions, the cooperative transmissions are not always beneficial and redistribute the interference over the network coverage area due to relay transmissions. This chapter proposes an opportunistic cooperation strategy for a wireless ad hoc network, where each source-destination pair activates the cooperative transmission only when the number of potential relays is not smaller than a cooperation threshold. Such a threshold determines the proportion of concurrent cooperative transmissions and it can be adjusted to enhance the overall network performance. Under the physical interference model, the correlation of node locations induces spatial and temporal correlation of interference power. Based on tools from stochastic geometry, we derive the correlation coefficient of interference power at a destination node during the transmission periods of the source and relay nodes. The outage probability of opportunistic cooperation is derived, while taking into account the interference correlation, relay selection strategy, and spatial distributions of source and relay nodes. Extensive simulations are conducted to validate the performance analysis.

4.1 Motivation

For a fair comparison with the direct transmission and due to the half-duplex constraint, a higher transmission rate is required in both hops of the cooperative transmission to transmit one packet in one time-slot. To support a higher transmission rate, a higher

reception threshold is required for successful packet receptions. When no relays that have good channel quality to both the source and destination nodes can be found to forward the packet, the cooperative transmission performs worse than the direct transmission because of the higher reception threshold. Due to the randomness of channel fading coefficients and node locations, the availability of reliable relays varies for different source-destination pairs. Hence, the cooperative transmission should be activated by each source-destination pair when necessary and beneficial. In particular, the overall network performance can be enhanced by allowing only a fraction of source-destination pairs to activate cooperative transmissions, which motivates this work.

The direct and cooperative links coexist in the network and generate interference to each other. The cooperative links redistribute the interference over the network coverage area due to relay transmissions. Because of the common and adjacent locations of the interferers, the interference power is spatially correlated across adjacent locations and temporally correlated in consecutive time-slots. The correlation level of interference power depends on the fraction of concurrent cooperative transmissions as well as the relay selection strategy. The correlation of interference power results in the correlation of successful packet receptions. Such a correlation poses significant challenges on characterizing interference power as well as on making network-wide beneficial cooperation decisions. Taking into account the interference redistribution and correlation as well as the spatial distributions of source and relay nodes, we derive the correlation coefficient of interference power and outage probability of opportunistic cooperation, in terms of the source density, relay density, cooperation threshold, and link length.

4.2 Opportunistic Cooperation and Interference Characterization

4.2.1 Opportunistic Cooperation

To enhance the overall network performance, an opportunistic cooperation strategy is required to activate cooperative transmissions when necessary and beneficial. For each source-destination pair, a constrained region is considered for relay selection. For instance, the relay selection region, denoted as CR_0, for the typical source-destination pair is centered at $O = (L_D - \kappa, 0)$, $0 < \kappa < L_D$, with radius $r_C \leq L_D/2$, where the source and destination nodes are located at $s_0 = (L_D, 0)$ and $d_0 = (0, 0)$ respectively, as shown in Figure 4.1. In particular, the distance between source node S_0 and center of relay selection

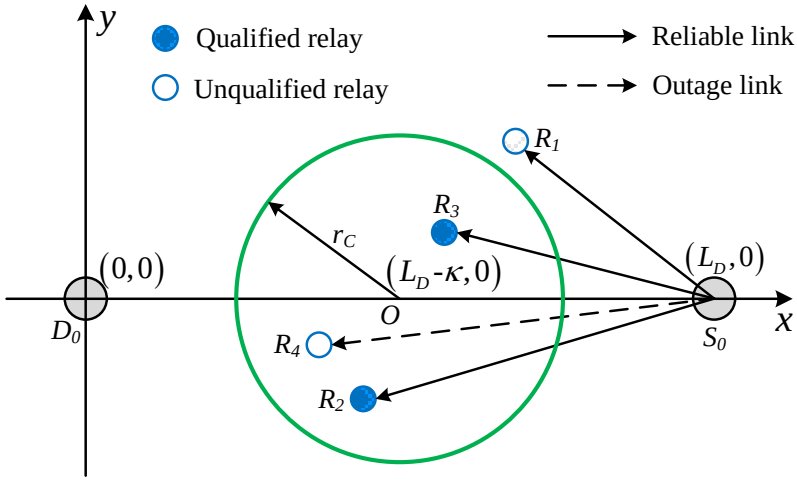

Figure 4.1: An illustration of the constrained relay selection region centered at O with radius r_C for the typical source-destination pair under the 2D Cartesian coordinate system.

region is denoted as κ, while the distance between center of relay selection region and destination node D_0 is $L_D - \kappa$. Such a constrained relay selection region can be identified by coordination signaling and location estimation at each node via the localization technique [66]. Performance analysis with other different relay selection regions can be carried out similarly. Note that it is desirable to select the best relay within a constrained region due to the following reasons: 1) the relays geographically far away from the source and/or destination nodes are not beneficial [36]; 2) the protocol overhead and implementation complexity of a relay selection scheme increase with the number of relays that contending to be the best relay [55, 67]; and 3) the efficiency of spatial frequency reuse reduces with a larger relay selection region [49].

The relays within the relay selection region are referred to as potential relays and only the potential relays contend to be the best relay. The existence of more potential relays for a source-destination pair implies a higher probability of selecting a reliable relay. Hence, the number of potential relays determines the achievable performance of cooperative transmissions and such local information can be obtained by each source node via coordination signaling. Note that each source node does not have two-hop instantaneous CSI (i.e., channel qualities of source-relay and relay-destination links) to help making the cooperation decision, which is always the case in decentralized wireless networks. As a result, each source node makes an independent decision on whether or not to enable a cooperative

transmission based on the limited available information (i.e., number of potential relays).

Threshold-based opportunistic cooperation is considered here due to its efficiency and simplicity for implementation. To make a cooperation decision, a source node, S_i, compares the number of potential relays, K_i, with a cooperation threshold, θ_C. For example, source node S_0 schedules a cooperative transmission when $K_0 \geq \theta_C$, and enables a direct transmission otherwise. To guarantee an acceptable outage probability for each source-destination pair, the concurrent transmissions should keep a distance away with high probability, which leads to a low possibility of having overlapped constrained relay selection regions. Hence, we assume that the numbers of potential relays for different source-destination pairs are independent. Because of the independent cooperation decisions of all source nodes and by applying the independent thinning property of the PPP, the final cooperative transmission set (consisting of spatial locations of source nodes of cooperative links)

$$\Phi_C = \{s_i \in \Phi_S : K_i \geq \theta_C\} \tag{4.1}$$

is a homogeneous PPP with density

$$\begin{aligned} \lambda_C &= \lambda_S \cdot \sum_{k=\theta_C}^{\infty} \mathbb{P}\left(K = k\right) \\ &\overset{(a)}{=} \lambda_S \cdot \sum_{k=\theta_C}^{\infty} \frac{\left(\lambda_R \mathcal{A}_R\right)^k}{k!} \exp\left(-\lambda_R \mathcal{A}_R\right) \end{aligned} \tag{4.2}$$

where $\mathcal{A}_R = \pi r_C^2$ is the area of a relay selection region and (a) holds as the number of potential relays is a Poisson random variable with mean $\lambda_R \mathcal{A}_R$. Similarly, the final direct transmission set $\Phi_D = \{s_i \in \Phi_S : K_i < \theta_C\}$ is a homogeneous PPP with density $\lambda_D = \lambda_S - \lambda_C$.

Based on the opportunistic cooperation strategy, the concurrent transmissions within the network are a mixture of direct and cooperative transmissions, as shown in Figure 4.2, except two special cases (i.e., direct transmissions only when $\theta_C = \infty$ and cooperative transmissions only when $\theta_C = 0$). For a one-hop direct transmission, a source node utilizes the whole time-slot to transmit a packet at rate ν. An outage event occurs when the received SIR at the destination node within the time-slot is smaller than required reception threshold β_ν. Similar to the relay selection scheme in Chapter 3, a single-relay DF scheme is considered for a two-hop cooperative transmission and a time-slot is partitioned equally to two sub-time-slots [59]. The fading coefficients remain invariant during one sub-time-slot and vary independently in different sub-time-slots. Each source node transmits a packet at

rate 2ν in the first sub-time-slot. Each potential relay can successfully receive the packet if the received SIR is not smaller than $\beta_{2\nu}$, depending on both instantaneous signal and interference power. Note that for $\beta_{2\nu} > 1$, each potential relay can correctly decode at most one packet over each time-slot [34]. With a potential of more than one qualified relay for each cooperative link, a distributed relay selection scheme is required. Assuming that, via coordination signaling, each qualified relay has instantaneous CSI to the intended destination node. When relay set Ω_0 is not empty, a qualified relay with the best channel to the destination node is selected as the best relay, R_b^0, which is given by

$$R_b^0 = \arg \max_{R_i \in \Omega_0} \{H_{R_i D_0:2} \cdot g(r_i)\} \tag{4.3}$$

where $\Omega_0 = \{R_i : r_i \in \Phi_R \cap CR_0, \gamma_{S_0 R_i:1} \geq \beta_{2\nu}\}$ denotes the set of qualified relays for the typical source-destination pair, $\gamma_{S_0 R_i:1}$ denotes the SIR at relay R_i when receiving a packet from source node S_0 in the first sub-time-slot, $H_{R_i D_0:2}$ denotes the fading coefficient between relay R_i and destination node D_0 in the second sub-time-slot, and $g(r_i)$ denotes the path loss between relay R_i and destination node D_0 as defined in (2.1).

In the second sub-time-slot, the best relay forwards the packet to the intended destination node at rate 2ν and the source node does not repeat the packet transmission. If the relay set is empty (i.e., no qualified relays), the packet is not forwarded to the intended destination node. Finally, the destination node decodes the packet using SC, by which the destination node selects a better link from the direct and forward links for packet decoding. Hence, an outage event occurs when both the direct and forward links cannot support the required transmission rate.

4.2.2 Interference Characterization

Under the physical interference model, power levels of the signals transmitted from all unintended transmitters are added and the sum is considered as interference power. Transmission power P_t is normalized to one without loss of generality. Due to the mixture of direct and cooperative transmissions, as shown in Figure 4.2(a), the aggregate interference power observed by a potential relay (e.g., R_k) of the typical source-destination pair in the first sub-time-slot is given by

$$I_{R_k:1}(\Phi_D, \Phi_C) = I_{DR_k:1}(\Phi_D) + I_{CR_k:1}(\Phi_C) \tag{4.4}$$

where $I_{DR_k:1}(\Phi_D) = \sum_{s_i \in \Phi_D} H_{S_i R_k:1} \cdot g(s_i - r_k)$ and $I_{CR_k:1}(\Phi_C) = \sum_{s_j \in \Phi_C} H_{S_j R_k:1} \cdot g(s_j - r_k)$ denote the interference power observed by relay R_k from the source nodes of direct and

cooperative links, respectively.

Due to the interference redistribution incurred by concurrent cooperative transmissions, as shown in Figure 4.2(b), the aggregate interference power observed by destination node D_0 in the first and second sub-time-slots can be expressed respectively as

$$\begin{aligned} I_{D_0:1}(\Phi_D, \Phi_C) &= I_{DD_0:1}(\Phi_D) + I_{CD_0:1}(\Phi_C) \\ I_{D_0:2}(\Phi_D, \Phi_F) &= I_{DD_0:2}(\Phi_D) + I_{FD_0:2}(\Phi_F) \end{aligned} \tag{4.5}$$

where $I_{DD_0:1}(\Phi_D) = \sum_{s_i \in \Phi_D} H_{S_i D_0:1} \cdot g(s_i)$ and $I_{DD_0:2}(\Phi_D) = \sum_{s_i \in \Phi_D} H_{S_i D_0:2} \cdot g(s_i)$ are the interference power from the source nodes of direct links in the first and second sub-time-slots respectively, $I_{CD_0:1}(\Phi_C) = \sum_{s_j \in \Phi_C} H_{S_j D_0:1} \cdot g(s_j)$ and $I_{FD_0:2}(\Phi_F) = \sum_{r_m \in \Phi_F} H_{R_m D_0:2} \cdot g(r_m)$ denote the interference power from the source nodes and selected relays of cooperative links in the first and second sub-time-slots respectively, and Φ_F denotes the PPP formed by the spatial locations of selected relays that forward the packets in the second sub-time-slot [68].

Due to the common locations of source nodes of direct links in both sub-time-slots, interference power $I_{DD_0:1}(\Phi_D)$ and $I_{DD_0:2}(\Phi_D)$ are temporally correlated. Similarly, as the source node (e.g., S_j) locates close to its selected relay (e.g., R_b^j) for each cooperative link, interference power $I_{CD_0:1}(\Phi_C)$ and $I_{FD_0:2}(\Phi_F)$ are temporally correlated. As a result, the interference power observed by destination node D_0 in two sub-time-slots, i.e., $I_{D_0:1}(\Phi_D, \Phi_C)$ and $I_{D_0:2}(\Phi_D, \Phi_F)$ defined in (4.5), are temporally correlated. On the other hand, the potential relays (e.g., R_k) of the typical source-destination pair and destination node D_0 are geographically close and suffer from the interference originated from the same or adjacent interferers, which yield to the spatial correlation between interference power $I_{R_k:1}(\Phi_D, \Phi_C)$ and $I_{D_0:1}(\Phi_D, \Phi_C)$ or $I_{D_0:2}(\Phi_D, \Phi_F)$. The correlation of interference power is taken into account in the following analysis of correlation coefficient and outage probability.

4.3 Temporal Correlation Coefficient of Interference

In this section, we analyze the temporal correlation coefficient of interference power observed by destination node D_0 in the first and second sub-time-slots, i.e., $I_{D_0:1}(\Phi_D, \Phi_C)$ and $I_{D_0:2}(\Phi_D, \Phi_F)$. The spatial correlation coefficient of interference power can be derived similarly. As in [41], a non-singular path loss model (i.e., $\epsilon > 0$) is utilized to ensure the

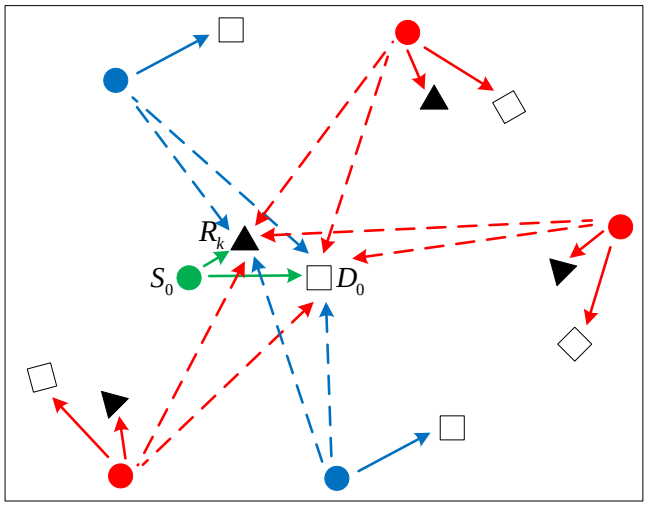

(a) Transmissions in the first sub-time-slot

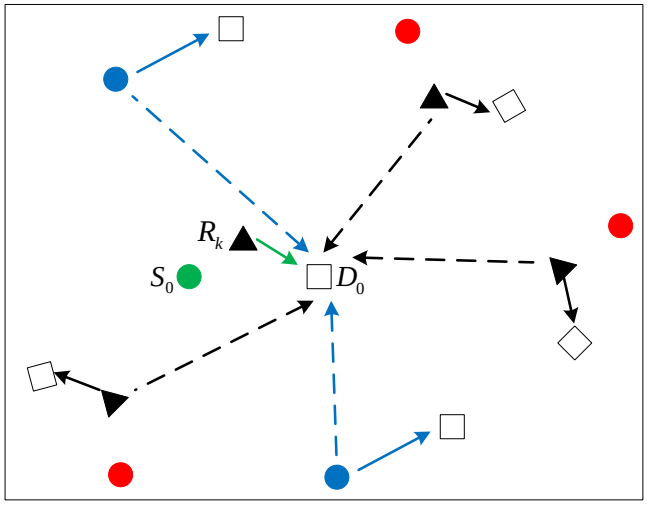

(b) Transmissions in the second sub-time-slot

Figure 4.2: An illustration of the interference power, originating from both the direct and cooperative links over the network, observed by relay R_k and destination node D_0 in the first and second sub-time-slots. Each circle, triangle, and square represent a source, selected relay, and destination, respectively. The solid and dashed lines represent the transmitted signal and interference, respectively.

mean and variance of interference power to be finite when deriving the correlation coefficient, while a singular path loss model (i.e., $\epsilon = 0$) is used to determine whether or not a packet is successfully received[1]. The correlation coefficient can be represented in terms of important network and protocol parameters, as stated in the following proposition (with proof in Appendix A.4).

Proposition 4. *For Rayleigh fading channels, the temporal correlation coefficient of interference power observed by destination node D_0 in the first and second sub-time-slots (i.e., $I_{D_0:1}(\Phi_D, \Phi_C)$ and $I_{D_0:2}(\Phi_D, \Phi_F)$) is given by*

$$\rho = \frac{\lambda_D \int_{\mathbb{R}^2} g^2(s)\mathrm{d}s + \lambda_F \int_{\mathbb{R}^2} g(s)\,\mathbb{E}_\tau\left[g(s+\tau)\right]\mathrm{d}s}{2\sqrt{\lambda_S}\sqrt{\lambda_D+\lambda_F}\int_{\mathbb{R}^2} g^2(s)\mathrm{d}s} \tag{4.6}$$

where $\int_{\mathbb{R}^2} g^2(s)\mathrm{d}s = \delta(1-\delta)\pi^2/\left[\epsilon^{2-\delta}\sin(\pi\delta)\right]$, $\delta = 2/\alpha$, τ denotes the coordinate difference between the source node and the best relay, and $\lambda_F = \lambda_C(1-q_e)$ is the spatial density of PPP Φ_F with

$$q_e = \sum_{k=\theta_C}^{\infty} \frac{(\lambda_R \mathcal{A}_R)^k}{k!}\exp(-\lambda_R\mathcal{A}_R)\sum_{m=0}^{k}\binom{k}{m}(-1)^m \frac{1}{\mathcal{A}_R}\int_{CR_0}\exp\left(-\lambda_S C_1 d_{S_0R}^2\right)\mathrm{d}r \tag{4.7}$$

and

$$C_1 = -\pi\delta\beta_{2\nu}^{\delta}\Gamma(-\delta)\,\Gamma(\delta+m)/\Gamma(m). \tag{4.8}$$

In (4.8), $\Gamma(x)$ is the Gamma function.

Due to random relay locations, the coordinate difference between the source node and the best relay is a random variable and utilizing its probability density function [26] to directly calculate the correlation coefficient in (4.6) is complex. For simplicity of performance analysis, we obtain the lower bound of the temporal correlation coefficient, as stated in the following corollary.

Corollary 2. *For Rayleigh fading channels, the temporal correlation coefficient of interference power observed by destination node D_0 in the first and second sub-time-slots (i.e.,*

[1]The singularity has a negligible effect on determining whether or not a packet is successfully received [31]. For instance, if an interferer locates very close to a receiver, the singular path loss model would result in a very small SIR and hence an unsuccessful packet reception at the receiver. On the other hand, the receiver would also very likely fail to decode the packet even if the singularity is removed (i.e., non-singular path loss model).

$I_{D_0:1}(\Phi_D, \Phi_C)$ and $I_{D_0:2}(\Phi_D, \Phi_F)$) is lower bounded by

$$\rho \geq \frac{\lambda_D \int_{\mathbb{R}^2} g^2(s)\mathrm{d}s + \lambda_F \int_{\mathbb{R}^2} g(s)\, g(s + \mathbb{E}_\tau[\tau])\mathrm{d}s}{2\sqrt{\lambda_S}\sqrt{\lambda_D + \lambda_F} \int_{\mathbb{R}^2} g^2(s)\mathrm{d}s}. \tag{4.9}$$

Proof. As $g(s)$ is a convex function and according to Jensen's inequality, we have

$$\mathbb{E}_\tau[g(s+\tau)] \geq g(s + \mathbb{E}_\tau[\tau]). \tag{4.10}$$

As a result, (4.9) follows directly from (4.6). □

As mentioned in Section 4.2.2, both the common locations of source nodes of direct links and the adjacent locations of source and relay nodes of cooperative links yield to the temporal correlation of interference power in the first and second sub-time-slots. To distinguish the temporal interference correlation incurred by these two factors, we obtain the temporal correlation coefficient due to the common locations of source nodes of direct links, as stated in the following corollary.

Corollary 3. *The temporal correlation coefficient of interference power observed by destination node D_0 due to the common locations of source nodes of direct links in the first and second sub-time-slots is given by*

$$\rho_D = \frac{\lambda_D}{2\sqrt{\lambda_S}\sqrt{\lambda_D + \lambda_F}}. \tag{4.11}$$

Similarly, the temporal correlation coefficient of interference power observed by destination node D_0 due to the adjacent locations of source and relay nodes of cooperative links in the first and second sub-time-slots is $\rho_C = \rho - \rho_D$. The temporal correlation coefficient incorporates the effect of interference redistribution incurred by concurrent cooperative transmissions and reflects the level of interference correlation at the destination node in two consecutive sub-time-slots. The impact of interference redistribution on the temporal correlation coefficient is illustrated in Section 4.5.1.

4.4 Outage Probability of Opportunistic Cooperation

In this section, we derive the outage probability of opportunistic cooperation based on tools from stochastic geometry, while taking into account the spatial distributions of sources and

relays, cooperation threshold, and interference correlation. By conditioning on whether or not cooperation is activated by the typical source-destination pair, the outage probability of opportunistic cooperation can be expressed as

$$q_{out}^{OC} = \sum_{k=0}^{\theta_C - 1} \mathbb{P}\left(K_0 = k\right) q_{DT} + \sum_{k=\theta_C}^{\infty} \mathbb{P}\left(K_0 = k\right) q_{out}^{CT}\left(k\right) \tag{4.12}$$

where q_{DT} and $q_{out}^{CT}\left(k\right)$ denote the outage probabilities of the direct transmission and cooperative transmission given k potential relays, derived in the following two subsections, respectively.

4.4.1 Direct Transmission

For a direct transmission of the typical source-destination pair, an outage event occurs when the received SIR at destination node D_0 in either the first or second sub-time-slot is smaller than β_ν. The outage probability, q_{DT}, is given by

$$q_{DT} = 1 - \mathbb{P}\left(\gamma_{S_0 D_0:1} \geq \beta_\nu, \gamma_{S_0 D_0:2} \geq \beta_\nu\right) \tag{4.13}$$

where $\gamma_{S_0 D_0:1} = \frac{H_{S_0 D_0:1} L_D^{-\alpha}}{I_{D_0:1}(\Phi_D, \Phi_C)}$ and $\gamma_{S_0 D_0:2} = \frac{H_{S_0 D_0:2} L_D^{-\alpha}}{I_{D_0:2}(\Phi_D, \Phi_F)}$ denote the received SIRs at destination node D_0 in the first and second sub-time-slots, respectively.

Over a Rayleigh fading channel, the received signal power at the destination node follows an exponential distribution. As PPP Φ_D is independent of PPP Φ_C and PPP Φ_F, we have

$$\begin{aligned} q_{DT} = 1 - &\underbrace{\mathbb{E}\left[\exp\left(-\beta_\nu L_D^\alpha \left[I_{DD_0:1}\left(\Phi_D\right) + I_{DD_0:2}\left(\Phi_D\right)\right]\right)\right]}_{\mathcal{B}_1} \\ &\times \underbrace{\mathbb{E}\left[\exp\left(-\beta_\nu L_D^\alpha \left[I_{CD_0:1}\left(\Phi_C\right) + I_{FD_0:2}\left(\Phi_F\right)\right]\right)\right]}_{\mathcal{B}_2}. \end{aligned} \tag{4.14}$$

Taking the Laplace transforms of fading coefficients between the interferers and desti-

nation node D_0, we have

$$\begin{aligned}\mathcal{B}_1 &= \mathbb{E}\left[\prod_{s_i\in\Phi_D}\frac{1}{\left(1+\beta_\nu L_D^\alpha g\left(s_i\right)\right)^2}\right]\\ &\overset{(a)}{=} \exp\left(-\lambda_D 2\pi\int_0^\infty\left[1-\frac{1}{\left(1+\beta_\nu L_D^\alpha l^{-\alpha}\right)^2}\right]l\mathrm{d}l\right)\\ &\overset{(b)}{=} \exp\left(-\lambda_D\pi\beta_\nu^\delta\Gamma\left(1+\delta\right)\Gamma\left(1-\delta\right)\left(1+\delta\right)L_D^2\right)\end{aligned} \tag{4.15}$$

where (a) follows from the probability generating functional (PGFL) of the PPP [69] and (b) follows from the diversity polynomial [70].

As PPP Φ_C is not independent of PPP Φ_F, we have

$$\begin{aligned}\mathcal{B}_2 &= \mathbb{E}\left[\left(\prod_{s_i\in\Phi_C}\frac{1}{1+\beta_\nu L_D^\alpha g\left(s_i\right)}\right)\left(\prod_{r_m\in\Phi_F}\frac{1}{1+\beta_\nu L_D^\alpha g\left(r_m\right)}\right)\right]\\ &\overset{(a)}{=} \mathbb{E}\left[\left(\prod_{s_i\in\Phi_C}\frac{1}{1+\beta_\nu L_D^\alpha g\left(s_i\right)}\right)\left(\prod_{s_i\in\Phi_C}\left[\frac{1-q_e}{1+\beta_\nu L_D^\alpha g\left(s_i+\tau\right)}+q_e\right]\right)\right]\\ &\overset{(b)}{=} \exp\left(-\lambda_C\int_{\mathbb{R}^2}\left[1-\frac{1}{1+\beta_\nu L_D^\alpha g\left(s\right)}\left(\frac{1-q_e}{1+\beta_\nu L_D^\alpha g\left(s+\mathbb{E}_\tau[\tau]\right)}+q_e\right)\right]\mathrm{d}s\right)\end{aligned} \tag{4.16}$$

where (a) follows from the transformation between PPP Φ_C and PPP Φ_F and the expectation with respect to the event of an empty relay set, and (b) follows from the PGFL of the PPP.

By substituting (4.15) and (4.16) into (4.14), we can derive the outage probability of the direct transmission, which can be efficiently calculated such as in Mathematica.

4.4.2 Cooperative Transmission

For a cooperative transmission of the typical source-destination pair with selection combining at the destination, an outage event occurs when both the direct and forward links cannot support the required transmission rate. Specifically, the direct link fails when the SIR at the destination node is smaller than $\beta_{2\nu}$, as the source node transmits a packet at rate 2ν in the first sub-time-slot. On the other hand, the forward link fails when one of the following events occurs: 1) Event $\mathcal{E}_{21}$ - relay set Ω_0 is empty; 2) Event $\mathcal{E}_{22}$ - the received SIR at destination node D_0 in the second sub-time-slot is smaller than $\beta_{2\nu}$ when

relay set Ω_0 is not empty. Hence, the conditional outage probability given that there exist k potential relays, $q_{out}^{CT}(k)$, is given by

$$q_{out}^{CT}(k) = \mathbb{P}\left(\gamma_{S_0D_0:1} < \beta_{2\nu}, \mathcal{E}_{21} \cup \mathcal{E}_{22} \,|K_0 = k\right) \tag{4.17}$$

where $\gamma_{S_0D_0:1} = H_{S_0D_0:1}L_D^{-\alpha}/I_{D_0:1}\left(\Phi_D, \Phi_C\right)$, and outage events $\mathcal{E}_{21}$ and $\mathcal{E}_{22}$ can be expressed as

$$\begin{aligned} \mathcal{E}_{21} &= \{\Omega_0 = \emptyset\} \\ \mathcal{E}_{22} &= \{\Omega_0 \neq \emptyset, \gamma_{R_b^0D_0:2} < \beta_{2\nu}\}. \end{aligned} \tag{4.18}$$

Outage event $(\mathcal{E}_{21} \cup \mathcal{E}_{22})$ is equivalent to the event that no potential relays have reliable links to both the source and destination nodes. Given that k potential relays locate within a relay selection region, we have

$$q_{out}^{CT}(k) = \mathbb{E}\left[\underbrace{\mathbb{P}\left(\gamma_{S_0D_0:1} < \beta_{2\nu}\right)}_{\mathcal{P}_1} \prod_{n=1}^{k}\left(1 - \underbrace{\mathbb{P}\left(\gamma_{S_0R_n:1} \geq \beta_{2\nu}\right)}_{\mathcal{P}_2}\underbrace{\mathbb{P}\left(\gamma_{R_nD_0:2} \geq \beta_{2\nu}\right)}_{\mathcal{P}_3}\right)\right]. \tag{4.19}$$

The success probability of the relay-destination link can be expressed as

$$\begin{aligned} \mathcal{P}_3 &\overset{(a)}{=} \mathbb{E}\left[\exp\left(-\beta_{2\nu}d_{R_nD_0}^{\alpha}I_{DD_0:2}\left(\Phi_D\right)\right) \cdot \exp\left(-\beta_{2\nu}d_{R_nD_0}^{\alpha}I_{FD_0:2}\left(\Phi_F\right)\right)\right] \\ &\overset{(b)}{=} \prod_{s_i \in \Phi_D} \frac{1}{1 + \beta_{2\nu}d_{R_nD_0}^{\alpha}g\left(s_i\right)} \cdot \prod_{r_m \in \Phi_F} \frac{1}{1 + \beta_{2\nu}d_{R_nD_0}^{\alpha}g\left(r_m\right)} \\ &\overset{(c)}{=} \prod_{s_i \in \Phi_D} \frac{1}{1 + \beta_{2\nu}d_{R_nD_0}^{\alpha}g\left(s_i\right)} \cdot \prod_{s_j \in \Phi_C} \left[\frac{1 - q_e}{1 + \beta_{2\nu}d_{R_nD_0}^{\alpha}g\left(s_j + \tau\right)} + q_e\right] \end{aligned} \tag{4.20}$$

where $d_{R_nD_0} = \|r_n\|$ denotes the distance between potential relay R_n and destination node D_0, (a) follows from the expectation with respect to the channel fading between the relay and destination node, (b) follows from the Laplace transforms of the channel fading between the interferers and destination node, and (c) follows from the transformation between PPP Φ_C and PPP Φ_F.

Similarly, the outage and success probabilities of the source-destination and source-relay

links can be expressed respectively as

$$\begin{aligned}\mathcal{P}_1 &= 1 - \prod_{s_i \in \Phi_D} \left[1 + \beta_{2\nu} L_D^{\alpha} g\left(s_i\right)\right]^{-1} \prod_{s_j \in \Phi_C} \left[1 + \beta_{2\nu} L_D^{\alpha} g\left(s_j\right)\right]^{-1} \\ \mathcal{P}_2 &= \prod_{s_i \in \Phi_D} \left[1 + \beta_{2\nu} d_{S_0 R_n}^{\alpha} g\left(s_i - r_n\right)\right]^{-1} \prod_{s_j \in \Phi_C} \left[1 + \beta_{2\nu} d_{S_0 R_n}^{\alpha} g\left(s_j - r_n\right)\right]^{-1}\end{aligned} \tag{4.21}$$

where $d_{S_0 R_n} = \|s_0 - r_n\|$ denotes the distance between source node S_0 and potential relay R_n.

The conditional outage probability, given that there exist k potential relays, is given by

$$\begin{aligned} q_{out}^{CT}(k) &= \mathbb{E}\left[\mathcal{P}_1 \cdot \prod_{n=1}^{k} \left(1 - \mathcal{P}_2 \cdot \mathcal{P}_3\right)\right] \\ &\overset{(a)}{=} \mathbb{E}\left[\mathcal{P}_1 \cdot \left(1 - \mathcal{P}_2 \cdot \mathcal{P}_3\right)^k\right] \\ &\overset{(b)}{=} \sum_{m=0}^{k} \binom{k}{m} (-1)^m \underbrace{\mathbb{E}\left[\mathcal{P}_1 \cdot \mathcal{P}_2^m \cdot \mathcal{P}_3^m\right]}_{\mathcal{P}} \end{aligned} \tag{4.22}$$

where (a) follows as k potential relays are uniformly distributed within the relay selection region, and (b) follows from the binomial expansion [33, 70]. Note that the spatial and temporal correlation of interference power observed by the destination node and potential relays is considered by taking a joint expectation over the spatial locations of the same set of interferers.

Instead of averaging over all possible relay locations within the constrained relay selection region, we divide it evenly into ζ equal sub-regions and average over the centers of all sub-regions, so as to reduce the computation complexity. As shown in the simulations, a small value of ζ provides an accurate approximation. As PPP Φ_D and PPP Φ_C are

independent, applying the PGFL of the PPP, we have

$$\begin{aligned}\mathcal{P} \approx \frac{1}{\zeta}\sum_{i=1}^{\zeta}\Bigg[&\exp\left(-\lambda_D\int_{\mathbb{R}^2}\left[1-\mathcal{L}^m\left(\|s_0-r_i\|,-r_i\right)\mathcal{L}^m\left(\|r_i\|,d_0\right)\right]\mathrm{d}s\right)\\ &\times\exp\left(-\lambda_C\int_{\mathbb{R}^2}\left[1-\mathcal{L}^m\left(\|s_0-r_i\|,-r_i\right)\left(\left(1-q_e\right)\mathcal{L}^m\left(\|r_i\|,\mathbb{E}_\tau[\tau]\right)+q_e\right)\right]\mathrm{d}s\right)\\ &-\exp\left(-\lambda_D\int_{\mathbb{R}^2}\left[1-\mathcal{L}\left(L_D,d_0\right)\mathcal{L}^m\left(\|s_0-r_i\|,-r_i\right)\mathcal{L}^m\left(\|r_i\|,d_0\right)\right]\mathrm{d}s\right)\\ &\times\exp\left(-\lambda_C\int_{\mathbb{R}^2}\left[1-\mathcal{L}\left(L_D,d_0\right)\mathcal{L}^m\left(\|s_0-r_i\|,-r_i\right)\left(\left(1-q_e\right)\mathcal{L}^m\left(\|r_i\|,\mathbb{E}_\tau[\tau]\right)+q_e\right)\right]\mathrm{d}s\right)\Bigg]\end{aligned} \tag{4.23}$$

where

$$\mathcal{L}\left(u,v\right)=\frac{1}{1+\beta_{2\nu}u^{\alpha}g\left(s+v\right)}. \tag{4.24}$$

The conditional outage probability of opportunistic cooperation, given k potential relays, can be derived by substituting (4.23) and (4.24) into (4.22). Finally, the outage probability of opportunistic cooperation can be obtained by substituting (4.14) and (4.22) into (4.12).

4.5 Numerical Results

This section presents both analytical (A) and simulation (S) results for the direct transmission and opportunistic cooperation. In the simulations, a circular network coverage area with radius 1000 m is considered. Based on Shannon's formula, the required reception thresholds for direct and cooperative transmissions (i.e., β_ν and $\beta_{2\nu}$) are set to be 2 and 8, respectively. In addition, we set both α and ζ equal to 4. The simulation results are obtained by averaging 10^6 realizations of the random network topology.

4.5.1 Correlation Coefficient of Interference Power

Figure 4.3 shows the temporal correlation coefficient of interference power $I_{D_0:1}\left(\Phi_D,\Phi_C\right)$ and $I_{D_0:2}\left(\Phi_D,\Phi_F\right)$ versus cooperation threshold θ_C and distance between a source node and the center of a relay selection region κ with parameters $\lambda_S=0.001$ nodes/m^2, $\lambda_R=0.2$

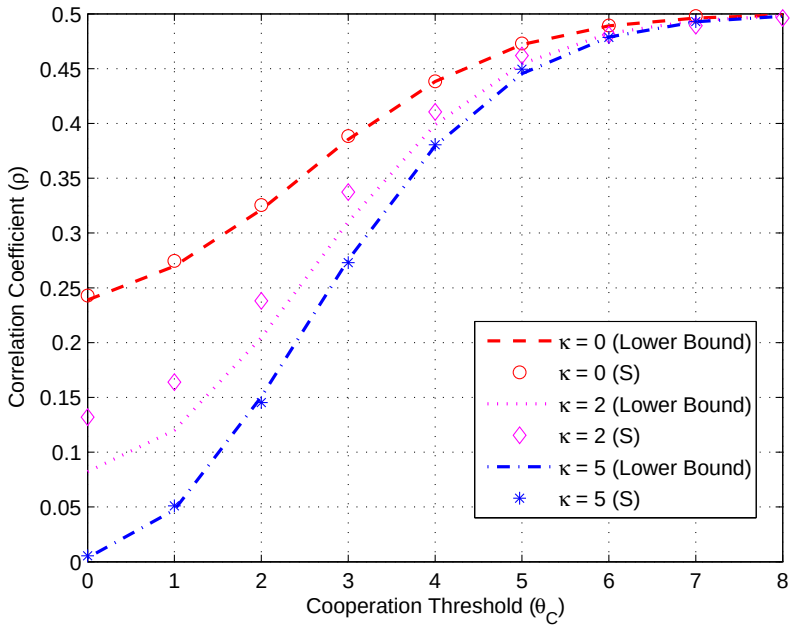

Figure 4.3: Correlation coefficient of interference power $I_{D_0:1}(\Phi_D, \Phi_C)$ and $I_{D_0:2}(\Phi_D, \Phi_F)$ versus cooperation threshold θ_C and distance between a source node and the center of a relay selection region κ when $\lambda_S = 0.001$ nodes/m^2, $\lambda_R = 0.2$ nodes/m^2, $r_C = 2$ m, and $L_D = 12$ m.

nodes/m^2, $r_C = 2$ m, and $L_D = 12$ m. The analytical lower bound of temporal correlation coefficient is obtained based on (4.9). To guarantee that each source-destination pair has enough potential relays and to show the impact of the number of potential relays, source density λ_S is set to be much smaller than relay density λ_R. In addition, we set $\epsilon = 1$ for the non-singular path loss model. It is observed that the correlation coefficient increases with the cooperation threshold. This is due to the fact that, with an increase of the cooperation threshold, the probability of each source-destination pair activating cooperative transmissions becomes smaller, which results in a higher level of interference correlation. In other words, the interference redistribution incurred by cooperative transmissions reduces the level of interference correlation. Over a quasi-static Rayleigh fading channel with $\mathbb{E}[H^2] = 2$, the correlation coefficient increases up to 0.5. On the other hand, with an increase of κ, the average distance between the source node and the best relay becomes larger, which reduces the level of interference correlation as well as the correlation coefficient.

4.5.2 Outage Probability and Transmission Capacity

In this subsection, we study the impact of the relay density, cooperation threshold, distance between a source node and the center of a relay selection region, size of the relay selection region, and link length on the outage probability and transmission capacity (average number of source-destination pairs per square kilometer) [11]. The transmission capacity measures the maximum spatial density of concurrent successful transmissions that can be supported in a network without violating the outage probability constraint, which is set to 5% in the simulation.

Figure 4.4 shows the outage probabilities of DT where $\theta_C = \infty$ and opportunistic cooperation (OC) with $\theta_C = 1$ versus the relay density with parameters $\lambda_S = 0.0001$ nodes/m^2, $r_C = 4$ m, $\kappa = 6$ m, and $L_D = 12$ m, where the analytical results are obtained based on (4.12) and (4.14). It is observed that the outage probability of opportunistic cooperation decreases with the relay density, while that of the direct transmission does not change. This is due to the fact that, with an increase of the relay density, more potential relays are available for each source-destination pair, which results in a higher probability of selecting a reliable relay. The outage probability of opportunistic cooperation is always lower than that of the direct transmission, as cooperation is activated only when there exists at least one potential relay within the best relay locations.

Figure 4.5 illustrates the transmission capacity of DT and OC versus the cooperation threshold for $\lambda_R = 0.01$ nodes/m^2 and $\lambda_R = 0.02$ nodes/m^2 when $r_C = 4$ m, $\kappa = 6$ m, and $L_D = 12$ m. When all source-destination pairs activate cooperative transmissions regardless of the number of potential relays (i.e., $\theta_C = 0$), the achievable transmission capacity is smaller than that of opportunistic cooperation with $\theta_C = 1$. When there are no potential relays, the cooperative transmission performs worse than the direct transmission as the cooperative transmission requires a higher reception threshold for the SIR. It is observed that the transmission capacity of opportunistic cooperation reaches the maximum value when cooperation threshold $\theta_C = 1$. With an increase of the cooperation threshold, the transmission capacity of opportunistic cooperation approaches to that of the direct transmission as the probability of enabling cooperative transmissions decreases. Moreover, the transmission capacity increases with the relay density, as the probability of selecting a reliable relay becomes higher.

Figure 4.6 shows the outage probabilities of DT and OC with $\theta_C = 1$ versus the distance between a source node and the center of a relay selection region for $r_C = 3$ m and $r_C = 4$ m with parameters $\lambda_S = 0.0001$ nodes/m^2, $\lambda_R = 0.03$ nodes/m^2, and $L_D = 12$ m. It can be observed that the opportunistic cooperation achieves the best performance when the center of the relay selection region is located at the link center. This is because the

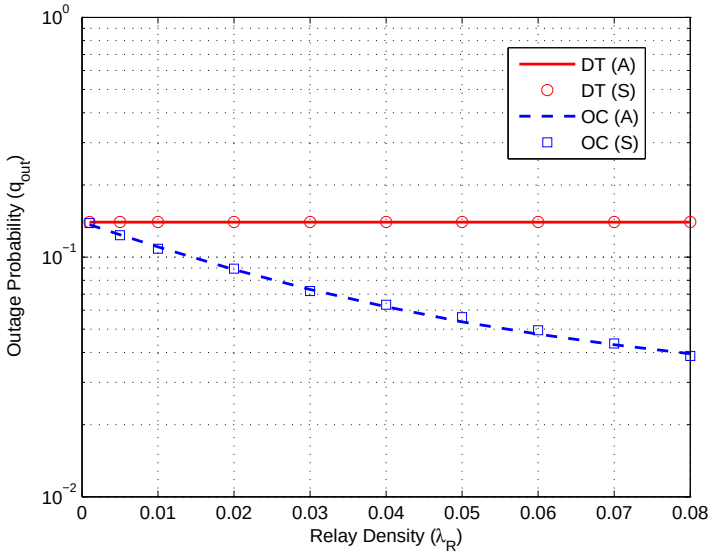

Figure 4.4: Outage probability versus relay density (in nodes/m^2) when $\lambda_S = 0.0001$ nodes/m^2, $r_C = 4$ m, $\kappa = 6$ m, and $L_D = 12$ m.

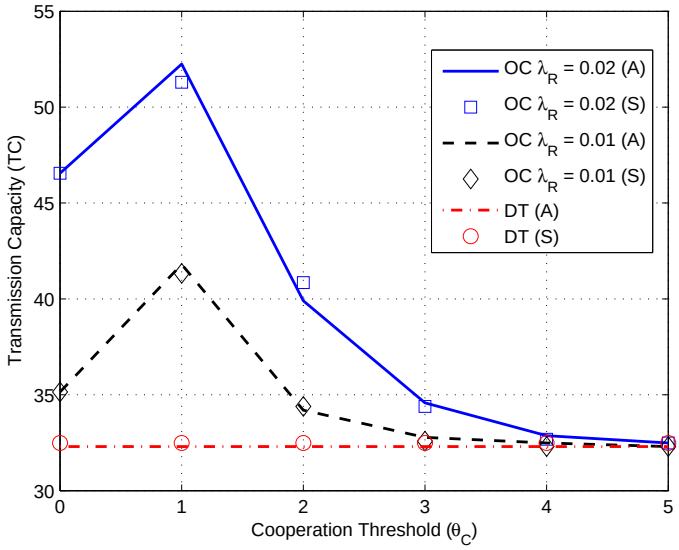

Figure 4.5: Transmission capacity in links/km^2 versus cooperation threshold for $\lambda_R = 0.01$ nodes/m^2 and $\lambda_R = 0.02$ nodes/m^2 when $r_C = 4$ m, $\kappa = 6$ m, and $L_D = 12$ m.

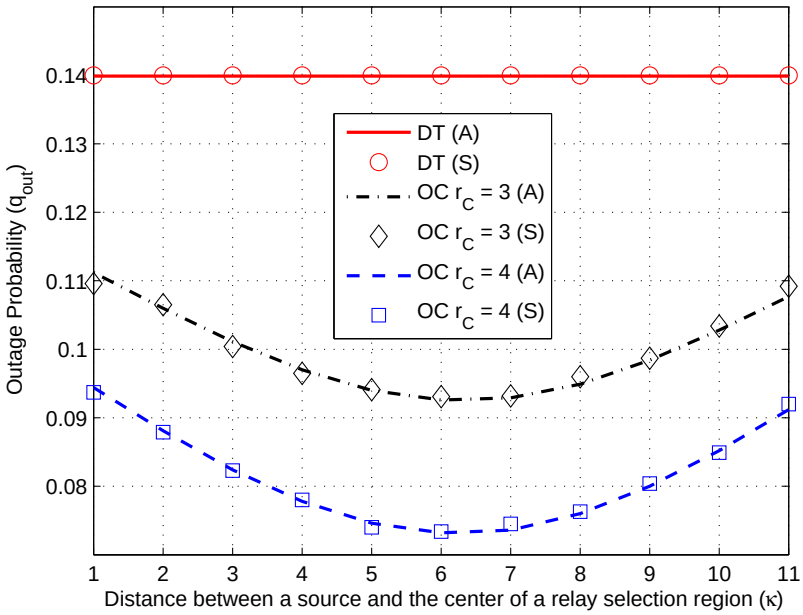

Figure 4.6: Outage probabilities versus distance between a source node and the center of a relay selection region for $r_C = 3$ m and $r_C = 4$ m when $\lambda_S = 0.0001$ nodes/m^2, $\lambda_R = 0.03$ nodes/m^2, and $L_D = 12$ m.

performance of the two-hop cooperative transmission is determined by the qualities of both the source-relay and relay-destination links. Furthermore, with an increase of the size of the relay selection region, better performance is achieved as more relays are available for each source-destination pair.

Figure 4.7 shows the transmission capacity of DT, CT (i.e., OC with $\theta_C = 0$), and OC with $\theta_C = 1$ versus the link length for $\lambda_R = 0.005$ nodes/m^2 and $\lambda_R = 0.02$ nodes/m^2 when $r_C = 4$ m and $\kappa = L_D/2$. With an increase of the link length, the outage probabilities of all transmission schemes increase due to a larger path loss, which leads to a lower transmission capacity. When the relay density is low (e.g., $\lambda_R = 0.005$ nodes/m^2), the cooperative transmission performs worse than the direct transmission, because the probability of having a reliable relay is low and the cooperative transmission requires a higher reception threshold for the SIR. On the other hand, by activating cooperation when there exists at least one potential relay, the transmission capacity of opportunistic cooperation achieves better performance. Furthermore, with an increase of the relay density (e.g., $\lambda_R = 0.02$ nodes/m^2), higher performance gains are achieved by both cooperative transmission schemes.

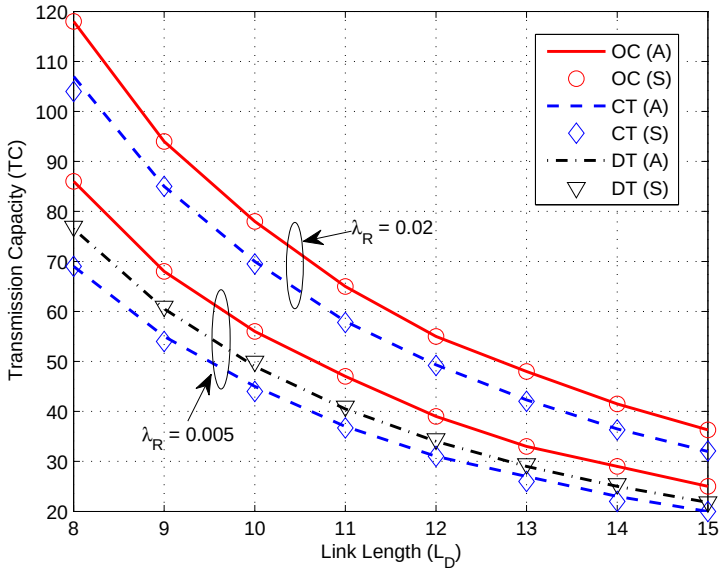

Figure 4.7: Transmission capacity in links/km^2 versus link length for $\lambda_R = 0.005$ nodes/m^2 and $\lambda_R = 0.02$ nodes/m^2 when $r_C = 4$ m and $\kappa = L_D/2$.

4.6 Summary

This chapter presents an opportunistic cooperation strategy for a wireless ad hoc network with randomly positioned single-hop source-destination pairs and relays, which leads to a mixture of direct and cooperative transmissions as well as the spatial and temporal correlation of interference power. We derive the correlation coefficient of interference power and outage probability of opportunistic cooperation as a function of important network and protocol parameters. We demonstrate that cooperation is not always beneficial and its effectiveness depends on the number of available potential relays. Extensive simulations are conducted to validate the performance analysis. The analytical framework can be extended to analyze more advanced cooperation strategies.

Chapter 5

Cooperative Communication with Unsaturated Traffic

This chapter investigates the performance of cooperative communication in a wireless ad hoc network under unsaturated traffic conditions, where interference is the main performance limiting factor. The traffic unsaturation and concurrent cooperative transmissions introduce correlation between the interferer density and packet retransmission probability, and correlation of interference power in both spatial and time domains, which complicate the interference characterization. Based on queueing theory and stochastic geometry, the stationary interferer density is derived by solving a fixed-point equation, which is proved to have a unique solution. According to the relay selection scheme, we characterize the correlation of interference power in two consecutive time-slots by identifying the densities of source and relay retransmissions. Based on the stationary interferer density and interference correlation, we derive the outage probability and average packet delay for a typical source-destination pair, while taking into account the dynamic traffic arrival, interference correlation, relay selection scheme, and spatial node distribution. The performance analysis is validated by extensive simulations.

5.1 Motivation

In Chapter 4, we focus on analyzing the performance of opportunistic cooperation in a saturated traffic scenario, where each source node always has a packet for transmission. In this chapter, we consider a practically important scenario, where the packets arrive at each

source node dynamically. However, the dynamic traffic arrivals and concurrent cooperative transmissions complicate the characterization of both interferer density and interference correlation. Specifically, the interferer density depends on the traffic arrival rate and affects the packet retransmission probability. In addition, the packet retransmission probability affects the packet service rate and in turn affects the probability of an empty queue and interferer density. Such a correlation should be considered when characterizing the interferer density. On the other hand, as each (interfering) relay is geographically close to its intended source node, the interference power observed by a destination node in two consecutive time-slots is correlated. Similarly, the interference power observed by a destination node and its neighboring relays in the same time-slot is also correlated. The spatial and temporal correlation of interference power leads to the correlation of successful packet receptions at adjacent locations and in consecutive time-slots. The level of interference correlation depends on the packet retransmission probability as well as the relay selection scheme, which should be considered when characterizing the interference correlation.

5.2 Cooperation Scheme

At the beginning of each time-slot, the source node of each potential source-destination pair[1] is granted access to the medium with probability $p_m > 0$, which is independent of the transmission decisions of all other source nodes and its buffer status. Each source node, being granted access to the medium and having a non-empty buffer, transmits a packet to its intended destination node with rate ν. Hence, a packet transmitted from source node S_0 is successfully received by destination node D_0 at time-slot t if the instantaneous SIR satisfies

$$\gamma_{S_0D_0}(t) = \frac{H_{S_0D_0}(t) \cdot L_D^{-\alpha}}{\sum\limits_{x \in \Phi_I(t)} H_{XD_0}(t) \cdot d_{XD_0}^{-\alpha}(t)} \geq \beta_\nu \tag{5.1}$$

where $H_{S_0D_0}(t)$ denotes the random distance-independent fading coefficient between source node S_0 and destination node D_0 at time-slot t, $\Phi_I(t)$ denotes the set of the spatial locations of unintended (active) transmitters at time-slot t, x denotes the location coordinate of unintended transmitter X, the denominator is the aggregate interference power observed by destination node D_0 (i.e., summation of power levels of the signals from all unintended

[1] A potential source-destination pair refers to the source-destination pair that its source node or selected relay does not retransmit a packet in the current time-slot.

transmitters), transmission power P_t is normalized to one without loss of generality, and $\epsilon = 0$ models the singular path loss model.

Consider a cooperative truncated automatic repeat request (ARQ) scheme with one-time retransmission. If the destination node correctly decodes a packet, it sends an acknowledgement (ACK) frame. In the subsequent time-slot, $t+1$, the source node is granted access to the medium with probability p_m to transmit a new packet. Otherwise, a negative acknowledgement (NACK) frame is broadcasted. The undelivered packet is retransmitted in the subsequent time-slot by either the source node or a selected relay according to the following relay selection scheme. Both the ACK and NACK frames are reported back via an error-free and delay-free control channel.

For each source-destination pair requiring a packet retransmission, a constrained relay selection region as in Chapter 4 is considered. Let $\Omega_0(t)$ denote the relay set formed by the qualified relays of the typical source-destination pair at time-slot t. Mathematically, relay set $\Omega_0(t)$ can be expressed as

$$\Omega_0(t) = \{R_i : r_i(t) \in \Phi_R(t) \cap CR_0, \gamma_{S_0R_i}(t) \geq \beta_\nu\} \tag{5.2}$$

where CR_0 denotes the constrained relay selection region for the typical source-destination pair, and $\gamma_{S_0R_i}(t)$ denotes the SIR observed by relay R_i at time-slot t.

Assuming that, via measuring the NACK frame, each qualified relay has instantaneous CSI towards the intended destination node. The source node is treated equivalently as a qualified relay. At the beginning of time-slot $t+1$, a qualified relay with the best channel to destination node D_0 is selected as the best relay. In particular, source node S_0 is selected as the best relay R_b^0 when either relay set $\Omega_0(t)$ is empty or source node S_0 has the best channel quality to destination node D_0. Otherwise, a qualified relay in $\Omega_0(t)$ with the best channel quality to destination node D_0 acts as the best relay R_b^0. At time-slot $t+1$, the best relay R_b^0 retransmits the packet to intended destination node D_0 with rate ν, while all other qualified relays for the typical source-destination pair keep silent. Mathematically, the SIR observed by destination node D_0 at time-slot $t+1$ can be expressed as

$$\gamma_{R_b^0D_0}(t+1) = \max\left\{\max_{R_i \in \Omega_0(t)}\{\gamma_{R_iD_0}(t+1)\}, \gamma_{S_0D_0}(t+1)\right\} \tag{5.3}$$

where relay set $\Omega_0(t)$ is defined in (5.2).

The retransmitted packet is correctly received by destination node D_0 if $\gamma_{R_b^0D_0}(t+1) \geq \beta_\nu$. Otherwise, an outage event occurs as both the original transmission and retransmission fail to deliver the packet, i.e., $\gamma_{S_0D_0}(t) < \beta_\nu$ and $\gamma_{R_b^0D_0}(t+1) < \beta_\nu$. Upon the failure of

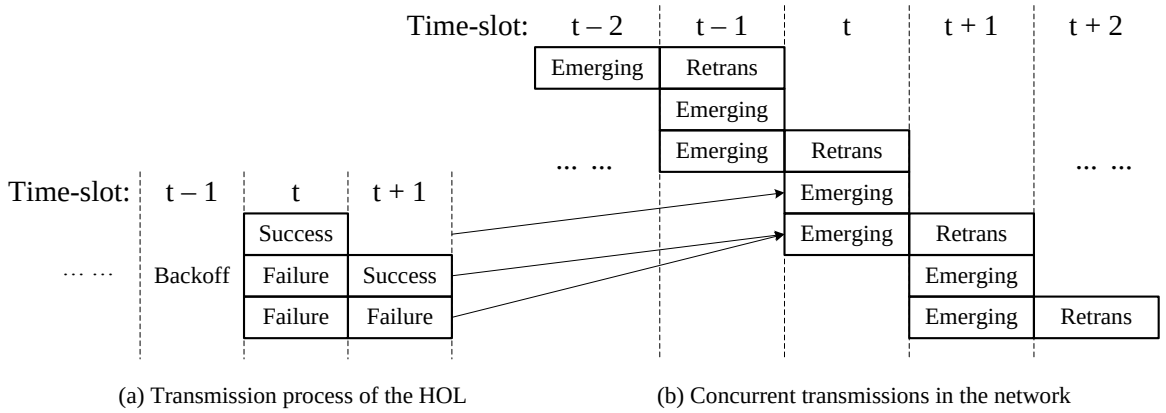

(a) Transmission process of the HOL (b) Concurrent transmissions in the network

Figure 5.1: An illustration of the transmission processes of the HOL and all packets in the network, respectively.

the packet retransmission, the packet is dropped from the queue, and the source node is granted access to the medium with probability p_m to transmit a new packet in the subsequent time-slot, $t + 2$.

Figure 5.1(a) illustrates the transmission process of each packet. Upon being granted access to the medium, the head-of-line (HOL) departs from the buffer of the source node when either it is correctly decoded by the destination node or it is not correctly decoded by the destination node after one retransmission attempt. After the transmission of one packet, the node location changes according to a high mobility random walk model as in [39, 71], which allows for decoupling the interaction among the queues and providing tractable performance analysis. With the mobility model, the displacement theorem [24] can be applied, which results in location independence across the transmission periods of different packets.

From a perspective of the overall network, the cooperative truncated ARQ scheme is enabled by all source-destination pairs, leading to asynchronous concurrent cooperative transmissions over different spatial locations. As shown in Figure 5.1(b), the concurrent transmitters at any time-slot include emerging and retransmitting nodes. An emerging node refers to the node transmitting a new packet in the current time-slot, while a retransmitting node refers to the node retransmitting the packet undelivered in the previous time-slot. Enabling more concurrent transmissions is beneficial for the efficiency of spatial frequency reuse. However, as the concurrent transmissions generate interference to each other, a higher density of unintended transmissions increases the packet retransmission probability, and vice versa. Such a correlation should be considered when deriving

the interferer density. On the other hand, the correlation of interferer locations in two consecutive time-slots, due to packet retransmissions, induces the correlation of interference power, which leads to the correlation of successful packet receptions and affects the transmission outage probability. As a result, to evaluate the overall network performance, we characterize the interferer density and interference correlation in Sections 5.3 and 5.4, respectively.

5.3 Interferer Density

The interferer density determines the average interference power observed by each node and hence the probability of transmission failure. In this section, utilizing the tools from queueing theory and stochastic geometry, we derive the interferer density (i.e., density of unintended transmitters) when the network is in a steady state, in terms of the data traffic arrival rate, source density, medium access probability, and link length.

In deriving the interferer density, the typical source-destination pair is not included in the following sets. Let $\Phi_{em}(t)$ and $\Phi_{re}(t)$ be the sets of the spatial locations of emerging and retransmitting nodes at time-slot t, respectively. As in [38] and [68], $\Phi_{em}(t)$ and $\Phi_{re}(t)$ can be approximated as PPPs with densities $\lambda_{em}(t)$ and $\lambda_{re}(t)$ respectively, and the accuracy is validated by simulations. As an unintended transmitter is either an emerging node or a retransmitting node, we have $\Phi_I(t) = \Phi_{em}(t) \cup \Phi_{re}(t)$ and $\lambda_I(t) = \lambda_{em}(t) + \lambda_{re}(t)$, where $\lambda_I(t)$ is the interferer density at time-slot t. When the network is in a steady state, the interferer density is stationary, i.e., $\lambda_I(t) = \lambda_I$. Due to the i.i.d. channel fading coefficients in different time-slots and the stationary interferer density, the retransmission probability (i.e., failure probability of the packets transmitted by emerging nodes) is stationary, denoted as q_f. Let σ denote the packet transmission rate of each source-destination pair, which depends on medium access probability p_m and retransmission probability q_f. Hence, the probability that each source node has a non-empty buffer is given by the utilization factor, denoted as $\varrho_u = \Lambda_T/\sigma$.

At the beginning of time-slot t, the density of source nodes of potential source-destination pair is $\lambda_S - \lambda_{re}(t)$. As these source nodes are granted access to the medium with probability p_m, the density of emerging nodes at time-slot t is given by $\lambda_{em}(t) = \varrho_u p_m [\lambda_S - \lambda_{re}(t)]$. Because of one-time packet retransmission, the density of retransmitting nodes at time-slot $t+1$ can be expressed as $\lambda_{re}(t+1) = \lambda_{em}(t) \cdot q_f$. Hence, the following equation holds

$$\varrho_u p_m [\lambda_S - \lambda_{re}(t)] \cdot q_f = \lambda_{re}(t+1) \tag{5.4}$$

where $\lambda_{re}(t) = \lambda_{re}(t+1) = \lambda_{re}$ when the network is in a steady state.

The time index is dropped whenever the quantities remain invariant over time. According to (5.4), the densities of retransmitting and emerging nodes at any time-slot can be expressed respectively as

$$\begin{aligned} \lambda_{re} &= \frac{q_f}{1+\varrho_u p_m q_f}\varrho_u p_m \lambda_S \\ \lambda_{em} &= \frac{1}{1+\varrho_u p_m q_f}\varrho_u p_m \lambda_S. \end{aligned} \tag{5.5}$$

As a result, the stationary interferer density is given by

$$\lambda_I = \lambda_{em} + \lambda_{re} = \frac{1+q_f}{1+\varrho_u p_m q_f}\varrho_u p_m \lambda_S. \tag{5.6}$$

The utilization factor ϱ_u and retransmission probability q_f are derived in the following two propositions.

Proposition 5. *Given that all source nodes have stable queues and the network is in a steady state, the utilization factor of each source node is given by*

$$\varrho_u = \Lambda_T(1 + p_m q_f)/p_m. \tag{5.7}$$

After obtaining utilization factor ϱ_u, we derive retransmission probability q_f and interferer density λ_I in the following proposition.

Proposition 6. *Given that all source nodes have stable queues and the network is in a steady state, the interferer density is given by*

$$\lambda_I = \Lambda_T \lambda_S \cdot G(q_f) \tag{5.8}$$

where q_f is a unique solution of the following fixed-point equation

$$q_f = 1 - \exp\left[-\Lambda_T \lambda_S C_2 \cdot G(q_f)\right] \tag{5.9}$$

with $\delta = 2/\alpha$, and

$$C_2 = \frac{\pi^2 \delta}{\sin(\pi\delta)} \beta_\nu^\delta L_D^2 \tag{5.10}$$

$$G\left(q_f\right) = \frac{\left(1+q_f\right)\left(1+p_m q_f\right)}{1+\Lambda_T\left(1+p_m q_f\right)q_f}. \tag{5.11}$$

The retransmission probability q_f can be easily calculated by solving a fixed-point equation in (5.9). Equations (5.8) and (5.9) capture the correlation between interferer density λ_I and retransmission probability q_f.

Propositions 5 and 6 present utilization factor ϱ_u, interferer density λ_I, and retransmission probability q_f under the condition that the network is stable. In the following corollary, we provide a sufficient condition for the network stability.

Corollary 4. *A sufficient condition for the queues of all source nodes to be stable is given by*

$$\Lambda_T < p_m/(1+p_m q_f) \tag{5.12}$$

where q_f is a unique solution of the following fixed-point equation

$$q_f = 1 - \exp\left(-\frac{\left(1+q_f\right)p_m}{1+p_m q_f}\lambda_S C_2\right). \tag{5.13}$$

5.4 Interference Correlation

The transmission of one packet lasts for two time-slots when a retransmission is required. For each source-destination pair requiring a packet retransmission, the locations of transmitting and retransmitting nodes are correlated. Due to concurrent packet retransmissions, the interference power correlates in two consecutive time-slots. In this section, we characterize and distinguish the interference correlation incurred by (interfering) source and relay retransmissions by deriving their respective densities.

At time-slot $t+1$, the set of retransmitting nodes, $\Phi_{re}\left(t+1\right)$, can be further partitioned into two independent PPPs, $\Phi_{reS}\left(t+1\right)$ and $\Phi_{reR}\left(t+1\right)$. Mathematically, we have

$$\Phi_{re}\left(t+1\right) = \Phi_{reS}\left(t+1\right) \cup \Phi_{reR}\left(t+1\right) \tag{5.14}$$

where $\Phi_{reS}\left(t+1\right)$ and $\Phi_{reR}\left(t+1\right)$ denote the sets of the geographical locations of retransmitting sources and relays at time-slot $t+1$, respectively.

The sets of the locations of retransmitting source and relay nodes can be expressed

respectively as

$$\Phi_{reS}(t+1) = \{s_i(t+1) \in \Phi_{re}(t+1) : s_i(t+1) = s_i(t)\} \tag{5.15}$$

and

$$\Phi_{reR}(t+1) = \{r_i(t+1) \in \Phi_{re}(t+1) : r_i(t+1) = s_i(t) + \tau\} \tag{5.16}$$

where $s_i(t) \in \Phi_{em}(t)$ and τ is the location difference between a source and the selected relay.

At any time-slot t, the relays within constrained relay selection region CR_0 and destination node D_0 locate geographically close and suffer from the same set of interferers $\Phi_I(t)$, yielding to the spatial correlation of interference power observed by these nodes. On the other hand, the common locations of transmitting and retransmitting sources, $\Phi_{reS}(t+1)$ defined in (5.15), and the adjacent locations of transmitting sources and retransmitting relays, $\Phi_{reR}(t+1)$ defined in (5.16), yield to the temporal correlation of interference power observed by destination node D_0 in consecutive time-slots t and $t+1$. The temporal interference correlation is characterized by the densities of retransmitting sources and relays, denoted as λ_{reS} and λ_{reR} respectively, which are derived based on the relay selection scheme. The effect of interference correlation on the network performance is considered in the following analysis.

According to the relay selection scheme, source node S_0 retransmits the packet at time-slot $t+1$ when one of the following events occurs: 1) Event $\mathcal{E}_{31}$ - destination node D_0 fails to decode the packet at time-slot t, and relay set $\Omega_0(t)$ is empty; 2) Event $\mathcal{E}_{32}$ - destination node D_0 fails to decode the packet at time-slot t, and source node S_0 has the best channel to destination node D_0 while relay set $\Omega_0(t)$ is not empty. The probability of Event $\mathcal{E}_{31}$ can be expressed as

$$\begin{aligned}\mathbb{P}(\mathcal{E}_{31}) &= \mathbb{P}(\gamma_{S_0D_0}(t) < \beta_\nu, \Omega_0(t) = \emptyset) \\ &\overset{(a)}{=} \sum_{k=0}^{\infty} \mathbb{P}(K_0 = k) \cdot \mathbb{P}(\gamma_{S_0D_0}(t) < \beta_\nu, M_0 = 0 \,|K_0 = k)\end{aligned} \tag{5.17}$$

where K_0 and M_0 denote the number of relays within CR_0 and qualified relays respectively, and (a) follows by conditioning on the value of K_0.

Denote Event $\mathcal{E}_{33}$ as the event that source node S_0 has the best channel to destination

node D_0. By definition, the probability of Event $\mathcal{E}_{32}$ is given by

$$\begin{aligned}\mathbb{P}\left(\mathcal{E}_{32}\right) &= \mathbb{P}\left(\gamma_{S_0D_0}\left(t\right) < \beta_\nu, \Omega_0(t) \neq \emptyset, \mathcal{E}_{33}\right) \\ &\overset{(a)}{=} \sum_{k=1}^{\infty} \mathbb{P}\left(K_0 = k\right) \left[\sum_{m=1}^{k} \mathbb{P}\left(\gamma_{S_0D_0}\left(t\right) < \beta_\nu, M_0 = m, \mathcal{E}_{33}(m) \,|K_0 = k\right)\right]\end{aligned} \tag{5.18}$$

where (a) follows by conditioning on the value of K_0, and $\mathcal{E}_{33}(m)$ denotes the event that $\mathcal{E}_{33}$ happens when there are m qualified relays.

The probability that destination node D_0 fails to decode the packet while there exist m qualified relays (i.e., $k-m$ potential relays fail to decode the packet) is given by

$$\begin{aligned}&\mathbb{P}\left(\gamma_{S_0D_0}\left(t\right) < \beta_\nu, M_0 = m, \mathcal{E}_{33}(m) \,|K_0 = k\right) \\ \overset{(a)}{=}&\mathbb{E}_{\Phi_I(t),H}\left[\left[1-\exp\left(-\beta_\nu L_D^\alpha I_{D_0}\left(t\right)\right)\right]\binom{k}{m}\prod_{i=1}^{m}\exp\left(-\beta_\nu\kappa^\alpha I_{R_i}\left(t\right)\right)\right. \\ &\left.\times\prod_{j=1}^{k-m}\left[1-\exp\left(-\beta_\nu\kappa^\alpha I_{R_j}\left(t\right)\right)\right]\right]\cdot\mathbb{P}(\mathcal{E}_{33}(m)) \\ =&\mathcal{P}_4\cdot\mathbb{P}(\mathcal{E}_{33}(m))\end{aligned} \tag{5.19}$$

where $I_{D_0}\left(t\right) = \sum_{x\in\Phi_I(t)} H_{XD_0}\left(t\right) d_{XD_0}^{-\alpha}\left(t\right)$ and $I_{R_i}\left(t\right) = \sum_{x\in\Phi_I(t)} H_{XR_i}\left(t\right) d_{XR_i}^{-\alpha}\left(t\right)$ denote the aggregate interference power observed by destination node D_0 and relay R_i at time-slot t respectively, (a) follows by taking expectations over independent exponential channel fading coefficients $H_{S_0D_0}\left(t\right)$ and $H_{S_0R_i}\left(t\right)$, by setting the distances between source node S_0 and its potential relays to be κ for small constrained relay selection regions, and by applying the independent channel fading in different time-slots and for different channels. Note that the spatial interference correlation is taken into account by taking a joint expectation over the same set of interferers $\Phi_I(t)$.

Similarly, by taking the Laplace transforms of independent channel fading coefficients $H_{XD_0}\left(t\right)$ and $H_{XR_i}\left(t\right)$, we have

$$\mathcal{P}_4 = \mathbb{E}_{\Phi_I(t)}\left[\binom{k}{m}\left(1-\prod_{x\in\Phi_I(t)}\eta_{11}\right)\left(\prod_{x\in\Phi_I(t)}\eta_{22}\right)^m\left(1-\prod_{x\in\Phi_I(t)}\eta_{22}\right)^{k-m}\right] \tag{5.20}$$

where $\eta_{jl} = \left(1+\beta_\nu u_j^\alpha v_l^{-\alpha}\right)^{-1}$. Note that $u_j \in \{L_D, \kappa, L_D-\kappa\}$ and $v_l \in \{d_{XD_0}\left(t\right), d_{XR_0}\left(t\right)\}$,

where $d_{XD_0}(t) = \|x\|$ and $d_{XR_0}(t) = \|x - r_0\|$.

By applying the binomial expansion in (5.20), we have

$$\begin{aligned}\mathcal{P}_4 &= \binom{k}{m}\sum_{n=0}^{k-m}\binom{k-m}{n}(-1)^n\left\{\mathbb{E}\left[\prod_{x\in\Phi_I(t)}\eta_{22}^{m+n}\right]-\mathbb{E}\left[\prod_{x\in\Phi_I(t)}\eta_{11}\eta_{22}^{m+n}\right]\right\}\\ &\overset{(a)}{=}\binom{k}{m}\sum_{n=0}^{k-m}\binom{k-m}{n}(-1)^n\left\{\exp\left(-\lambda_I Q_{m+n}\right)-\exp\left[-\lambda_I\int_{\mathbb{R}^2}\left(1-\eta_{11}\eta_{22}^{m+n}\right)\mathrm{d}x\right]\right\}\end{aligned} \tag{5.21}$$

where (a) follows from the PGFL of the PPP [23], and

$$Q_{m+n} = -\delta\pi\beta_\nu^\delta\kappa^2\Gamma(-\delta)\,\Gamma(\delta+m+n)/\Gamma(m+n). \tag{5.22}$$

By setting $m = 0$ and substituting (5.21) into (5.17), we obtain $\mathbb{P}(\mathcal{E}_{31})$.

Given that there are m qualified relays, the probability that source node S_0 has the best channel to destination node D_0 is given by

$$\begin{aligned}\mathbb{P}(\mathcal{E}_{33}(m)) &= \mathbb{P}\left(H_{S_0D_0}(t+1) > \left(\frac{L_D}{L_D-\kappa}\right)^\alpha \max_{R_i\in\Omega_0(t)}\left\{H_{R_iD_0}(t+1)\right\}\right)\\ &= \prod_{i=1}^{m}\mathbb{P}\left(H_{S_0D_0}(t+1) > \left(\frac{L_D}{L_D-\kappa}\right)^\alpha H_{R_iD_0}(t+1)\right)\\ &= \left[1+\left(\frac{L_D}{L_D-\kappa}\right)^\alpha\right]^{-m}.\end{aligned} \tag{5.23}$$

Substituting (5.21) and (5.23) into (5.18), we obtain $\mathbb{P}(\mathcal{E}_{32})$. With $\mathbb{P}(\mathcal{E}_{31})$ and $\mathbb{P}(\mathcal{E}_{32})$, the probability of source node retransmitting, denoted as q_s, is given by $q_s = \mathbb{P}(\mathcal{E}_{31}) + \mathbb{P}(\mathcal{E}_{32})$. As a result, the densities of retransmitting sources and relays are given by

$$\begin{aligned}\lambda_{reS} &= q_s\lambda_{re}/q_f\\ \lambda_{reR} &= (q_f - q_s)\,\lambda_{re}/q_f\end{aligned} \tag{5.24}$$

where λ_{re} and q_f are defined in (5.5) and (5.9), respectively.

5.5 Performance Analysis

After deriving the stationary interferer density in Section 5.3 and characterizing the interference correlation in two consecutive time-slots in Section 5.4, we derive the outage probability and average delay in terms of important network and protocol parameters in this section.

For performance comparison, we first consider a conventional truncated ARQ scheme, where only the source nodes retransmit the packets upon transmission failure. An outage event occurs when the received SIRs at the destination node (e.g., D_0) are smaller than reception threshold β_ν in two consecutive time-slots. The outage probability, denoted as q_{out}^{Conv}, is given in the following proposition.

Proposition 7. *The outage probability of the conventional truncated ARQ scheme is given by*

$$q_{out}^{Conv} = 1 - 2\exp\left(-\lambda_I C_2\right) + \left[\exp\left(-\lambda_{em} C_2\right)\right]^2 \exp\left(-\lambda_{re} C_3\right) \tag{5.25}$$

where C_2 is defined in (5.10), and

$$C_3 = \pi \beta_\nu^\delta \Gamma\left(1+\delta\right) \Gamma\left(1-\delta\right) \left(1+\delta\right) L_D^2. \tag{5.26}$$

For a cooperative truncated ARQ scheme, an outage event occurs when both of the following events occur: 1) Event $\mathcal{E}_{41}$ - the direct link is not reliable in both time-slots t and $t+1$; 2) Event $\mathcal{E}_{42}$ - no relays have reliable links to the source and destination nodes in time-slots t and $t+1$, respectively. The outage probability, denoted as q_{out}^{Coop}, is given in the following proposition.

Proposition 8. *The outage probability of the cooperative truncated ARQ scheme is given by*

$$q_{out}^{Coop} = \sum_{k=0}^{\infty} \frac{\left(\lambda_R \mathcal{A}_R\right)^k}{k!} \exp\left(-\lambda_R \mathcal{A}_R\right) \cdot \sum_{m=0}^{k} \binom{k}{m} (-1)^m \cdot C_4 \tag{5.27}$$

where

$$\begin{aligned} C_4 = &\exp\left(-2\lambda_{em}Q_m - \lambda_{reS}\int_{\mathbb{R}^2}\left(1-\eta_{22}^m\eta_{31}^m\right)\mathrm{d}x - \lambda_{reR}\int_{\mathbb{R}^2}\left(1-\eta_{21}^m\eta_{31}^m\right)\mathrm{d}x\right) \\ &-\exp\left(-\lambda_{em}\left(Q_m+Q_{m+1}\right) - \lambda_{reS}\int_{\mathbb{R}^2}\left(1-\eta_{11}\eta_{22}^m\eta_{31}^m\right)\mathrm{d}x - \lambda_{reR}\int_{\mathbb{R}^2}\left(1-\eta_{11}\eta_{21}^m\eta_{31}^m\right)\mathrm{d}x\right) \\ &-\exp\left(-\lambda_{em}\left(Q_m+Q_{m+1}\right) - \lambda_{reS}\int_{\mathbb{R}^2}\left(1-\eta_{11}\eta_{22}^m\eta_{31}^m\right)\mathrm{d}x - \lambda_{reR}\int_{\mathbb{R}^2}\left(1-\eta_{12}\eta_{21}^m\eta_{31}^m\right)\mathrm{d}x\right) \\ &+\exp\left(-2\lambda_{em}Q_{m+1} - \lambda_{reS}\int_{\mathbb{R}^2}\left(1-\eta_{11}^2\eta_{22}^m\eta_{31}^m\right)\mathrm{d}x - \lambda_{reR}\int_{\mathbb{R}^2}\left(1-\eta_{11}\eta_{12}\eta_{21}^m\eta_{31}^m\right)\mathrm{d}x\right) \end{aligned} \tag{5.28}$$

with λ_{em}, λ_{reS}, λ_{reR}, and Q_m are defined in (5.5), (5.24), and (5.22), respectively.

The average delay is composed of queueing delay and service delay. Queueing delay is the duration between the time that a packet arrives at the queue and the time that it becomes the HOL. Service delay is the duration between the time that a packet becomes the HOL until it leaves the queue. According to the service time distribution in (A.30) derived in Appendix A.5, the second moment of the service time is given by

$$\begin{aligned} \mathbb{E}\left[U^2\right] &= p_m\left(1-q_f\right) + \sum_{k=2}^{\infty} k^2\left[\left(1-p_m\right)^{k-1}p_m\left(1-q_f\right) + \left(1-p_m\right)^{k-2}p_m p_f\right] \\ &= \left(2-p_m+2p_m q_f + p_m^2 q_f\right)/p_m^2. \end{aligned} \tag{5.29}$$

In an M/G/1 queue, the queueing delay, denoted as Z_q, can be obtained by using the P-K formula [72]

$$Z_q = \frac{\Lambda_T \mathbb{E}\left[U^2\right]}{2\left(1-\Lambda_T\mathbb{E}\left[U\right]\right)} \tag{5.30}$$

where $\mathbb{E}[U]$ is provided in (A.31).

The service delay of a successful packet transmission is given by

$$Z_s = \left[1+\left(q_f - q_{out}^{Coop}\right)p_m\right]/p_m \tag{5.31}$$

where q_f and q_{out}^{Coop} are given in (5.9) and (5.27), respectively.

As a result, by combining (5.30) and (5.31), we can obtain the average delay of a

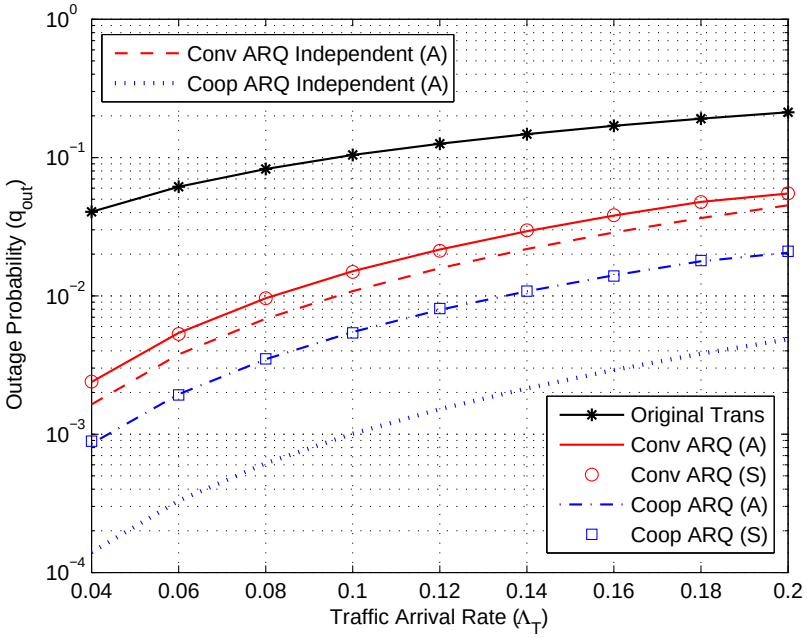

Figure 5.2: Outage probability versus traffic arrival rate (in packets/time-slot) when $\lambda_S = 0.001$ nodes/m^2, $\lambda_R = 0.2$ nodes/m^2, $p_m = 0.2$, $\kappa = 5$ m, and $L_D = 10$ m.

successful packet transmission by

$$Z = Z_q + Z_s. \tag{5.32}$$

5.6 Numerical Results

This section presents both analytical (A) and simulation (S) results for conventional and cooperative truncated ARQ schemes in a wireless ad hoc network. In the simulations, a circular network coverage area with radius 1000 m is considered. The reception threshold β_ν and radius of relay selection region r_C are set to 4 and 2, respectively, with path loss exponent $\alpha = 4$. The simulation results are obtained by averaging 10^6 realizations of the random network topology.

Figure 5.2 shows the outage probabilities of both conventional and cooperative truncated ARQ schemes versus traffic arrival rate Λ_T with parameters $\lambda_S = 0.001$ nodes/m^2,

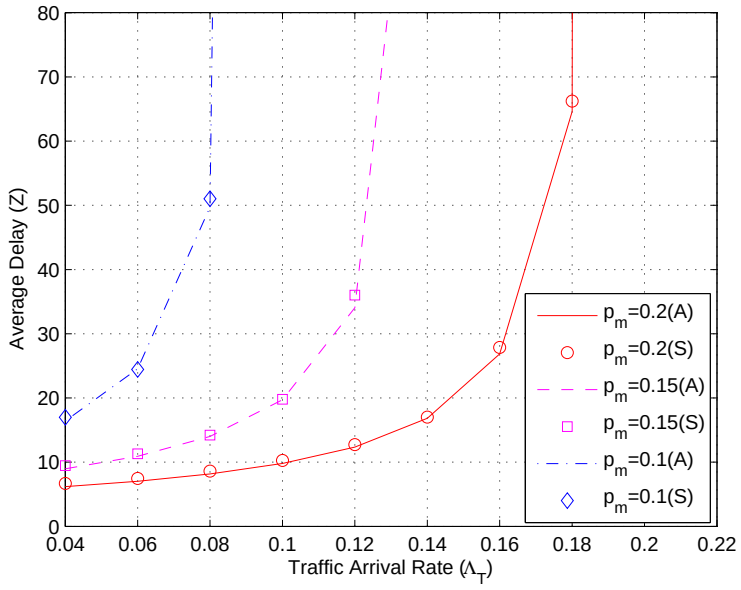

Figure 5.3: Average delay versus traffic arrival rate (in packets/time-slot) when $\lambda_S = 0.001$ nodes/m^2, $\lambda_R = 0.2$ nodes/m^2, $\kappa = 5$ m, and $L_D = 10$ m.

$\lambda_R = 0.2$ nodes/m^2, $p_m = 0.2$, $\kappa = 5$ m, and $L_D = 10$ m, where the analytical results are obtained based on (5.25) and (5.27), respectively. To illustrate the impact of interference correlation, the analytical results of outage probabilities of both schemes under the assumption that the interference power is independent at adjacent locations and in consecutive time-slots are also plotted in Figure 5.2. It is shown that the outage probability incorporating the effect of interference correlation is always higher than that assuming independent interference power, as the correlated interference power reduces the benefit achieved by exploiting the spatial diversity gain. The simulation results match well with the analytical results incorporating the effect of interference correlation, which validates the performance analysis. In addition, it is observed that the outage probabilities of both schemes increase with the traffic arrival rate. With an increase of the traffic arrival rate, the probability of an empty queue at a source node decreases, which leads to a higher density of concurrent transmitters as well as higher interference power observed by a receiver. Compared to the failure probability of the original transmission, both schemes enhance the transmission reliability. By exploiting the spatial diversity gain, the outage probability of the cooperative truncated ARQ scheme is always lower than that of the conventional truncated ARQ scheme.

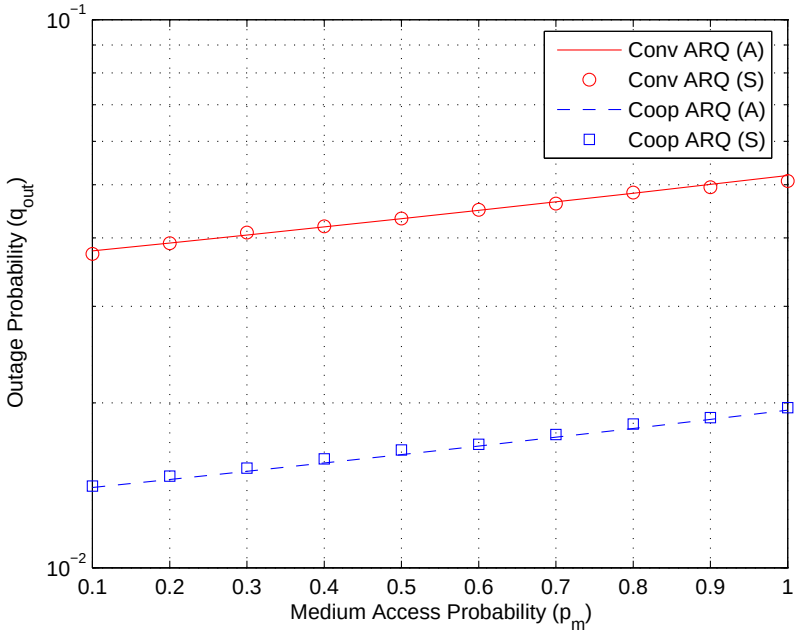

Figure 5.4: Outage probability versus medium access probability when $\lambda_S = 0.002$ nodes/m^2, $\lambda_R = 0.2$ nodes/m^2, $\Lambda_T = 0.08$ packets/time-slot, $\kappa = 5$ m, and $L_D = 10$ m.

Figure 5.3 illustrates the average delay of the cooperative truncated ARQ scheme versus traffic arrival rate Λ_T for medium access probability $p_m = 0.1$, 0.15, and 0.2 when $\lambda_S = 0.001$ nodes/m^2, $\lambda_R = 0.2$ nodes/m^2, $\kappa = 5$ m, and $L_D = 10$ m, where the analytical result is obtained based on (5.32). It is observed that the average delay increases significantly with the traffic arrival rate. With an increase of the traffic arrival rate, the queueing delay becomes a more dominant component of the total delay and approaches to infinity when utilization factor ϱ_u tends to 1. On the other hand, with an increase of medium access probability p_m, the packet transmission rate of each source-destination pair increases, which in turn decreases the average delay.

Figure 5.4 shows the outage probabilities of both conventional and cooperative truncated ARQ schemes versus medium access probability p_m with parameters $\lambda_S = 0.002$ nodes/m^2, $\lambda_R = 0.2$ nodes/m^2, $\Lambda_T = 0.08$ packets/time-slot, $\kappa = 5$ m, and $L_D = 10$ m. With an increase of the medium access probability, the outage probabilities of both schemes increase due to a higher interferer density at each time-slot. Comparing the results in Figures 5.2 and 5.4, it is observed that the impact of medium access probability p_m on the outage probability is smaller than the impact of traffic arrival rate Λ_T on the

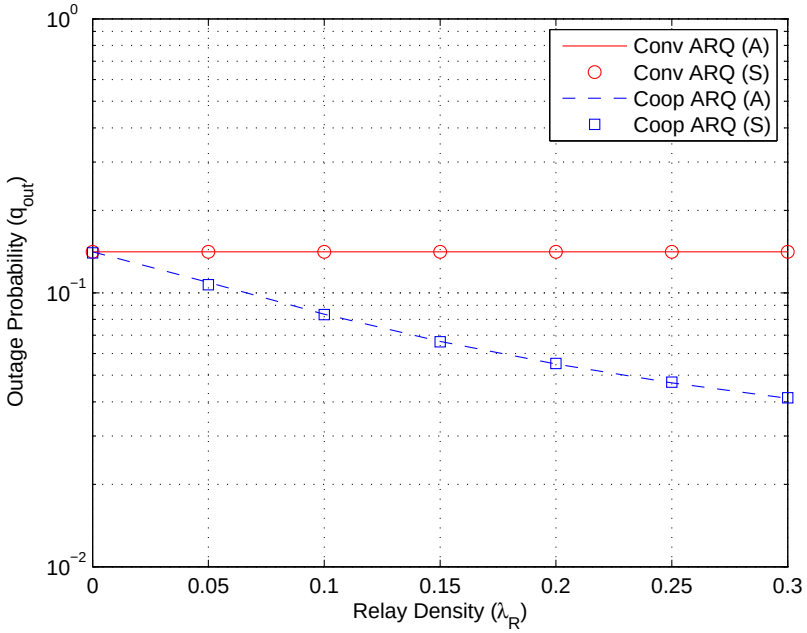

Figure 5.5: Outage probability versus relay density when $\lambda_S = 0.0015$ nodes/m^2, $\Lambda_T = 0.2$ packets/time-slot, $p_m = 0.4$, $\kappa = 5$ m, and $L_D = 10$ m.

outage probability. This is due to the fact that, with an increase of medium access probability p_m, the probability of having an empty queue at each source node increases, which in turn reduces the interferer density. As a result, combining these two conflict effects on the interferer density, the outage probabilities increase slowly with the medium access probability. On the other hand, comparing the results in Figures 5.3 and 5.4, the average delay deceases with the medium access probability while the outage probability increases with the medium access probability. This implies that the medium access probability can be adjusted to balance the tradeoff between the average delay and outage probability.

Figure 5.5 illustrates the outage probabilities of both conventional and cooperative truncated ARQ schemes versus relay density λ_R with parameters $\lambda_S = 0.0015$ nodes/m^2, $p_m = 0.4$, $\kappa = 5$ m, $\Lambda_T = 0.2$ packets/time-slot, and $L_D = 10$ m. It is observed that the outage probability of the cooperative truncated ARQ scheme decreases with the relay density, while that of the conventional truncated ARQ scheme does not change. With an increase of the relay density, more potential relays are available, which results in a higher probability of selecting a reliable relay. The outage probability of the cooperative truncated ARQ scheme is always lower than that of the conventional truncated ARQ scheme, as the

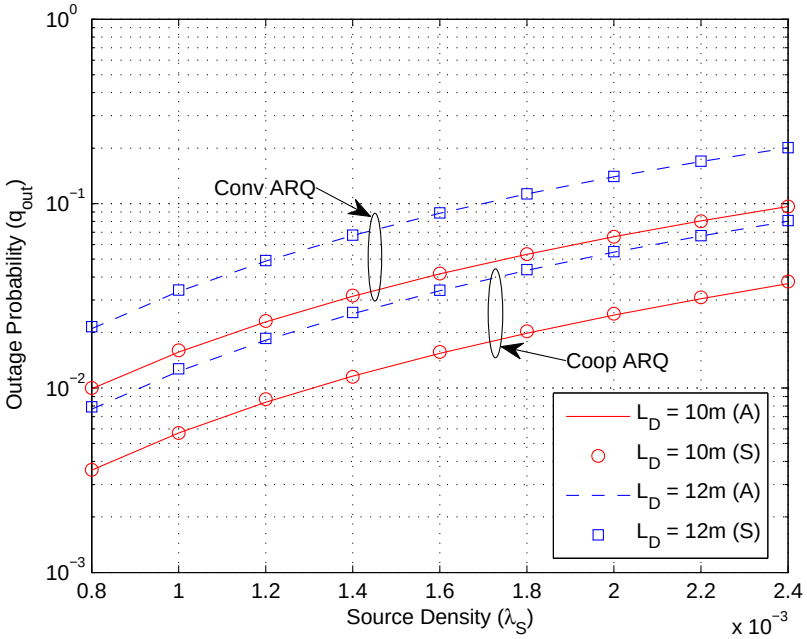

Figure 5.6: Outage probability versus source density and link length when $\lambda_R = 0.2$ nodes/m^2, $\Lambda_T = 0.1$ packets/time-slot, $\kappa = L_D/2$, and $p_m = 0.4$.

node (i.e., a source node or qualified relay) with the best channel quality to the destination node is selected to retransmit the packet.

Figure 5.6 shows the outage probabilities of both conventional and cooperative truncated ARQ schemes versus source density λ_S and link length L_D with parameters $\lambda_R = 0.2$ nodes/m^2, $\Lambda_T = 0.1$ packets/time-slot, $\kappa = L_D/2$, and $p_m = 0.4$. With an increase of the source density, the outage probabilities of both schemes increase, because activating more concurrent transmissions leads to higher interference power observed by a destination node. On the other hand, the outage probabilities of both schemes increases with the link length due to a larger path loss between the source and destination nodes.

5.7 Summary

This chapter studies the performance of a cooperative truncated ARQ scheme in a wireless ad hoc network with unsaturated traffic and randomly positioned single-hop source-

destination pairs, where the interference power is spatially and temporally correlated. To evaluate the network performance, we characterize the interference power by deriving the stationary interferer density and identifying the interference correlation in two consecutive time-slots, utilizing the tools from queueing theory and stochastic geometry. The outage probability and average delay for a typical source-destination pair are derived as a function of important network and protocol parameters. Extensive simulations are conducted to validate the performance analysis. The analytical results show that the performance analysis under the assumption of independent interference power overestimates the network performance.

Chapter 6

Conclusions and Future Work

6.1 Conclusions

Wireless ad hoc networks have recently been recognized as a promising solution to increase network coverage and enhance spectrum efficiency in next generation cellular networks. Through exploiting both spatial diversity and frequency reuse gains, supporting concurrent cooperative transmissions can further enhance the network performance, where co-channel interference is the main performance-limiting factor. To evaluate the overall network performance, one of the main research challenges is interference characterization, which is complicated by the randomness of spatial node locations, transmission decisions, and packet traffic patterns. The main objective of this research is to evaluate the effectiveness of cooperative communication in a wireless ad hoc network from a perspective of overall network performance. To achieve this objective, this thesis presents a theoretical performance analysis framework for cooperative communication in a wireless ad hoc network with randomly positioned single-hop source-destination pairs and relays.

Compared to direct transmissions, cooperative transmissions can enhance single-link transmission reliability, but reduce network-wide spatial frequency reuse due to relay transmissions. We construct a geographically constrained relay selection region to balance the tradeoff between these two competing effects. The single-link cooperation gain is characterized by comparing the success probabilities of cooperative and direct links. In particular, the outage probabilities of a cooperative link with SC and MRC are derived based on stochastic geometry. On the other hand, the network-wide reduced spatial frequency reuse is characterized by comparing the expected numbers of concurrent direct and cooperative transmissions that can be accommodated within the network coverage area, which

are derived based on a randomized scheduling scheme. Combining these two aspects, the network throughput is derived to evaluate the effectiveness of cooperative communication, in terms of the total number of links, relay density, size of relay selection region, and link length. It is shown that a locally beneficial cooperative transmission is not guaranteed to be network-wide beneficial.

We propose an opportunistic cooperation strategy to activate the cooperative transmission by each source-destination pair only when the number of potential relays is not smaller than a cooperation threshold, leading to a mixture of direct and cooperative transmissions. The correlation of node locations induces the correlation of interference power at adjacent locations and in consecutive sub-time-slots. By modeling the interferer locations as a PPP and by identifying the dependency among different PPPs, we derive the correlation coefficient of interference power observed by a typical destination node during the transmission periods of source and relay nodes. Conditioning on whether or not cooperation is activated by the typical source-destination pair, the outage probability of opportunistic cooperation is derived, while taking into account interference correlation. It is shown that cooperation is not always beneficial and its effectiveness depends on the number of potential relays available for relay selection. In addition, it is observed that the interference redistribution incurred by cooperative transmissions reduces the level of interference correlation.

The dynamic traffic arrival and concurrent cooperative transmissions introduce a correlation between the interferer density and packet retransmission probability. We investigate the impact of traffic unsaturation on the performance of a cooperative truncated ARQ scheme in a wireless ad hoc network. We derive the stationary interferer density by establishing and solving a fixed-point equation, which captures the correlation between the interferer density and packet retransmission probability. The fixed-point equation is proved to have a unique solution according to the Contraction Mapping Theorem. In addition, a sufficient condition for a stable queue at all source nodes is presented. Based on the interference correlation according to the relay selection scheme, we derive the outage probability and average packet delay for a typical source-destination pair. It is shown that the performance analysis under the assumption of independent interference power overestimates the network performance.

6.2 Future Research Topics

This research focuses on the scenario with randomly positioned single-hop source-destination pairs. An extension to consider multi-hop source-destination pairs is very interesting but challenging, in which the spatial and temporal correlation of interference power across

multiple hops should be considered. There exists a tradeoff between end-to-end outage probability and delay. In particular, a larger hopping number results in a shorter hopping distance, which provides higher transmission reliability. On the other hand, a larger hopping number implies that more relays are needed to forward the packet, which incurs a longer delay. Hence, it is interesting to optimize the number of hops to balance the tradeoff.

In the future, more powerful nodes and advanced signal processing methods can be utilized to alleviate the adverse effect of interference in cooperative communication. For instance, in a multi-channel scenario, a relay with cognitive radio capability can select a channel with least interference, so as to reduce the impact on its neighboring links. To enhance signal quality and reduce interference power, joint relay and channel selection need further investigation. Interference cancellation is a promising technique to boost the network performance by canceling received interference from the received signal, at the cost of introducing additional complexity. The tradeoff between single-link cooperation gain and network-wide reduced spatial frequency reuse should be reinvestigated.

In this research, it is assumed that all nodes transmit with the same power. With a constant transmission power, the received SINR of a high-quality link may be higher than the required reception threshold. As a result, unnecessary interference is introduced to increase the interference power at other destination nodes. Transmission power is a key degree of freedom in the management of interference. To reduce unnecessary interference and further enhance spatial frequency reuse, transmission power of each node should be adjusted based on instantaneous channel quality and interference power. Hence, joint relay selection and transmission power control need further investigation.

Another important research topic is to generalize to multiple relay selection, in which the number of relays should be optimized to balance the tradeoff between cooperation gain and additional interference. In addition, the protocol overhead incurred by relay selection increases with the number of relays, and it reduces the diversity gain achieved by cooperative communication. The impacts of both additional protocol overhead and interference redistribution on the achievable cooperation gain should be investigated, so as to fully understand the benefits and limitations of cooperative communication.

Appendix A

Proofs of Propositions and Corollaries

A.1 Proof of Proposition 1

The probability that the direct link fails in the first sub-time-slot is given by

$$\begin{aligned}\mathbb{P}\left(\psi_{S_0D_0} < \beta_{2\nu}\right) &= \mathbb{P}\left(H_{S_0D_0} < \frac{\beta_{2\nu}W}{P_t}L_D^{\alpha}\right) \\ &\overset{(a)}{=} 1 - \exp(-ML_D^{\alpha})\end{aligned} \tag{A.1}$$

where (a) follows from the exponential distribution of $H_{S_0D_0}$.

Similarly, with a relay located at r_i instead of at a distance L_D away, the success probabilities of the source-relay and relay-destination links can be expressed as

$$\begin{aligned}\mathbb{P}\left(\psi_{S_0R_i} \geq \beta_{2\nu}\right) &= \exp\left(-Md_{S_0R_i}^{\alpha}\right) \\ \mathbb{P}\left(\psi_{R_iD_0} \geq \beta_{2\nu}\right) &= \exp\left(-Md_{R_iD_0}^{\alpha}\right).\end{aligned} \tag{A.2}$$

As the potential relays form a homogeneous PPP, the probability of existing k relays within $DR_0(\omega)$ is given by

$$\mathbb{P}\left(K_0 = k\right) = \frac{\left(\lambda_R\mathcal{A}_{DR_0(\omega)}\right)^k}{k!}\exp\left(-\lambda_R\mathcal{A}_{DR_0(\omega)}\right) \tag{A.3}$$

where $\mathcal{A}_{DR_0(\omega)} = \frac{L_D^2}{2} \tan\omega$ represents the area of $DR_0(\omega)$.

Outage event $\mathcal{E}_{11}$ means that no potential relays have a reliable link to the source node. Outage event $\mathcal{E}_{12}$ means that no qualified relays have a reliable link to the destination node when the relay set is not empty. Hence, outage event $(\mathcal{E}_{11} \cup \mathcal{E}_{12})$ is equivalent to the event that no potential relays have a reliable link to both the source and destination nodes. Given that k potential relays locate within $DR_0(\omega)$, we have

$$\mathbb{P}(\mathcal{E}_{11} \cup \mathcal{E}_{12} | K_0 = k) = \mathbb{E}\left[\prod_{i=1}^{k} \left[1 - \mathbb{P}(\psi_{S_0R_i} \geq \beta_{2\nu}) \cdot \mathbb{P}(\psi_{R_iD_0} \geq \beta_{2\nu})\right]\right]. \tag{A.4}$$

As k potential relays are uniformly distributed within $DR_0(\omega)$, we have

$$\begin{aligned} &\mathbb{P}(\mathcal{E}_{11} \cup \mathcal{E}_{12} | K_0 = k) \\ \overset{(a)}{=} &\left(\frac{\int_{DR_0(\omega)} \left[1 - \mathbb{P}(\psi_{S_0R_i} \geq \beta_{2\nu})\, \mathbb{P}(\psi_{R_iD_0} \geq \beta_{2\nu})\right] \mathrm{d}s}{\mathcal{A}_{DR_0(\omega)}}\right)^k \\ \equiv &\mathcal{J}^k \end{aligned} \tag{A.5}$$

where (a) follows from the PGFL of the BPP [23].

Combining (A.3) and (A.5), we have

$$\begin{aligned} &\mathbb{P}(K_0 = 0) + \sum_{k=1}^{\infty} \mathbb{P}(K_0 = k) \cdot \mathbb{P}(\mathcal{E}_{11} \cup \mathcal{E}_{12} | K_0 = k) \\ = &\exp\left(-\lambda_R \mathcal{A}_{DR_0(\omega)}\right) + \sum_{k=1}^{\infty} \frac{\left(\lambda_R \mathcal{A}_{DR_0(\omega)}\right)^k}{k!} \exp\left(-\lambda_R \mathcal{A}_{DR_0(\omega)}\right) \cdot \mathcal{J}^k \\ = &\exp\left[-\lambda_R \mathcal{A}_{DR_0(\omega)} (1 - \mathcal{J})\right] \\ = &\exp\left[-\lambda_R \int_{DR_0(\omega)} \mathbb{P}(\psi_{S_0R_i} \geq \beta_{2\nu}) \cdot \mathbb{P}(\psi_{R_iD_0} \geq \beta_{2\nu}) \mathrm{d}s\right]. \end{aligned} \tag{A.6}$$

Consider a rectangular coordinate system with origin at link center O, as shown in Figure 3.2. Due to the constrained relay selection region, the coordinate of any qualified

relay should satisfy one of the following two constraints

$$\begin{cases} x \in \left[\frac{y}{\tan\omega} - \frac{L_D}{2}, -\frac{y}{\tan\omega} + \frac{L_D}{2}\right], \text{ if } y \in \left[0, \frac{L_D}{2}\tan\omega\right] \\ x \in \left[-\frac{y}{\tan\omega} - \frac{L_D}{2}, \frac{y}{\tan\omega} + \frac{L_D}{2}\right], \text{ if } y \in \left[-\frac{L_D}{2}\tan\omega, 0\right]. \end{cases} \tag{A.7}$$

Due to the symmetry, we focus on the upper half of the constrained relay selection region, where $y \in \left[0, \frac{L_D}{2}\tan\omega\right]$. By substituting (A.1), (A.2), and (A.6) into (3.5), we get the result in (3.7).

A.2 Proof of Proposition 2

As the qualified relay with the best channel to the destination node is selected, the outage probability can be expressed as

$$\begin{aligned} q_{CT}^{MRC} &= \mathbb{P}\left(\psi_{S_0D_0} + \max\left\{\psi_{R_b^0D_0}, \psi_{S_0D_0}\right\} < \beta_{2\nu}\right) \\ &= \mathbb{P}\left(\psi_{S_0D_0} + \max_{R_i\in\Omega_0}\left\{\psi_{R_iD_0}\right\} < \beta_{2\nu}, 2\psi_{S_0D_0} < \beta_{2\nu}\right) \\ &= \mathbb{P}\left(\psi_{S_0D_0} + \max_{R_i\in\Omega_0}\left\{\psi_{R_iD_0}\right\} < \beta_{2\nu} \middle| \psi_{S_0D_0} < \frac{\beta_{2\nu}}{2}\right) \cdot \mathbb{P}\left(\psi_{S_0D_0} < \frac{\beta_{2\nu}}{2}\right). \end{aligned} \tag{A.8}$$

With $H_{S_0D_0}$ following an exponential distribution, we have $\mathbb{P}(\psi_{S_0D_0} < \beta_{2\nu}/2) = 1 - \exp(-ML_D^{\alpha}/2)$.

By selecting the best relay, the outage event is equivalent to that all qualified relays are in outage. The conditional probability of transmission failure with MRC can be obtained as

$$\begin{aligned} &\mathbb{P}\left(\psi_{S_0D_0} + \max_{R_i\in\Omega_0}\left\{\psi_{R_iD_0}\right\} < \beta_{2\nu} \middle| \psi_{S_0D_0} < \frac{\beta_{2\nu}}{2}\right) \\ =&\mathbb{E}\left[\prod_{R_i\in\Omega_0} \mathbb{P}\left(\psi_{S_0D_0} + \psi_{R_iD_0} < \beta_{2\nu} \middle| \psi_{S_0D_0} < \frac{\beta_{2\nu}}{2}\right)\right]. \end{aligned} \tag{A.9}$$

As different source-relay links experience independent channel fading, the set of qualified relays Ω_0 is an independent thinning of Φ_R. Statistically, a relay closer to the source node has a higher probability to receive the packet successfully in the first sub-time-slot.

Hence, the probability of successful packet reception at each relay is location-dependent, which results in an inhomogeneous PPP Ω_0. According to the PGFL of the PPP [23], we have

$$\begin{aligned}&\mathbb{P}\left(\psi_{S_0D_0}+\max_{R_i\in\Omega_0}\left\{\psi_{R_iD_0}\right\}<\beta_{2\nu}\left|\psi_{S_0D_0}<\frac{\beta_{2\nu}}{2}\right.\right)\\&=\exp\left[-\int_{DR_0(\omega)}\left(1-\mathbb{P}\left(\psi_{S_0D_0}+\psi_{RD_0}<\beta_{2\nu}\left|\psi_{S_0D_0}<\frac{\beta_{2\nu}}{2}\right.\right)\right)\mu\left(\mathrm{d}s\right)\right].\end{aligned}\tag{A.10}$$

where $\mu\left(\mathrm{d}s\right)$ represents the intensity measure.

The intensity measure of Ω_0 is equal to the average number of qualified relays in $DR_0(\omega)$. It is given by

$$\begin{aligned}\mu\left(DR_0\left(\omega\right)\right)&\overset{(a)}{=}\mathbb{E}\left[\sum_{r_i\in\Phi_R\cap DR_0(\omega)}\mathbf{1}\left(R_i\in\Omega_0\right)\right]\\&\overset{(b)}{=}\int_{DR_0(\omega)}\lambda_R\exp\left(-Md_{S_0R_i}^{\alpha}\right)\mathrm{d}s\end{aligned}\tag{A.11}$$

where $\mathbf{1}(\cdot)$ is the indicator function, (a) follows from the definition of intensity measure, and (b) follows from the Campbell's theorem [23].

According to the definition of conditional probability, we have

$$\mathbb{P}\left(\psi_{S_0D_0}+\psi_{RD_0}<\beta_{2\nu}\left|\psi_{S_0D_0}<\frac{\beta_{2\nu}}{2}\right.\right)=\frac{\mathbb{P}\left(\psi_{S_0D_0}+\psi_{RD_0}<\beta_{2\nu},\psi_{S_0D_0}<\frac{\beta_{2\nu}}{2}\right)}{\mathbb{P}\left(\psi_{S_0D_0}<\frac{\beta_{2\nu}}{2}\right)}.\tag{A.12}$$

In (A.12), we should first calculate $\mathbb{P}\left(\psi_{S_0D_0}+\psi_{RD_0}<\beta_{2\nu},\psi_{S_0D_0}<\frac{\beta_{2\nu}}{2}\right)$. As both $H_{S_0D_0}$ and H_{RD_0} follow an exponential distribution, we have

$$\begin{aligned}&\mathbb{P}\left(\psi_{S_0D_0}+\psi_{RD_0}<\beta_{2\nu},\psi_{S_0D_0}<\tfrac{\beta_{2\nu}}{2}\right)\\&=\mathbb{P}\left(L_D^{-\alpha}H_{S_0D_0}+d_{RD_0}^{-\alpha}H_{RD_0}<M,H_{S_0D_0}<\tfrac{M}{2}L_D^{\alpha}\right)\\&=\int_0^{\frac{M}{2}L_D^{\alpha}}\int_0^{ML_D^{\alpha}-\left(\frac{L_D}{d_{RD_0}}\right)^{\alpha}x}\exp\left(-x\right)\exp\left(-y\right)\mathrm{d}y\mathrm{d}x\\&=\begin{cases}1-\exp\left(-\frac{M}{2}L_D^{\alpha}\right)+\frac{\exp\left(-Md_{RD_0}^{\alpha}\right)-\exp\left(-\frac{M}{2}\left(L_D^{\alpha}+d_{RD_0}^{\alpha}\right)\right)}{\left(d_{RD_0}/L_D\right)^{\alpha}-1}, & \text{if } L_D\neq d_{RD_0}\\1-\exp\left(-\frac{M}{2}L_D^{\alpha}\right)\left[1+\frac{M}{2}L_D^{\alpha}\exp\left(-\frac{M}{2}L_D^{\alpha}\right)\right], & \text{if } L_D=d_{RD_0}.\end{cases}\end{aligned}\tag{A.13}$$

Due to the constrained relay selection region, L_D is not equal to d_{RD_0}. By substituting (A.11), (A.12), and (A.13) into (A.10), we obtain (3.12).

A.3 Proof of Proposition 3

Let random variable $V_2 = \frac{L_D}{2}\tan\omega - V_1$, as shown in Figure 3.4. The expected value of V_2 can be expressed as

$$\begin{aligned}\mathbb{E}[V_2] &= \int_0^{\frac{L_D}{2}\tan\omega} v \cdot f_{V_2}(v)\mathrm{d}v \\ &= \int_0^{\frac{L_D}{2}\tan\omega} \overline{F}_{V_2}(v)\mathrm{d}v\end{aligned} \tag{A.14}$$

where $f_{V_2}(v)$ and $\overline{F}_{V_2}(v)$ represent the probability density function and complementary cumulative density function of random variable V_2, respectively. Note that $\overline{F}_{V_2}(v)$ is the same as the probability that there are no potential relays within the shaded triangular region. Hence, we have

$$\begin{aligned}\overline{F}_{V_2}(v) &= \mathbb{P}(V_2 > v) \\ &= \mathbb{P}(\text{No potential relays within } TR(v)) \\ &\overset{(a)}{=} \exp\left(-\frac{\lambda_R}{\tan\omega}v^2\right)\end{aligned} \tag{A.15}$$

where (a) follows from the definition of the PPP, $TR(v)$ represents the shaded triangular region, and its area is $\mathcal{A}_{TR(v)} = v^2/\tan\omega$.

By substituting (A.15) into (A.14), we have

$$\mathbb{E}[V_2] = \sqrt{\frac{\pi\tan\omega}{4\lambda_R}}\,\mathrm{erf}\left(\frac{L_D}{2}\sqrt{\lambda_R\tan\omega}\right). \tag{A.16}$$

As $\mathbb{E}[V_1] = \frac{L_D}{2}\tan\omega - \mathbb{E}[V_2]$, we get the result in (3.16).

A.4 Proof of Proposition 4

According to the definition of the correlation coefficient between two random variables, we have

$$\rho=\frac{\mathbb{E}\left[I_{D_0:1}\left(\Phi_D,\Phi_C\right)I_{D_0:2}\left(\Phi_D,\Phi_F\right)\right]-\mathbb{E}\left[I_{D_0:1}\left(\Phi_D,\Phi_C\right)\right]\mathbb{E}\left[I_{D_0:2}\left(\Phi_D,\Phi_F\right)\right]}{\sqrt{\mathrm{Var}\left(I_{D_0:1}\left(\Phi_D,\Phi_C\right)\right)}\sqrt{\mathrm{Var}\left(I_{D_0:2}\left(\Phi_D,\Phi_F\right)\right)}} \tag{A.17}$$

where $\mathbb{E}\left[X\right]$ and $\mathrm{Var}\left(X\right)$ represent the mean and variance of random variable X, respectively.

Due to the unit mean of fading coefficients, the mean of interference power $I_{D_0:1}\left(\Phi_D,\Phi_C\right)$ is given by

$$\begin{aligned}\mathbb{E}\left[I_{D_0:1}\left(\Phi_D,\Phi_C\right)\right]&=\mathbb{E}\left[\sum_{s_i\in\Phi_D}H_{S_iD_0:1}\cdot g\left(s_i\right)+\sum_{s_j\in\Phi_C}H_{S_jD_0:1}\cdot g\left(s_j\right)\right]\\&\overset{(a)}{=}\lambda_S\int_{\mathbb{R}^2}g\left(s\right)\mathrm{d}s\end{aligned} \tag{A.18}$$

where (a) follows from the Campbell's Theorem [22].

Similarly, we have $\mathbb{E}\left[I_{D_0:2}\left(\Phi_D,\Phi_F\right)\right]=\left(\lambda_D+\lambda_F\right)\int_{\mathbb{R}^2}g\left(s\right)\mathrm{d}s$, where $\lambda_F=\lambda_C\cdot\mathbb{P}\left(\Omega_0\neq\emptyset\right)$ denotes the spatial density of PPP Φ_F. As the cooperative transmission is activated only when there exist at least θ_C potential relays, the probability of an empty relay set (i.e., no qualified relays), denoted as $q_e=\mathbb{P}\left(\Omega_0=\emptyset\right)$, is given by

$$q_e=\sum_{k=\theta_C}^{\infty}\mathbb{P}\left(K_0=k\right)\cdot\underbrace{\mathbb{P}\left(\gamma_{S_0R_1:1}<\beta_{2\nu},\cdots,\gamma_{S_0R_k:1}<\beta_{2\nu}\left|K_0=k\right.\right)}_{A} \tag{A.19}$$

where $\gamma_{S_0R_k:1}=H_{S_0R_k:1}\cdot g\left(s_0-r_k\right)/I_{R_k:1}\left(\Phi_D,\Phi_C\right)$ denotes the SIR at relay R_k when receiving a packet from source node S_0.

The probability that k potential relays fail to decode the packet from source node S_0

is given by

$$\begin{aligned}
A &\overset{(a)}{=} \mathbb{E}\left[\prod_{i=1}^{k}\left(1-\exp\left[-\beta_{2\nu}d_{S_0R_i}^{\alpha}\left(I_{DR_i:1}\left(\Phi_D\right)+I_{CR_i:1}\left(\Phi_C\right)\right)\right]\right)\right] \\
&\overset{(b)}{=} \mathbb{E}\left[\left(1-\prod_{s_i\in\Phi_D}\frac{1}{1+\beta_{2\nu}d_{S_0R_k}^{\alpha}g\left(s_i-r_k\right)}\prod_{s_j\in\Phi_C}\frac{1}{1+\beta_{2\nu}d_{S_0R_k}^{\alpha}g\left(s_j-r_k\right)}\right)^{k}\right] \\
&\overset{(c)}{=} \sum_{m=0}^{k}\binom{k}{m}(-1)^m\underbrace{\mathbb{E}\left[\prod_{s_i\in\Phi_D}\frac{1}{\left(1+\beta_{2\nu}d_{S_0R_k}^{\alpha}g\left(s_i-r_k\right)\right)^{m}}\right]}_{A_1} \\
&\quad\times\underbrace{\mathbb{E}\left[\prod_{s_j\in\Phi_C}\frac{1}{\left(1+\beta_{2\nu}d_{S_0R_k}^{\alpha}g\left(s_j-r_k\right)\right)^{m}}\right]}_{A_2}
\end{aligned} \tag{A.20}$$

where (a) follows by taking expectations over independent exponential channel fading between source node S_0 and potential relays, (b) follows by taking Laplace transforms of independent channel fading between the interferers and potential relays, and (c) follows from the binomial expansion and the independence between PPP Φ_D and PPP Φ_C. Note that the spatial correlation of interference power at potential relays is considered by taking a joint expectation over the spatial locations of the same set of interferers.

Via applying the PGFL of the PPP [69] and performing a coordinate transformation, we have

$$\begin{aligned}
A_1 &= \frac{1}{\mathcal{A}_R}\int_{CR_0}\exp\left(-2\pi\lambda_D\int_0^{\infty}\left[1-\left(1+\beta_{2\nu}d_{S_0R}^{\alpha}l^{-\alpha}\right)^{-m}\right]l\mathrm{d}l\right)\mathrm{d}r \\
&= \frac{1}{\mathcal{A}_R}\int_{CR_0}\exp\left(-\lambda_D C_1 d_{S_0R}^{2}\right)\mathrm{d}r \\
A_2 &= \frac{1}{\mathcal{A}_R}\int_{CR_0}\exp\left(-\lambda_C C_1 d_{S_0R}^{2}\right)\mathrm{d}r
\end{aligned} \tag{A.21}$$

where C_1 is defined in (4.8).

By substituting (A.20) and (A.21) into (A.19), λ_F and $\mathbb{E}\left[I_{D_0:2}\left(\Phi_D,\Phi_F\right)\right]$ can be derived.

The mean product of $I_{D_0:1}(\Phi_D, \Phi_C)$ and $I_{D_0:2}(\Phi_D, \Phi_F)$ is given by

$$\begin{aligned}
&\mathbb{E}\left[I_{D_0:1}(\Phi_D, \Phi_C) I_{D_0:2}(\Phi_D, \Phi_F)\right] \\
=\ &\mathbb{E}\left[I_{DD_0:1}(\Phi_D) I_{DD_0:2}(\Phi_D)\right] + \mathbb{E}\left[I_{DD_0:1}(\Phi_D) I_{FD_0:2}(\Phi_F)\right] \\
+\ &\mathbb{E}\left[I_{CD_0:1}(\Phi_C) I_{DD_0:2}(\Phi_D)\right] + \mathbb{E}\left[I_{CD_0:1}(\Phi_C) I_{FD_0:2}(\Phi_F)\right].
\end{aligned} \tag{A.22}$$

As PPP Φ_D is independent of PPP Φ_C and PPP Φ_F, we have

$$\begin{aligned}
\mathbb{E}\left[I_{DD_0:1}(\Phi_D) I_{FD_0:2}(\Phi_F)\right] &= \lambda_D \lambda_F \left(\int_{\mathbb{R}^2} g(s)\,\mathrm{d}s\right)^2 \\
\mathbb{E}\left[I_{CD_0:1}(\Phi_C) I_{DD_0:2}(\Phi_D)\right] &= \lambda_C \lambda_D \left(\int_{\mathbb{R}^2} g(s)\,\mathrm{d}s\right)^2.
\end{aligned} \tag{A.23}$$

As PPP Φ_C and PPP Φ_F are not independent of each other, the mean product of $I_{CD_0:1}(\Phi_C)$ and $I_{FD_0:2}(\Phi_F)$ is given by

$$\begin{aligned}
&\mathbb{E}\left[I_{CD_0:1}(\Phi_C) I_{FD_0:2}(\Phi_F)\right] \\
\overset{(a)}{=}&\mathbb{E}\left[\left(\sum_{s_j\in\Phi_C} g(s_j)\right)\left(\sum_{r_m\in\Phi_F} g(r_m)\right)\right] \\
\overset{(b)}{=}&\mathbb{E}\left[\left(\sum_{s_j\in\Phi_C} g(s_j)\right)\left(\sum_{s_j\in\Phi_C} (1-q_e)\cdot g(s_j+\tau)\right)\right] \\
=&\mathbb{E}\left[\sum_{s_j\in\Phi_C} (1-q_e)\cdot g(s_j)\, g(s_j+\tau)\right] + \mathbb{E}\left[\sum_{s_i,s_j\in\Phi_C}^{s_i\neq s_j} (1-q_e)\cdot g(s_j)\, g(s_j+\tau)\right] \\
\overset{(c)}{=}&\lambda_F \int_{\mathbb{R}^2} g(s)\,\mathbb{E}_\tau\left[g(s+\tau)\right]\mathrm{d}s + \lambda_C\lambda_F\left(\int_{\mathbb{R}^2} g(s)\,\mathrm{d}s\right)^2
\end{aligned} \tag{A.24}$$

where (a) holds as the fading coefficients of different links are independent random variables with unit mean, (b) follows from the transformation between PPP Φ_C and PPP Φ_F and τ is the coordinate difference between a source node and its selected relay (i.e., $\tau = r_m - s_j$), and (c) follows from the Campbell's Theorem and second-order product density formula of the PPP [22].

Similarly, by replacing τ with $(0,0)$, we have

$$\mathbb{E}\left[I_{DD_0:1}\left(\Phi_D\right) I_{DD_0:2}\left(\Phi_D\right)\right] = \lambda_D \int_{\mathbb{R}^2} g^2\left(s\right)\mathrm{d}s + \lambda_D^2 \left(\int_{\mathbb{R}^2} g\left(s\right)\mathrm{d}s\right)^2. \tag{A.25}$$

By substituting (A.23), (A.24), and (A.25) into (A.22), the numerator of (A.17), denoted as N_ρ, is given by

$$N_\rho = \lambda_D \int_{\mathbb{R}^2} g^2\left(s\right)\mathrm{d}s + \lambda_F \int_{\mathbb{R}^2} g\left(s\right)\mathbb{E}_\tau\left[g\left(s+\tau\right)\right]\mathrm{d}s. \tag{A.26}$$

The second moment of $I_{DD_0:1}\left(\Phi_D\right)$ is given by

$$\mathbb{E}\left[I_{DD_0:1}^2\left(\Phi_D\right)\right] \overset{(a)}{=} 2\lambda_D \int_{\mathbb{R}^2} g^2\left(s\right)\mathrm{d}s + \lambda_D^2 \left(\int_{\mathbb{R}^2} g\left(s\right)\mathrm{d}s\right)^2 \tag{A.27}$$

where (a) follows from the similar arguments in (A.24) and $\mathbb{E}\left[H^2\right] = 2$ for Rayleigh fading channels.

Using (A.27), the variance of $I_{D_0:1}\left(\Phi_D, \Phi_C\right)$ and $I_{D_0:2}\left(\Phi_D, \Phi_F\right)$ can be expressed respectively as

$$\begin{aligned}
\mathrm{Var}\left(I_{D_0:1}\left(\Phi_D, \Phi_C\right)\right) &= \mathbb{E}\left[I_{D_0:1}^2\left(\Phi_D, \Phi_C\right)\right] - \mathbb{E}[I_{D_0:1}\left(\Phi_D, \Phi_C\right)]^2 \\
&= 2\lambda_S \int_{\mathbb{R}^2} g^2\left(s\right)\mathrm{d}s \\
\mathrm{Var}\left(I_{D_0:2}\left(\Phi_D, \Phi_F\right)\right) &= 2\left(\lambda_D + \lambda_F\right)\int_{\mathbb{R}^2} g^2\left(s\right)\mathrm{d}s.
\end{aligned} \tag{A.28}$$

For the non-singular path loss model defined in (2.1), we have

$$\int_{\mathbb{R}^2} g^2\left(s\right)\mathrm{d}s = \frac{\delta\left(1-\delta\right)\pi^2}{\epsilon^{2-\delta}\sin\left(\pi\delta\right)}. \tag{A.29}$$

By substituting (A.26), (A.28), and (A.29) into (A.17), we obtain (4.6).

A.5 Proof of Proposition 5

Let U denote the number of time-slots required to transmit the HOL. Starting from time-slot 1, u time-slots are required if 1) the source node is granted access to the medium and transmits the HOL successfully at the uth time-slot; 2) the source node is granted access to the medium at the $(u-1)$th time-slot and retransmits the HOL at the uth time-slot. As the packet arrivals follow a Poisson distribution, the queue of each source node can be modeled by an M/G/1 queue and its service time distribution is given by

$$\begin{aligned} &\mathbb{P}\left(U=1\right)=p_m\left(1-q_f\right), && u=1 \\ &\mathbb{P}\left(U=u\right)=\left(1-p_m\right)^{u-1}p_m\left(1-q_f\right)+\left(1-p_m\right)^{u-2}p_m q_f, && u\geq 2. \end{aligned} \tag{A.30}$$

Hence, the expectation of the service time is given by

$$\mathbb{E}\left[U\right]=\sum_{u=1}^{\infty}u\cdot\mathbb{P}\left(U=u\right)=(1+p_m q_f)/p_m. \tag{A.31}$$

By definition, the utilization factor is

$$\varrho_u=\Lambda_T/\sigma=\Lambda_T\mathbb{E}\left[U\right]=\Lambda_T(1+p_m q_f)/p_m. \tag{A.32}$$

A.6 Proof of Proposition 6

By substituting (5.7) into (5.6), we obtain interferer density λ_I as a function of retransmission probability q_f, as shown in (5.8). The next step is to derive retransmission probability q_f and prove its uniqueness. The original transmission fails when the SIR observed by the destination node (e.g., D_0) is smaller than the required reception threshold. The retransmission probability is given by

$$\begin{aligned} q_f &= \mathbb{P}\left(\gamma_{S_0D_0}\left(t\right)<\beta_\nu\right) \\ &\overset{(a)}{=} 1-\exp\left(-\lambda_I C_2\right) \\ &\overset{(b)}{=} 1-\exp\left[-\Lambda_T\lambda_S C_2\cdot G(q_f)\right] \end{aligned} \tag{A.33}$$

where C_2 and $G(q_f)$ are defined in (5.10) and (5.11) respectively, (a) follows from the results presented in [24], and (b) follows by substituting (5.8).

Let $\Delta(q_f)$ denote the right hand side of fixed-point equation (A.33). As $0 < \Delta(0) < \Delta(1) < 1$ and $0 \leq q_f \leq 1$, there exists at least one solution. In order to prove that (A.33) has a unique solution, based on the Contraction Mapping Theorem [73], we need to show that the first derivative of $\Delta(q_f)$ with respect to q_f is smaller than one. As a result, we need to show that

$$\Delta'(q_f) = \exp\left[-\Lambda_T \lambda_S C_2 \cdot G(q_f)\right] \cdot \Lambda_T \lambda_S C_2 \cdot G'(q_f) < 1 \tag{A.34}$$

where $\Delta'(q_f)$ and $G'(q_f)$ are the first derivatives of $\Delta(q_f)$ and $G(q_f)$, respectively.

Equivalently, we need to prove that

$$\Psi(q_f) = \exp\left[\Lambda_T \lambda_S C_2 \cdot G(q_f)\right] - \Lambda_T \lambda_S C_2 \cdot G'(q_f) > 0. \tag{A.35}$$

The above inequality holds if 1) $\Psi(q_f)$ is an increasing function of q_f; and 2)

$$\exp\left[\Lambda_T \lambda_S C_2 \cdot G(0)\right] > \Lambda_T \lambda_S C_2 \cdot G'(0). \tag{A.36}$$

In order to show that $\Psi(q_f)$ is an increasing function of q_f, we need to prove that the first derivative $\Psi'(q_f)$ is larger than 0. The first derivative is given by

$$\Psi'(q_f) = \exp\left[\Lambda_T \lambda_S C_2 \cdot G(q_f)\right] \cdot \Lambda_T \lambda_S C_2 \cdot G'(q_f) - \Lambda_T \lambda_S C_2 \cdot G''(q_f) \tag{A.37}$$

where $G''(q_f)$ is the second derivative of $G(q_f)$, and

$$G'(q_f) = \frac{-\Lambda_T p_m^2 q_f^2 + 2p_m(1-\Lambda_T) q_f + 1 + p_m - \Lambda_T}{\left[1 + \Lambda_T(1 + p_m q_f) q_f\right]^2}. \tag{A.38}$$

Knowing that $0 < \Lambda_T < p_m \leq 1$ and $0 \leq q_f \leq 1$, we have $G'(q_f) > 0$. As all parameters are larger than or equal to 0, we have $\exp\left[\Lambda_T \lambda_S C_2 \cdot G(q_f)\right] \geq 1$. As a result, from (A.37), we need to show that $G'(q_f) - G''(q_f) > 0$. This inequality always holds by deriving and substituting $G''(q_f)$ and using the above relationships among parameters.

Since $G(0) = 1$ and $G'(0) = 1 + p_m - \Lambda_T$, according to (A.36), we need to show that

$$\exp(\Lambda_T \lambda_S C_2) > \Lambda_T \lambda_S C_2 (1 + q_m - \Lambda_T). \tag{A.39}$$

The Taylor series expansion of $\exp(\Lambda_T \lambda_S C_2)$ can be expressed as

$$\exp(\Lambda_T \lambda_S C_2) = 1 + \Lambda_T \lambda_S C_2 + (\Lambda_T \lambda_S C_2)^2/2 + \cdots. \tag{A.40}$$

Based on (A.39) and (A.40), we need to show that

$$\left(\Lambda_T \lambda_S C_2 - q_m\right)^2/2 + \left(1 - q_m^2/2\right) + \cdots > -\Lambda_T^2 \lambda_S C_2. \tag{A.41}$$

The above inequality always holds as the left hand side is positive and the right hand side is negative.

In summary, (A.34) holds and hence retransmission probability q_f is a unique solution of the fixed-point equation.

A.7 Proof of Corollary 4

To guarantee the network stability, we consider a dominant network [74], where all source nodes being granted access to the medium and having empty queues make dummy transmissions. The utilization factor of each source node in the dominant network equals to one, i.e., $\varrho_u = 1$, which represents the worst case scenario for interference. As a result, the interferer density is given by

$$\lambda_I = \frac{(1 + q_f)\, p_m}{1 + p_m q_f} \lambda_S. \tag{A.42}$$

Since the arrival and departure processes are jointly ergodic and stationary, by Loynes's theorem [75], the sufficient condition for the network stability is that $\Lambda_T < \mu = p_m/(1 + p_m q_f)$, where retransmission probability q_f is the solution of fixed-point equation (5.13). Note that (5.13) is obtained by substituting (A.42) into $q_f = 1 - \exp\left(-\lambda_I \cdot C_2\right)$. Following an argument similar to that in Appendix A.6, the uniqueness of the solution of (5.13) can be proved by setting

$$G\left(q_f\right) = \frac{1 + q_f}{1 + p_m q_f}. \tag{A.43}$$

A.8 Proof of Proposition 7

The outage probability of the conventional truncated ARQ scheme can be expressed as

$$\begin{aligned} q_{out}^{Conv} &= \mathbb{P}\left(\gamma_{S_0D_0}(t) < \beta_\nu, \gamma_{S_0D_0}(t+1) < \beta_\nu\right) \\ &\overset{(a)}{=} \mathbb{E}_{\Phi_I(t),\Phi_I(t+1)}\left[\left(1 - \prod_{x\in\Phi_I(t)} \eta_{11}\right)\left(1 - \prod_{x\in\Phi_I(t+1)} \eta_{11}\right)\right] \end{aligned} \tag{A.44}$$

where $\Phi_I(t) = \Phi_{em}(t) \cup \Phi_{reS}(t)$, $\Phi_I(t+1) = \Phi_{em}(t+1) \cup \Phi_{reS}(t+1)$, and (a) follows by taking expectations over the independent fading coefficients between source node S_0 and destination node D_0 and by taking Laplace transforms of the independent fading coefficients between interferers and destination node D_0.

In these two consecutive time-slots, $\Phi_{em}(t+1)$ is independent of $\Phi_I(t)$ and $\Phi_{reS}(t+1)$, while $\Phi_{reS}(t+1)$ is a subset of $\Phi_{em}(t)$ because of the source retransmissions, which leads to the temporal correlation of interference power. As only the source nodes retransmit the packets in the conventional truncated ARQ scheme, λ_{reS} equals to λ_{re}. As a result, we have

$$\begin{aligned} q_{out}^{Conv} &= 1 - \mathbb{E}\left[\prod_{x\in\Phi_I(t)} \eta_{11}\right] - \mathbb{E}\left[\prod_{x\in\Phi_I(t+1)} \eta_{11}\right] \\ &\quad + \mathbb{E}\left[\prod_{x\in\Phi_I(t)\setminus\Phi_{reS}(t+1)} \eta_{11}\right]\mathbb{E}\left[\prod_{x\in\Phi_{em}(t+1)} \eta_{11}\right]\mathbb{E}\left[\prod_{x\in\Phi_{reS}(t+1)} \eta_{11}^2\right] \\ &\overset{(a)}{=} 1 - 2\exp\left(-\lambda_I C_2\right) + \left[\exp\left(-\lambda_{em} C_2\right)\right]^2 \cdot \exp\left(-\lambda_{re} C_3\right) \end{aligned} \tag{A.45}$$

where (a) follows from the PGFL of the PPP, and C_2, η_{11}, and C_3 are given in (5.10), (5.20), and (5.26), respectively. Note that the temporal correlation of interference power observed by the destination node in two consecutive time-slots is considered by taking a joint expectation over the same set of interferers $\Phi_{reS}(t+1)$.

A.9 Proof of Proposition 8

For a typical source-destination pair, Events $\mathcal{E}_{41}$ and $\mathcal{E}_{42}$ can be expressed respectively as

$$\begin{aligned}\mathcal{E}_{41} &= \{\gamma_{S_0D_0}(t) < \beta_\nu \cap \gamma_{S_0D_0}(t+1) < \beta_\nu\} \\ \mathcal{E}_{42} &= \{\gamma_{S_0R_n}(t) < \beta_\nu \cup \gamma_{R_nD_0}(t+1) < \beta_\nu, \forall n \in [1,k]\}.\end{aligned} \tag{A.46}$$

Hence, the outage probability of the cooperative truncated ARQ scheme can be expressed as

$$\begin{aligned}q_{out}^{Coop} &= \sum_{k=0}^{\infty} \mathbb{P}(K_0 = k) \cdot \mathbb{P}[\mathcal{E}_{41} \cap \mathcal{E}_{42} | K_0 = k] \\ &\overset{(a)}{=} \sum_{k=0}^{\infty} \mathbb{P}(K_0 = k) \cdot \mathbb{E}[\mathbb{P}(\mathcal{E}_{41}) \cdot \mathbb{P}(\mathcal{E}_{42} | K_0 = k)]\end{aligned} \tag{A.47}$$

where the expectation is taken over the point process of interferers in two consecutive time-slots, and (a) follows from the independence of the fading coefficients for different channels.

Following the similar arguments in (5.19) and (5.20), we have

$$\mathbb{P}(\mathcal{E}_{41}) = \left[1 - \prod_{x \in \Phi_I(t)} \eta_{11}\right] \left[1 - \prod_{x \in \Phi_I(t+1)} \eta_{11}\right] \tag{A.48}$$

and

$$\mathbb{P}(\mathcal{E}_{42} | K_0 = k) = \left[1 - \prod_{x \in \Phi_I(t)} \eta_{22} \cdot \prod_{x \in \Phi_I(t+1)} \eta_{31}\right]^k = (1 - C)^k \tag{A.49}$$

where $\Phi_I(t) = \Phi_{em}(t) \cup \Phi_{reS}(t) \cup \Phi_{reR}(t)$ and $\Phi_I(t+1) = \Phi_{em}(t+1) \cup \Phi_{reS}(t+1) \cup \Phi_{reR}(t+1)$ are the sets of the interferer locations at time-slots t and $t+1$ respectively, and η_{11}, η_{22}, and η_{31} are given in (5.20).

By applying the binomial expansion in (A.49), we have

$$\mathbb{E}[\mathbb{P}(\mathcal{E}_{41}) \cdot \mathbb{P}(\mathcal{E}_{42} | K_0 = k)] = \sum_{m=0}^{k} \binom{k}{m} (-1)^m \mathbb{E}_{\Phi_I(t), \Phi_I(t+1)}[\mathbb{P}(\mathcal{E}_{41}) \cdot C^m] \tag{A.50}$$

where the joint expectation over the same set of interferers is taken to incorporate the effect of spatial and temporal interference correlation.

The correlation of node locations, defined in (5.15) and (5.16), induces the temporal correlation of interference power in consecutive time-slots t and $t+1$. By transforming the point process of transmitting sources at time-slot t to the point process of retransmitting relays at time-slot $t+1$, and by separating point process $\Phi_I(t) \cup \Phi_I(t+1)$ into independent point processes, we have

$$C = \prod_{x \in \Phi_I(t) \setminus \Phi_{re}(t+1)} \eta_{22} \cdot \prod_{x \in \Phi_{em}(t+1)} \eta_{31} \cdot \prod_{x \in \Phi_{reS}(t+1)} \eta_{22}\eta_{31} \cdot \prod_{x \in \Phi_{reR}(t+1)} \eta_{21}\eta_{31}. \tag{A.51}$$

Substituting (A.48) and (A.51) into (A.50), we can obtain outage probability q_{out}^{Coop} in (5.28) by applying the PGFL of the PPP.

References

[1] A. Ghosh, N. Mangalvedhe, R. Ratasuk *et al.*, "Heterogeneous cellular networks: from theory to practice," *IEEE Commun. Mag.*, vol. 50, no. 6, pp. 54–64, Jun. 2012.

[2] B. Alawieh, Y. Zhang, C. Assi, and H. Mouftah, "Improving spatial reuse in multihop wireless networks - a survey," *IEEE Commun. Surv. Tutor.*, vol. 11, no. 3, pp. 71–91, Aug. 2009.

[3] G. Foschini and M. Gans, "On limits of wireless communications in a fading environment when using multiple antennas," *Wireless Pers. Commun.*, vol. 6, no. 3, pp. 311–335, 1998.

[4] S. Alamouti, "A simple transmit diversity technique for wireless communications," *IEEE J. Select. Areas Commun.*, vol. 16, no. 8, pp. 1451–1458, Oct. 1998.

[5] A. Sendonaris, E. Erkip, and B. Aazhang, "User cooperation diversity. part I and part II," *IEEE Trans. Commun.*, vol. 51, no. 11, pp. 1927–1948, Nov. 2003.

[6] K. Liu, A. Sadek, W. Su, and A. Kwasinski, *Cooperative Communications and Networking.* Cambridge Press, 2009.

[7] W. Zhuang and Y. Zhou, "A survey of cooperative MAC protocols for mobile communication networks," *J. Internet Technology*, vol. 14, no. 4, pp. 541–559, Jul. 2013.

[8] A. Nosratinia, T. Hunter, and A. Hedayat, "Cooperative communication in wireless networks," *IEEE Commun. Mag.*, vol. 42, no. 10, pp. 74–80, Oct. 2004.

[9] H. Shan, W. Zhuang, and Z. Wang, "Distributed cooperative MAC for multihop wireless networks," *IEEE Commun. Mag.*, vol. 47, no. 2, pp. 126–133, Feb. 2009.

[10] W. Zhuang and M. Ismail, "Cooperation in wireless communication networks," *IEEE Wireless Commun. Mag.*, vol. 19, no. 2, pp. 10 –20, Apr. 2012.

[11] S. Weber, X. Yang, J. Andrews, and G. De Veciana, "Transmission capacity of wireless ad hoc networks with outage constraints," *IEEE Trans. Inf. Theory*, vol. 51, no. 12, pp. 4091–4102, Dec. 2005.

[12] A. Bletsas, A. Khisti, D. Reed, and A. Lippman, "A simple cooperative diversity method based on network path selection," *IEEE J. Select. Areas Commun.*, vol. 24, no. 3, pp. 659–672, Mar. 2006.

[13] E. Beres and R. Adve, "Selection cooperation in multi-source cooperative networks," *IEEE Trans. Wireless Commun.*, vol. 7, no. 1, pp. 118–127, Jan. 2008.

[14] Q. Yang, Y. Zhong, K. S. Kwak, and F. Fu, "Outage probability of opportunistic amplify-and-forward relaying in Nakagami-m fading channels," *ETRI Journal*, vol. 30, no. 4, pp. 609–611, 2008.

[15] S. Lee, M. Han, and D. Hong, "Average SNR and ergodic capacity analysis for opportunistic DF relaying with outage over Rayleigh fading channels," *IEEE Trans. Wireless Commun.*, vol. 8, no. 6, pp. 2807–2812, Jun. 2009.

[16] S. S. Ikki and M. H. Ahmed, "Performance analysis of adaptive decode-and-forward cooperative diversity networks with best-relay selection," *IEEE Trans. Commun.*, vol. 58, no. 1, pp. 68–72, Jan. 2010.

[17] Y. Jing and H. Jafarkhani, "Single and multiple relay selection schemes and their achievable diversity orders," *IEEE Trans. Wireless Commun.*, vol. 8, no. 3, pp. 1414–1423, Mar. 2009.

[18] C.-H. Yu and O. Tirkkonen, "Opportunistic multiple relay selection with diverse mean channel gains," *IEEE Trans. Wireless Commun.*, vol. 11, no. 3, pp. 885–891, Mar. 2012.

[19] J. Si, Z. Li, H. Huang, J. Chen, and R. Gao, "Capacity analysis of cognitive relay networks with the PU's interference," *IEEE Commun. Lett.*, vol. 16, no. 12, pp. 2020–2023, Dec. 2012.

[20] F. Yang, M. Huang, M. Zhao, S. Zhang, and W. Zhou, "Cooperative strategies for wireless relay networks with cochannel interference over time-correlated fading channels," *IEEE Trans. Veh. Technol.*, vol. 62, no. 7, pp. 3392–3408, Sept. 2013.

[21] J. Liu, W. Chen, Z. Cao, and Y. J. A. Zhang, "Cooperative beamforming for cognitive radio networks: a cross-layer design," *IEEE Trans. Commun.*, vol. 60, no. 5, pp. 1420–1431, May 2012.

[22] D. Stoyan, W. Kendall, J. Mecke, and L. Ruschendorf, *Stochastic Geometry and its Applications*. Wiley New York, 1987.

[23] M. Haenggi, *Stochastic Geometry for Wireless Networks*. Cambridge University Press, 2012.

[24] F. Baccelli and B. Blaszczyszyn, *Stochastic Geometry and Wireless Networks, Part I Theory*. Now Publishers, vol. 1, 2009.

[25] ——, *Stochastic Geometry and Wireless Networks, Part II Application*. Now Publishers, vol. 2, 2009.

[26] H. Wang, S. Ma, T.-S. Ng, and H. V. Poor, "A general analytical approach for opportunistic cooperative systems with spatially random relays," *IEEE Trans. Wireless Commun.*, vol. 10, no. 12, pp. 4122–4129, Dec. 2011.

[27] A. Behnad, A. Rabiei, N. Beaulieu, and H. Hajizadeh, "Generalized analysis of dual-hop DF opportunistic relaying with randomly distributed relays," *IEEE Commun. Lett.*, vol. 17, no. 6, pp. 1057–1060, Jun. 2013.

[28] C. Zhai, W. Zhang, and G. Mao, "Uncoordinated cooperative communications with spatially random relays," *IEEE Trans. Wireless Commun.*, vol. 11, no. 9, pp. 3126–3135, Sept. 2012.

[29] A. Tukmanov, S. Boussakta, Z. Ding, and A. Jamalipour, "On the impact of relay-side channel state information on opportunistic relaying," in *Proc. IEEE ICC'13*, 2013.

[30] K. S. Gilhousen, I. M. Jacobs, R. Padovani, A. J. Viterbi, J. LA Weaver, and C. E. Wheatley III, "On the capacity of a cellular CDMA system," *IEEE Trans. Veh. Technol.*, vol. 40, no. 2, pp. 303–312, May 1991.

[31] S. Weber, J. G. Andrews, and N. Jindal, "The effect of fading, channel inversion, and threshold scheduling on ad hoc networks," *IEEE Trans. Inf. Theory*, vol. 53, no. 11, pp. 4127–4149, Nov. 2007.

[32] F. Baccelli, P. Miihlethaler, and B. Blaszczyszyn, "Stochastic analysis of spatial and opportunistic ALOHA," *IEEE J. Select. Areas Commun.*, vol. 27, no. 7, pp. 1105–1119, Sept. 2009.

[33] C. Zhai, W. Zhang, and G. Mao, "Cooperative spectrum sharing between cellular and ad-hoc networks," *IEEE Trans. Wireless Commun.*, vol. 13, no. 7, pp. 4025–4037, Jul. 2014.

[34] R. K. Ganti and M. Haenggi, "Spatial analysis of opportunistic downlink relaying in a two-hop cellular system," *IEEE Trans. Commun.*, vol. 60, no. 5, pp. 1443–1450, May 2012.

[35] L. Wang and V. Fodor, "On the gain of primary exclusion region and vertical cooperation in spectrum sharing wireless networks," *IEEE Trans. Veh. Technol.*, vol. 61, no. 8, pp. 3746–3758, Oct. 2012.

[36] S. Cho, W. Choi, and K. Huang, "QoS provisioning relay selection in random relay networks," *IEEE Trans. Veh. Technol.*, vol. 60, no. 6, pp. 2680–2689, Jul. 2011.

[37] A. Altieri, L. Rey Vega, P. Piantanida, and C. Galarza, "Analysis of a cooperative strategy for a large decentralized wireless network," *IEEE/ACM Trans. Networking*, vol. 22, no. 4, pp. 1039–1051, Aug. 2014.

[38] K. Stamatiou and M. Haenggi, "Delay characterization of multihop transmission in a Poisson field of interference," *IEEE/ACM Trans. Networking*, vol. 22, no. 6, pp. 1794–1807, Dec. 2014.

[39] P. Nardelli, M. Kountouris, P. Cardieri, and M. Latva-aho, "Throughput optimization in wireless networks under stability and packet loss constraints," *IEEE Trans. Mobile Comput.*, vol. 13, no. 8, pp. 1883–1895, Aug. 2014.

[40] U. Schilcher, C. Bettstetter, and G. Brandner, "Temporal correlation of interference in wireless networks with Rayleigh block fading," *IEEE Trans. Mobile Comput.*, vol. 11, no. 12, pp. 2109–2120, Dec. 2012.

[41] R. Ganti and M. Haenggi, "Spatial and temporal correlation of the interference in ALOHA ad hoc networks," *IEEE Commun. Lett.*, vol. 13, no. 9, pp. 631–633, Sept. 2009.

[42] R. Tanbourgi, H. S. Dhillon, J. G. Andrews, and F. K. Jondral, "Effect of spatial interference correlation on the performance of maximum ratio combining," *IEEE Trans. Wireless Commun.*, vol. 13, no. 6, pp. 3307–3316, Jun. 2014.

[43] K. Gulati, R. Ganti, J. Andrews, B. Evans, and S. Srikanteswara, "Characterizing decentralized wireless networks with temporal correlation in the low outage regime," *IEEE Trans. Wireless Commun.*, vol. 11, no. 9, pp. 3112–3125, Sept. 2012.

[44] M. Haenggi, "Diversity loss due to interference correlation," *IEEE Commun. Lett.*, vol. 16, no. 10, pp. 1600–1603, Oct. 2012.

[45] U. Schilcher, S. Toumpis, A. Crismani, G. Brandner, and C. Bettstetter, "How does interference dynamics influence packet delivery in cooperative relaying?" in *Proc. ACM MSWiM'13*, 2013.

[46] R. Tanbourgi, H. Jakel, and F. K. Jondral, "Cooperative relaying in a Poisson field of interferers: a diversity order analysis," in *Proc. IEEE ISIT'13*, 2013.

[47] A. Crismani, S. Toumpis, U. Schilcher, G. Brandner, and C. Bettstetter, "Cooperative relaying under spatially and temporally correlated interference," *IEEE Trans. Veh. Technol.*, to appear.

[48] Y. Zhou and W. Zhuang, "Beneficial cooperation ratio in multi-hop wireless ad hoc networks," in *Proc. IEEE INFOCOM'13 (mini conference)*, 2013.

[49] ——, "Throughput analysis of cooperative communication in wireless ad hoc networks with frequency reuse," *IEEE Trans. Wireless Commun.*, vol. 14, no. 1, pp. 205–218, Jan. 2015.

[50] ——, "Opportunistic cooperation in wireless ad hoc networks with interference correlation," *Peer-to-Peer Networking and Applications*, submitted.

[51] ——, "Performance analysis of cooperative communication in decentralized wireless networks with unsaturated traffic," *IEEE Trans. Wireless Commun.*, submitted.

[52] S. Weber, J. G. Andrews, and N. Jindal, "An overview of the transmission capacity of wireless networks," *IEEE Trans. Commun.*, vol. 58, no. 12, pp. 3593–3604, Dec. 2010.

[53] I. Slivnyak, "Some properties of stationary flows of homogeneous random events," *Theory of Probability and its Applications*, vol. 7, no. 3, pp. 336–341, 1962.

[54] P. Cardieri, "Modeling interference in wireless ad hoc networks," *IEEE Commun. Surv. Tutor.*, vol. 12, no. 4, pp. 551–572, Nov. 2010.

[55] H. Shan, H. T. Cheng, and W. Zhuang, "Cross-layer cooperative MAC protocol in distributed wireless networks," *IEEE Trans. Wireless Commun.*, vol. 10, no. 8, pp. 2603–2615, Aug. 2011.

[56] H. Zhai and Y. Fang, "Physical carrier sensing and spatial reuse in multirate and multihop wireless ad hoc networks," in *Proc. IEEE INFOCOM'06*, 2006.

[57] T.-S. Kim, H. Lim, and J. C. Hou, "Understanding and improving the spatial reuse in multihop wireless networks," *IEEE Trans. Mobile Comput.*, vol. 7, no. 10, pp. 1200–1212, Oct. 2008.

[58] Y. Zhu and H. Zheng, "Understanding the impact of interference on collaborative relays," *IEEE Trans. Mobile Comput.*, vol. 7, no. 6, pp. 724–736, Jun. 2008.

[59] J. Laneman, D. Tse, and G. Wornell, "Cooperative diversity in wireless networks: efficient protocols and outage behavior," *IEEE Trans. Inf. Theory*, vol. 50, no. 12, pp. 3062–3080, Dec. 2004.

[60] Y. Zhou, J. Liu, L. Zheng, C. Zhai, and H. Chen, "Link-utility-based cooperative MAC protocol for wireless multi-hop networks," *IEEE Trans. Wireless Commun.*, vol. 10, no. 3, pp. 995–1005, Mar. 2011.

[61] S. Ramanathan, "A unified framework and algorithm for (T/F/C) DMA channel assignment in wireless networks," in *Proc. IEEE INFOCOM'97*, 1997.

[62] L. X. Cai, L. Cai, X. Shen, and J. Mark, "REX: a randomized exclusive region based scheduling scheme for mmWave WPANs with directional antenna," *IEEE Trans. Wireless Commun.*, vol. 9, no. 1, pp. 113–121, Jan. 2010.

[63] A. Jeffrey and D. Zwillinger, *Table of Integrals, Series, and Products*. Access Online via Elsevier, 2007.

[64] "IEEE standard for information technology-telecommunications and information exchange between systems-local and metropolitan area networks–specific requirements part 11: wireless LAN medium access control (MAC) and physical layer (PHY) specifications," *IEEE Std 802.11*, pp. 1–528, 1999.

[65] P. Liu, Z. Tao, S. Narayanan, T. Korakis, and S. S. Panwar, "CoopMAC: a cooperative MAC for wireless LANs," *IEEE J. Select. Areas Commun.*, vol. 25, no. 2, pp. 340–354, Feb. 2007.

[66] G. Mao, B. Fidan, and B. D. Anderson, "Wireless sensor network localization techniques," *Computer Networks*, vol. 51, no. 10, pp. 2529–2553, Jul. 2007.

[67] M. Mohammadi, H. Suraweera, and X. Zhou, "Outage probability of wireless ad hoc networks with cooperative relaying," in *Proc. IEEE GLOBECOM'12*, Dec. 2012.

[68] I. Krikidis, "Simultaneous information and energy transfer in large-scale networks with/without relaying," *IEEE Trans. Commun.*, vol. 62, no. 3, pp. 900–912, Mar. 2014.

[69] M. Haenggi, J. G. Andrews, F. Baccelli, O. Dousse, and M. Franceschetti, "Stochastic geometry and random graphs for the analysis and design of wireless networks," *IEEE J. Select. Areas Commun.*, vol. 27, no. 7, pp. 1029–1046, Sept. 2009.

[70] M. Haenggi and R. Smarandache, "Diversity polynomials for the analysis of temporal correlations in wireless networks," *IEEE Trans. Wireless Commun.*, vol. 12, no. 11, pp. 5940–5951, Nov. 2013.

[71] K. Stamatiou and M. Haenggi, "Random-access Poisson networks: stability and delay," *IEEE Commun. Lett.*, vol. 14, no. 11, pp. 1035–1037, Nov. 2010.

[72] D. P. Bertsekas, R. G. Gallager, and P. Humblet, *Data Networks*. Prentice-Hall International New Jersey, 1992.

[73] A. Granas and J. Dugundji, *Fixed Point Theory*. Springer Science & Business Media, 2003.

[74] W. Luo and A. Ephremides, "Stability of N interacting queues in random-access systems," *IEEE Trans. Inf. Theory*, vol. 45, no. 5, pp. 1579–1587, Jul. 1999.

[75] R. Loynes, "The stability of a queue with non-independent inter-arrival and service times," in *Proc. Camb. Phil. Soc.*, vol. 58, no. 3, pp. 497–520, 1962.